ADDIS ABABA UNIVERSITY

SCHOOL OF GRADUATE STUDIES

Extraction and Characterization of Cellulose and Microcrystalline Cellulose from Corn Husk, Corn Cob, and Lupine Husk, and Evaluation of Microcrystalline Cellulose as Directly Compressible Pharmaceutical Excipient

Hana Tesfaye

Dec, 2020

Addis Ababa, Ethiopia

Extraction and Characterization of Cellulose and Microcrystalline cellulose from Corn husk, Corn cob, and Lupine husk, and Evaluation of Microcrystalline Cellulose as Directly Compressible Pharmaceutical Excipient

A Thesis Submitted to the School of Graduate Studies, Addis Ababa University, Department of Pharmaceutics and Social Pharmacy, in Partial Fulfillment of the Requirements for the Degree of Master of Science in Pharmaceutics.

Hana Tesfaye

Advisors:

Prof. Tsige Gebre-Mariam
and
Dr. Nisha M. Joseph

Dec, 2020

Addis Ababa, Ethiopia

Addis Ababa University

School of Graduate Studies

Extraction and Characterization of Cellulose and Microcrystalline cellulose from Corn husk, Corn cob, and Lupine husk, and Evaluation of Microcrystalline Cellulose as Directly Compressible Pharmaceutical Excipient

By: Hana Tesfaye

Approved by:

Name	Signature	Date
Prof. Tsige Gebre-Mariam (Advisor)	_____	_____
Dr. Nisha M. Joseph (Advisor)	_____	_____
Dr. Getahun Paulos (External Examiner)	_____	_____
Mr. Tadele Eticha (Internal Examiner)	_____	_____

ABSTRACT

In recent years there has been a worldwide interest on sustainable use of resources. Isolation of cellulose from agro-industrial wastes has gained a great deal of interest from scientists and researchers due to its high demand in paper, food, cosmetics, textile and pharmaceutical industries. In Ethiopia, corn husk (CH), corn cob (CC), and lupine husk (LH) are abundant lignocellulosic agricultural wastes. Thus, the objective of this study was to prepare and characterize native cellulose and microcrystalline cellulose (MCC) from corn husk, corn cob, and lupine husk and evaluate MCC as directly compressible pharmaceutical excipient. Cellulose fibers were isolated from corn husk, corn cob, and lupine husk with NaOH and peroxiformic acid treatments and MCC was prepared through the hydrolysis of native celluloses using 0.1-M HCl. The isolated celluloses and MCC were characterized by Fourier-transform infrared spectroscopy (FTIR), X-ray diffraction (XRD), scanning electron microscope (SEM), and Thermogravimetric analysis (TGA). The mechanical properties of both plain MCC tablets and mebendazole-containing MCC tablets as a model drug were evaluated. The yields of cellulose from CH, CC, LH, were 42%, 33%, 36% and CH-MCC, CC-MCC, and LH-MCC, were 80%, 76%, and 78%, respectively. The degree of polymerization (DP) of CH-C, CC-C, and LH-C were 735.73, 667.29, and 576.75, respectively, while DP of MCC preparations ranged from 247.36 - 315.15. The FTIR spectra of cellulose from CH, CC, and LH were almost similar and MCCs were comparable to Avicel PH-101 spectra. The CI values of LH-C (75.39%) was slightly higher than CH-C (74.5%), CC-C (72.86%) and CI of LH-MCC (81.41 %) was lower than Avicel PH-101 (85.48%) and higher than CH-MCC (78.1%), CC-MCC (77.01%). The SEM pictures of cellulose showed micro-fibrillated structure, whereas MCC exhibited rod like shape and irregular aggregated particles. All samples of cellulose and MCC showed good thermal stability. All MCC powders showed monomodal normal particle size distribution. Both plain and mebendazole loaded CH-MCC, CC-MCC, and LH-MCC tablets showed acceptable crushing and tensile strength. The disintegration times and drug release profiles of all mebendazole loaded tablets prepared from CH-MCC, CC-MCC, LH-MCC, and Avicel PH-101 were comparable and within the acceptable Pharmacopeia range. Therefore, CH, CC, and LH could be promising locally available potential sources of cellulose and MCC.

Keywords*: Corn husk, Corn cob, Lupine husk, Cellulose, Microcrystalline Cellulose.*

ACKNOWLEDGMENTS

First and Fore most, I want to offer this endeavor to the God, Almighty, for the wisdom he best owed up on me, the peace of mind, and good health in order to finish this research.

I wish to express my sincere gratitude and heartfelt thanks to my advisors, Prof. Tsige Grebe-Mariam and Dr. Nisha M. Joseph for their encouragement, guidance, and mentorship during the thesis work as well as throughout the whole course of my postgraduate studies.

I would like to express my special thanks to Mr. Tesfaye Gabriel for his precious contribution to my thesis work by inspiring, advising and commenting during proposal development, Mr. Fekade Tefera, for his support and encouragement during laboratory work and the staff members of the Department of Pharmaceutics and Social Pharmacy.

I would also like to acknowledge, Department of Pharmacognosy for providing me with Soxhlet apparatus, Cadila Pharmaceutical Manufacturing Company for providing me access to their Fourier Transform Infrared spectroscopy (FTIR) and for donating mebendazole powder, Adama Science and Technology University for allowing access to X-ray diffractometer (XRD), Thermogravimetric and Differential Thermal Analysis Apparatus (TGA), Anna University Tamilnadu, India, providing access to Scanning electron microscope (SEM), and East Africa Pharmaceutical Manufacturing Share Company for allowing me access to their tablet compression machine.

I am highly thankful to Addis Ababa University and University of Gondar for sponsoring my study.

Finally, I am very grateful to my families for their encouragement and support throughout my entire life.

TABLE OF CONTENTS

LIST OF FIGURES

LIST OF TABLES

ACRONYMS AND ABBREVIATIONS

ASTM:	American Standard Test Methods
BP:	British Pharmacopoeia
CF:	Compression Force
CI:	Crystalinity index
CC-C:	Corn cob cellulose
CC-MCC:	Corn cob microcrystalline cellulose
CH-C:	Corn husk cellulose
CH-MCC:	Corn husk microcrystalline cellulose
Cuam:	Cuprammonium hydroxide
DP:	Degree of polymerization
DTA:	Differential thermal analysis
DC:	Direct compression
FTIR:	Fourier Transform Infrared Spectroscopy
HR:	Hausner ratio
LSR:	Lubricant sensitivity ratio
NF:	National Formulary
RH:	Relative Humidity
USP:	United States Pharmacopoeia
UV:	Ultraviolet - Visible
LH-C:	Lupine husk cellulose
LH-MCC:	Lupine husk microcrystalline cellulose
Rpm:	Revolution per minute

SEM:	Scanning electron microscope
TGA:	Thermogravimetric Analysis
XRD:	X-ray Diffraction

1. INTRODUCTION

In recent years there has been a great worldwide interest in environmental preservation and using resources sustainably. In the field of polymeric and composite materials production, numerous studies are carried out to produces cellulose and other polymers from waste materials. Among these studies the use of natural fibers, mainly of plant origin, due to the great biodiversity and waste generation by agribusiness standout (Costa *et al*., 2015).

Annually renewable agricultural wastes represent an abundant, inexpensive, and readily available source of renewable lignocellulosic biomass. Each year, farming and agricultural processing generate billions of tons of wastes, such as corn cobs, corn stalk, and corn husks, groundnut shells, rice straw, banana stems, soy hulls, and sugar beet pulp. These materials can be obtained from a variety of sources at a low cost, but the content and consistency of the three main structural polymer components (lignin, cellulose, and hemicellulose) depend on the material type. (Azubuike and Okhamafe, 2012; Krstic *et al*., 2018). Their utilizations are attracting increased interests around the world, particularly for the production of novel materials for environmentally friendly industrial applications after chemical modification (Azubuike and Okhamafe, 2012).

Lignocellulosic fibers are excellent raw materials for polymers and composites, which can be proven by the high number of patents and national and international articles, besides the large number of products like cellulose and its derivatives already marketed (Sa *et al*., 2015).

1.1. Cellulose

Cellulose was first discovered by the French scientist Anselme Payen in 1838, when he noticed a white, tasteless, odorless, resistant fibrous solid that remained behind after acid and ammonia treatment of plant tissue. (Hallac and Ragauskas, 2011). Cellulose is the backbone structure of plants and it is the chief constituent of plant cell wall and is the most widely used organic material in the world, representing around 1.5×10^{12} tons of the total annual biomass production. This natural polymer represents about one-third of plant tissues and it can be restocked by photosynthesis (Moran *et al*., 2008; Klemm *et al*., 2005). Cellulose, a linear homo polymer of glucose $(C_6H_{10}O_5)$ n and one of the major components of lignocellulosic biomass, is a poly disperse polymer of high molecular weight and comprising of long chains of D-glucose units

joined together by β-1, 4-glucosidic bonds (Haafiz *et al*., 2013). In the native cellulose (also called cellulose I), there are two different crystal forms, namely cellulose Iα and cellulose I β. Cellulose 1α has a triclinic cell arrangement and is usually found in algae and bacterial cellulose, while cellulose Iβ is a monoclinic allomorph that is common in plant cellulose (like wood, jute, cotton, etc.). Thus, cellulose from different biomass shows different properties of crystalline types. To remove the non-cellulosic materials like lignin, hemicellulose, ash and others from the cellulose alkali treatment is used. Regenerated cellulose, also known as cellulose II is produced by conversion of natural cellulose to a soluble cellulosic derivative and subsequent regeneration, which presents better thermal stability than cellulose I (Qian *et al*., 2017).

Cellulose is a semi-crystalline polymer having amorphous and crystalline regions which are bonded together by intra- and inter- molecular bonds. Cellulose in crystalline region is called cellulose crystallites and they are formed by glucose chains due to van der Waals interaction and hydrogen bonding. While cellulose in amorphous region is weak and readily hydrolyzed when exposed to an excessive amount of mineral acids, crystalline cellulose is the organized part and comprises the major proportion of cellulose, whereas amorphous cellulose formed by unorganized cellulose chains comprises a small amount (Kumar *et al*., 2009; Khalil *et al*., 2018). Thus, crystalline cellulose is obtained through hydrolysis of amorphous regions in micro fibrils of alpha cellulose, leaving the crystalline phases (Khalil *et al*., 2018; Kampeerapappun, 2015). Crystalline cellulose can be obtained from various biomasses ranging from wood to non-wood biomasses such as eucalyptus, birch (hardwood), pine (softwood), cotton slivers, corn cob, kenaf baste, orange mesocarp, empty fruit bunch, rice straw, bamboo, luffa cylindrical fiber, jute, banana fibers, rice husk and sugarcane bagasse. However, the crystalline cellulose obtained from different lingo cellulosic biomass sources usually differ in characteristics such as crystallinity, moisture content, surfaces area, molecular weight and porous structure (Khalil *et al*., 2018).

The main characteristics of cellulose are white, tasteless, odorless, semi crystalline, hydrophobic, and insoluble in organic solvents (Mishra *et al*., 2018). This is because of several factors relating to the chemical structure of cellulose. Among those, native cellulose is a macromolecule with a high degree of polymerization (DP), which is naturally hard to dissolve due to thermodynamics (decreased entropic gain for macromolecules in the dissolution process compared to small molecules). The other reasons are cellulose has many hydroxyl groups and, five oxygen atoms of the hydroxyl groups in addition to the ring and bridge oxygen, results in the formation of complex

patterns of hydrogen bonds, and the C- and H-atoms of cellulose may interact through hydrophobic interactions, indicating that cellulose has an amphiphilic nature (Jedvert and Heinze, 2017).

Hemicellulose is mainly amorphous, has branches with short lateral chains and a heteropolymer composed of different types of cycled saccharides include pentoses (xylose, rhamnose, and arabinose), hexoses (Glucose, mannose, and galactose), and uronic acids (e.g., 4-omethylglucuronic, D-glucuronic, and D-galactouronic acids). It forms a highly branched, random structure, has low DP, and is easy to hydrolyze to their monomer components (Moran *et al*., 2008; Jonsson and Martin, 2016; Taherzadeh and Karimi, 2008; Kumar *et al*., 2009). The backbone of hemicellulose is composed of either a homopolymer or a short-branched hetero polymer connected linked by β-(1, 4)-glycosidic bonds and sometimes β-(1, 3)-glycosidic bonds (Kumar *et al*., 2009). The structure of hemicellulose depends on the sources of plants. The most abundant hemicellulose, with the same D-glucose backbone as cellulose, is called xyloglucan (Szymanska-Chargot *et al*., 2017). The main hemicelluloses that are found in softwoods are O-acetylgalactoglucomannans and arabino-4-O-methylglucurono-D-xylans, while in hardwoods O-acetyl-4-O-methylglucurono-D-xylans are the most relevant ones (Jonsson and Martín, 2016). Hemicellulose sugars such as xylose, mannose and glucose are readily convertible to chemicals and fuels (Jahan *et al*., 2010).

Lignin is a very complex aromatic polymer composed of phenylpropanoid units linked in a three-dimensional structure (covalently and non-covalently cross-linked to the cellulose and hemicellulose), which is particularly difficult to biodegrade, and representing 25–39% of the dry weight of softwoods, and 17–32% of hardwoods (Jonsson and Martín, 2016; Taherzadeh and Karimi, 2008). Lignin is present in the primary cell wall, imparting structural support by binding the components of cell wall together, impermeability, and resistance against microbial attack (Kumar *et al*., 2009; Johnson and Martín, 2016) It is an amorphous phenolic polymer formed by phenyl-propane units (p-coumaryl, coniferyl and sinapyl alcohol), held together by different linkages. It mainly consists of aromatic units such as guaiacyl, syringyl and phenylpropan (Moran *et al*., 2018; Szymanska-Chargot *et al*., 2017). Lignin that presents in softwood is comprised predominantly by guaiacyl units while; hardwood lignin contains mainly syringyl units, but also important amounts of guaiacyl units. The lignins of annual plants also contain p-hydroxyphenyl units in addition to the guaiacyl and syringyl units (Jonsson and Martín, 2016).

1.2. Sources of cellulose

Cellulose is an abundant and naturally occurring polymer that can be obtained from numerous sources (Morsyleide *et al*., 2010). Cellulose is produced by plants, trees, bacteria, fungi, algae, and some animals (tunicates) via the condensation polymerization of glucose, which is a result of the photosynthesis process in plants and trees (Eichhorn, 2011). Cellulose can be produced from various biomasses ranging from wood to non-wood biomasses such as eucalyptus, birch (hardwood), pine (softwood), cotton slivers, corn husk, corn cob, kenaf bast, orange mesocarp, empty fruit bunch, rice straw, rice husk, bamboo, Luffa cylindrica fiber, jute, sisal, banana fibers, rice husk, sugarcane bagasse, soybean husk, oath hull, Sorghum caudatum and vegetable pomaces (Khalil *et al*., 2018; Jahan *et al*., 2010; Ohwoavworhua and Adelakun, 2010; Haafiz *et al*., 2013; Qian *et al*., 2017; Kambli *et al*., 2018; Johar *et al*., 2012). Except for the production of cellulose and its derivatives from lupine husk, there is no record available yet to the knowledge of the author on the production and characterization of cellulose, and microcrystalline cellulose (MCC) from lupine albus seed husk.

Typically, cellulose isolated mainly from wood pulp and cotton. Cotton is a high value-added crop and wood pulp generally originates in some manner from deforestation. Cotton may contain as much as ~90 % of cellulose (Jedvert and Heinze, 2017), and some types of wood may have as much as ~60-70% (Khalil *et al*., 2018). The need for environment friendly processes as well as the need to slow down the rapid global deforestation has stimulated renewed interest in waste products from agro-fiber plants (Ohwoavworhua and Adelakun, 2010).

The use of agricultural residues has high importance for developing countries like Ethiopia. Agricultural residues can be used by various manufacturing companies in the production of liganocellulosic biomass, such as cellulose and its derivatives. Teff straw, corn husk, corn cob, sugarcane bagasse, wheat, sorghum, and barley straw are the major agricultural residues produced in Ethiopia that contain liganocellulosic biomass.

1.3. Corn husk and Corn cob

Corn, (*maize or Zea mays*) is the third most important cereal crop in the world after rice and wheat and the second most important cereal next to Teff in Ethiopia (Kambli *et al*., 2017; Yami *et al*., 2020). Corn plays a key role in Ethiopia's food security. It is the lowest cost source of

cereal calories, providing one and half times and two times the calories per dollar compared to wheat and teff respectively (Yami *et al*., 2020). The corn stover (the stalk and leaves after harvesting), the corn husk, and the cobs are the primary waste from corn processing. Corn husk is one of the agricultural residues which are abundant, inexpensive, and readily available source of sustainable lignocellulosic biomass and it is the only fiber obtained from the byproduct of a food crop (Kampeerapappun, 2015; Kambli *et al*., 2016). Corn husk fiber, a liganocellulosic multicellular long-length fiber, is available in the global fiber market in the order of 9 million tons every year. It is the second largest source of natural fibers next to cotton (Kambli *et al*., 2016). The Corn cob is an essential cellulosic source, which is abundantly available annual liganocellulosic biomass that can be successfully cultivated in most regions of Ethiopia (Suvachitanont and Ratanapan, 2011). Corn husks and corn cobs are composed of mainly cellulose (~42%), (38%), lignin (~13%), (12%), ash (~4.2%), (4.5%), and other materials (~41%) (46%), respectively (Kampeerapappun, 2015).

Fig. 1. Image of Corn husk (left) and Corn cob (right)

1.4. Lupine husk

Lupine albus (Gibto), is an herbaceous plant of the leguminous family, belonging to the genus Lupinus, which comprising 450 species (Nadal *et al*., 2011). Gibto (Lupinus albus /White lupine) is a traditional crop in Ethiopia used for human and animal consumption, which grows at 1500-3000 m altitude. It is grown by small landholders in Amara and Benishangul Gumuz regions in the north-western part of the country. White lupine is locally known as Gibto and it is the predominant species produced by small scale farmers. The farmers produce the crop for its multipurpose benefits such as preservation of soil fertility, used as a green manure and for fixing atmospheric nitrogen to the soil, used as the control of some pests due to its alkaloids during the

flowering period, the nutritional value of seeds as a snack, local soup and local alcohol preparation, and for traditional therapy purposes of hypertensive patients (Azeze *et al*., 2016; Uzun *et al*, 2007). Two kinds of cultivated lupine plants are found in Ethiopia: a large-seeded type as grown in Egypt and Sudan, but also a small-seeded type with small leaves (Nigussie, 2012). Lupine is a good source of nutrients, not only proteins but also lipids, dietary fiber, minerals, and vitamins. Lupinus albus consists of Dietary fiber represents 40% of the kernel weight of white lupin which is a higher level than in most other legumes. The seed cover (hull) of Lupinus albus contains after the debittering process 89% of insoluble dietary fiber. The main component of the insoluble dietary fiber is cellulose (79%). Other ones, i.e., hemicelluloses and lignin, remain at the levels of 14 and 7%, respectively (Kohajdova *et al*., 2011).

a.  b  c. 

Fig. 2. Lupine albus (gibto) Plant (a), Seed (b) and husk(C) picture taken by Hanna Tesfaye.

1.5. Cellulose isolation methods from lignocellulose biomass

There are two effective methods used for the isolation of cellulose from lignin, hemicellulose and other extractives. The first one is the top-down approach, in which wood, cotton, annual plant or other agricultural residue can be used to produce a desired size of cellulose, and the other one is the bottom up approach, where cellulose is biosynthesized from glucose using bacteria (e.g. Acetobacter Xylinam) (Trache *et al.,* 2016).

The conversion of lignocellulosic biomass is strong and dependent not only on the biochemical composition, but also on the structural features of plant tissue. Lignocellulosic biomass

pretreatment is an essential step to increase the accessibility and quality of cellulose (Szymanska-Chargot *et al*., 2017). During the pretreatment process the compact structure of lignocellulosic biomass is disrupted and cellulose fibers are exposed. Pretreatment of the lignocellulosic material is carried out to overcome recalcitrance through the combination of chemical and structural changes to the lignin and carbohydrates (Amin *et al*., 2017).In liganocellulosic biomass, the disruption of hydrogen bonds, cross-linked matrix disruption, and increase in porosity as well as the surface area of cellulose are the primary tasks that are performed via suitable pretreatment methods. This pretreatment process can be a physical such as milling; a chemical treatment like alkali, or acids; biological pretreatment, e.g., by white-rot fungi or lignin-degrading enzymes; physicochemical pretreatment, like steam explosion; or a combination of the above two or three processes (Karimi and Taherzadeh, 2016).

Physical pretreatment enhance the accessibility to hydrolysable polymers within lignocellulosic material. In the application of physical pretreatment process pore size and surface area of lignocellulosic biomass can be increased, whereas crystallinity and DP of cellulose can be decreased. The reduction in DP and crystallinity is depending on the type of milling method adopted, processing time and also the type of biomass used. Physical pretreatment is eco-friendly, easier, and more effective pretreatment method. However, the main drawback of this pretreatment approach is the high power demand. Physical pretreatments include milling, microwave radiation, mechanical extrusion and pulse electric field (PEF) (Aftab *et al*., 2019: Baruah *et al*., 2018). Milling can be employed to alter the inherent ultrastructure of lignocelluloses and degree of crystallinity, and consequently make it more amenable to cellulose. The process of milling and size reduction have been applied prior to enzymatic hydrolysis, or even chemical and physico chemical pretreatment processes, on several lignocellulosic biomass (Taherzadeh and Karimi, 2008). There are different milling methods such as two-roll milling, ball milling, rod milling, hammer milling, vibratory milling, and colloid milling, (Baruah *et al*., 2018). Among the milling processes, colloid, vibratory and dissolver are suitable only for wet materials, e.g. wet paper from domestic waste separation or paper pulps, while the extruder, roller, cryogenic and hammer mills are usually used for dry materials. The ball mill can be used for either dry or wet materials (Taherzadeh and Karimi, 2008).

For waste materials, such as agricultural residues or any other crops and forestry residues, mechanical pretreatment is widely used among these physical pretreatments (Amin *et al*., 2017).

On the inherent ultrastructure of cellulose and degree of crystallinity, milling can be performed to render lignocelluloses more amenable to cellulases. Cellulases are enzyme that catalyze cellulose, but for the catalysis (Aftab *et al*., 2019). Microwave radiation accelerates biological, chemical, and physical processes due to heat and substantial collisions induced by the vibration of polar molecules and the movement of ions (Amin *et al*., 2017).

Chemical pretreatment is used more often than biological or physical pretreatment methods and the most effective method to get the most pure cellulose. A combination of alkali treatment, bleaching, and strong acid hydrolysis is the most common process used to isolate cellulose from the liganocellulosic biomass (Ching and Ng, 2014; Amin *et al*., 2017). Common chemicals used in chemical pretreatment methods for improving the accessibility of liganocellulosic biomass of agricultural residues are sulfuric acid, hydrochloric acid, acetic acid, sodium hydroxide, potassium hydroxide, calcium hydroxide, and hydrogen peroxide (Amin *et al*., 2017).

Alkali pretreatment involves the addition of bases like sodium hydroxide, potassium hydroxide, calcium hydroxide, aqueous ammonia and hydrogen peroxide or the combination of these to liganocellulosic biomass, leading to an increase of internal surface by swelling, a decrease of DP and crystallinity, destruction of links between hemicellulose, cellulose, and lignin and solubilize lignin, hemicellulose and other extractives like pectin (Ching and Ng, 2014; Amin *et al*., 2017; Behera *et al*., 2014). It removes acetyl group and various uronic acid substitutions in hemicelluloses that increase the accessibility of hemicelluloses and cellulose to hydrolytic enzymes. From the chemical pretreatments, alkali pretreatment provides the most effective method for breaking the ester bonds between lignin, hemicellulose and cellulose, and avoids fragmentation of the hemicellulose polymers (Behera *et al*., 2014; Ching and Ng, 2014). From alkaline pretreatment sodium hydroxide is the most popular base. Behera, and his coworkers (2014) reported that sodium hydroxide increased the hardwood digestibility from 14% to 55% by reducing the content of lignin from 24–55% to 20%.

Bleaching has the function of isolating halo cellulose from the raw cellulosic fiber. In addition to this bleaching also removes lignin and hemicellulose. Hydrogen per oxide and sodium hypochlorite are chemicals used for the bleaching process. However, hydrogen per oxide is frequently used bleaching agent because of its eco-friendly character. Sodium hypochlorite is the effective bleaching agent but it releases chlorine ions into the atmosphere (Galiwango *et al*., 2019). Otherwise, strong acid hydrolysis removes the amorphous parts of cellulose (Ching and

Ng, 2014). However, concentrated acids are not preferred because they are corrosive and to make the pretreatment economically feasible it must be recovered (Behera *et al*., 2014).

Acid pretreatment can be carried out either under concentrated acid (e.g. 30-70%) and low temperature (e.g. 40 ^{o}C) or under dilute acid (e.g. 0.1%) and high temperature (e.g. 230^{o} C) (Zheng *et al*., 2014). In this pretreatment process concentrated acids such as H_2SO_4 and HCl have also been used to treat lignocellulosic materials, however they are toxic, corrosive, and hazardous and thus require reactors that are resistant to corrosion, which makes the pretreatment process very expensive. Because of this dilute-acid hydrolysis has been successfully developed for pretreatment of lignocellulosic materials. For example most of the time sulfuric acid at concentrations below 4 %, and HCL 0.1M is used because it is inexpensive and effective (Kumar *et al*., 2009).

Physicochemical pretreatment is one of the most successful pretreatment methods. Steam explosion is one example of physicochemical pretreatment. It is a well-known technique for the pretreatment of various biomass feed stocks. During steam explosion pretreatment, lignocellulosic material is exposed to a high-pressure and temperature for a few minutes (Amin *et al*., 2017; Jonsson and Martin, 2016). It is more effective for the pretreatment of agricultural residues and hardwoods but less effective for softwoods. Due to high temperatures, this pretreatment procedure induces hemicellulose degradation and lignin transformation, thus increasing the potential for cellulose hydrolysis. The major disadvantages of steam exploration include the incomplete destruction of the lignin-carbohydrate matrix leading to the precipitation and condensation of soluble lignin components. This destroys a fragment of the xylan in hemicellulose and generates fermentation inhibitors at higher temperatures, thus making the biomass less digestible (Amin *et al*., 2017).

Biological pretreatment is mostly associated with the action of fungi (brown, white, and soft-rot fungi) and bacteria that are capable of producing enzymes to degrade lignin, hemicelluloses and polyphenols present in the liganocellulosic biomass (Behera *et al*., 2014).

Compared with physical and chemical pretreatment methods, biological pretreatment usually requires lower energy requirements, no generation of toxic compounds, no use of chemicals, and high yield of desired products and it is conducted under much milder environmental conditions so that few inhibitors, which could negatively affect anaerobic digestion, are generated (Zheng *et*

al., 2014; Behera *et al*., 2014; Vasco-Correa *et al*., 2016). However, long pretreatment time has limited the use of these processes in commercial applications (Vasco-Correa *et al*., 2016).

Most of the time biological pretreatments use ligninolytic enzyme system it is a group of oxidoreductases that are able to degrade lignin, and improving the degradation of biomass. This enzyme includes laccases and peroxidases with high redox potential that oxidize the lignin polymer directly, or by the use of low-molecular-weight organic compounds or mediators that can diffuse into the pores of cell wall and attack the structure of lignin, allowing access to holocellulose by hydrolytic enzyme (Vasco-Correa *et al*., 2016; Pointner *et al*., 2014).

1.6. Modification of cellulose

Chemical modification of cellulose has been investigated since 1800s (Jedvert and Heinze, 2017). Cellulose can adapt to a variety of its derivatives applying distinct methods. Cellulose derivatives were designed and fine-tuned to obtain certain desired properties. This was achieved by changing the network of inherent hydrogen bonds and by adding various substituents. These substituents either completely prevented spontaneous hydrogen bonding formation or created new interactions between the cellulose chains (Kampeerapappun, 2015). Several derivatives of cellulose are produced such as MCC, carboxy methyl cellulose (CMC), hydroxyl propyl methyl cellulose (HPMC) and Hydroxypropyl cellulose (HPC) (Shokri and Adibkia, 2013).

1.7. Microcrystalline cellulose (MCC)

MCC was discovered by Battista and Smith in 1955 and first marketed under the brand name Avicel in 1963 as a pharmaceutical tableting excipient (FMC, 2003; Doelke *et al*., 1995). MCC is purified, partially depolymerized cellulose prepared by treating alpha cellulose obtained as a pulp from fibrous plant material, by a different process such as reactive extrusion process, enzymes hydrolysis, steam explosion process, and acid hydrolysis process. The acid hydrolysis process is most preferred attributed to its shorter reaction time and economically feasible than other processes. The other benefits of acid hydrolysis are the ability to be used as a continuous process rather than a batch type process, limited quantity of acid consumption, the lower unit cost from less chemicals used, this process owned more fine particles of the MCC as the final

product (Carlin, 2008; Khalil *et al*., 2018). Acid hydrolysis can be performed using formic acid, phosphoric acid, nitric acid, sulfuric acid, and hydrochloric acid. However, the most commonly used acids for acid hydrolysis are sulfuric acid and hydrochloric acid. Because both hydrochloric acid and sulfuric acid have a high acid dissociation constant, they possess a superior ability to hydrolysis β-1, 4-glucosidic bond (Khaili *et al*., 2016). However, sulfuric acid significantly decreases the thermal stability of MCC (Morsyleide *et al*., 2010).

MCC is a fine (with particle sizes ranging between 30 to 50 μm in diameter), white, odorless, crystalline powder, biodegradable and composed of agglomerated porous particles, which can be isolated from cellulose and used as a suspension stabilizer and a water retainer, in the cosmetics, food, and pharmaceuticals industries (Haafiz *et al*., 2013; Mishra *et al*., 2018). In addition to this, the powdered cellulose and MCC has many applications in compounding pharmacies include the oral solid dosage form (capsules) as a bulking agent to increase the mass in formulations containing small amounts of the active ingredient. It is a base material for powder dosage forms, a suspending agent for aqueous per oral delivery and an adsorbent and thickening agent for topic preparations (Marques-Marinho and Vianna-Soares, 2013).

MCC has unique physicochemical properties such as, low density, strong mechanical properties, low/non-abrasive behavior, high reactivity, biodegradability, and renewability (Khali *et al*., 2018). MCC has strong mechanical properties such as high ductility (plastic deformation) because of the random orientation of the crystallites, low brittleness (fragmentation propensity), low elasticity (reversible deformation) due to additional inter-particle bonding, and high viscoelasticity (time-dependent behavior) (Doelker, 1993). MCC is increasingly considered as an important derivative from cellulose in the context of its potential applications in pharmaceutical, food, cosmetic, paper, and textile industries. Attributes like strength, fibrous nature, stiffness, crystallinity, lightness, biodegradability, water insolubility and renewability make MCC attractive for applications in diverse industrial fields (Kalita *et al*., 2013).

MCC is the most popular cellulose which extensively used in pharmaceutical industries. MCC grades are multifunctional pharmaceutical excipients which can be used as compressibility enhancer, disintegrating agent and binder in wet and dry granulation processes, thickener and viscosity builder in liquid dosage forms and free-flowing agents in solid dosage forms (Shokri and Adibkia, 2013). Typically, MCC isolated mainly from wood and cotton but cost has made it imperative that other materials be investigated as potential green sources (Khalil *et al*., 2018).

The rational and innovative utilization of agricultural crop residues such as corn husk, corn cob, jute, sisal, banana, and straws (rice and wheat) or non-wood (plant fibers) biomass as new sources of cellulose is of potential interest worldwide (Reddy *et al*., 2015).

In the pharmaceutical market, MCC is available under the brand names of Avicel, Emcocel, Vivacel etc. (Gohel and Jogani, 2005).

1.8. Physico-chemical Characterization of Cellulose and MCC

1.8.1. Structure of cellulose

Later, in 1920, Hermann Staudinger determined the chemical structure of cellulose (Trache *et al*., 2016). Cellulose consists un-branched β-(1,4)-D-glucose units linked together by β-1-4-glycosidic linkages, resulting in an alternate turning of the cellulose chain axis by 180°, i.e. the repeating unit of cellulose can be considered as two D-glucopyranose units, also called as cellobiose (Jedvert and Heinze, 2017; Nuruddin *et al*., 2014). Each monomer glucose unit carries three hydroxyl groups. These hydroxyl groups located at the secondary hydroxyl groups i.e. in the positions of C-2 and C-3 (anhydroglucose unit) and Primary hydroxyl groups (C-6) (CH2OH) can form intra and inter molecular hydrogen bond. These bonds can provide highly ordered three-dimensional crystalline structure, thus, these hydroxyl groups are able to form hydrogen bonds which control physical properties of cellulose (Nuruddin *et al*., 2014). The 20–300 chains of cellulosic components are bundled together to generate micro-fibrils, which are jointly grouped to form cellulose fibers (Trache *et al*., 2016).

The cellulose molecule contains three different kinds of an hydro glucose units, the reducing end with a free hemiacetal (or aldehyde) group at C-1, the non-reducing end with a free hydroxyl at C-4, and the internal rings joined at C-1 and C-4 (Khalil *et al*., 2015). The cellulose chain consists at one end of a D-glucose unit with an original C4-OH group (the non-reducing end); the other end is terminated with an original C1-OH group, which is in equilibrium with the aldehyde structure (the reducing end) (Klemm *et al*., 2005).

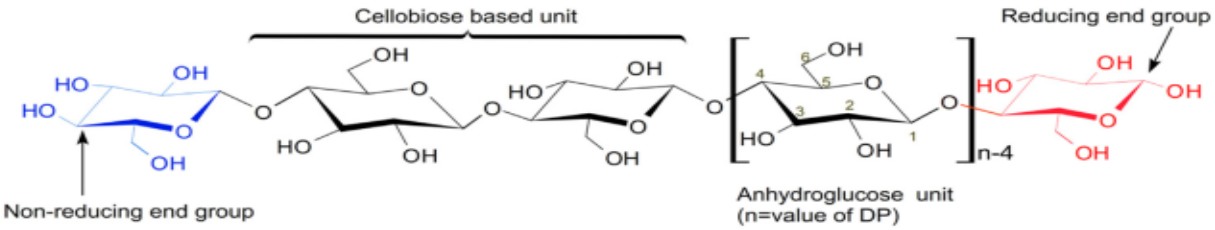

Fig. 3. Molecular structure of cellulose showing the numbering of carbon atoms, the reducing end with a hemiacetal, and the non-reducing end with free hydroxyl at C-4 (Trache *et al.*,2016).

1.8.2. Crystalline structure of MCC

There are both crystalline and amorphous regions of the cellulose micro fibrils, and the majority of cellulose (about 2/3 of the total cellulose) is in crystalline form (Taherzadeh and Karimi, 2008). These crystalline regions (cellulose crystallites) are formed by cellulose chains due to van der Waals interactions and hydrogen bonding (Trache *et al*., 2016). Depending on the various plant sources, the degree of crystallinity of the MCC products varies, and is not necessarily higher than that of the original cellulose because intensive agitation may destroy the crystal structure and short macromolecular chains are unfavorable to the formation of crystalline regions (Doelker, 1993). MCC is characterized by a high degree of crystallinity, and the values typically range between 60% and 80% (Trache *et al*., 2016).

1.8.3. Degree of polymerization (DP)

The DP is the number of glucose units $(C_6H_{10}O_5)$ n in the cellulose chain, and it can be as high as 15,000 and the individual molecules form microfibrils stabilized by hydrogen bonds (Jonson and Martín, 2016). The DP of cellulose varies with the origin and treatment of the raw materials. The DP of cellulose in wood pulp are typically 300 and 1,700, cotton and other plant fibers in the range of 800–10,000, depending on treatment process; comparable DP values are found in bacterial cellulose (Klemm *et al*., 2005). The DP of cellulose decreases exponentially as a function of acid hydrolysis conditions, which include temperature, acid concentration and time. When cellulose reacts with acid, the β (1–4) glycoside bond is attacked and the acetyl linkage is broken resulting in the hydrolysis of the chain, thus decrease the DP. The rate of hydrolysis slows to a certain level-off degree of polymerization (LODP). The LODP is a characteristic of a

particular pulp and is typically found in the 200–300 range (Thoorens *et al*., 2014; Setu *et al*., 2015). The viscometric technique is the most widely used method (the easiest and cheapest way) to access or measure cellulose DP. It needs dissolution of cellulose in a cellulose solvent, such as cuproethylenediamine, cuprammonium sulphate and cuprammonium hydroxide (Karimi and Taherzadeh, 2016).

1.8.4. Thermal analysis

Thermogravimetric analysis (TGA) and differential scanning calorimetry (DSC) are commonly used methods to investigate the thermal and degradation properties of cellulose (Trache *et al*., 2016). In line with the various treatments, TGA provides information about how the thermal stability of the material changes (Collazo-Bigliardi *et al.,* 2018). The investigation of the thermal stability is vital step to determine the application of polymers in different companies (Nwajiobi *et al*., 2019).

1.9. Application of MCC

There are several applications of MCC in food products, cosmetics, pharmaceutical, composite and packaging industries. Attributes like strength, fibrous nature, stiffness, crystallinity, lightness, biodegradability, water insolubility and renewability make MCC attractive for applications in diverse industrial fields (Kalita *et al*., 2013; Nwajiobi *et al*., 2019). MCC is used as bulking agent and fat substitute in food products such as baked foods, dairy products, desserts, frozen foods etc. It helps in enhancing mouth feel, texture and consistency of the food product. MCC is commonly used as a binder/filler, bulking agent, disintegrant, stabilizer, thickener, texturizer, and emulsifier in the pharmaceutical industry. MCC is used an excipient in almost every kind of oral dosage forms like tablets, pellets, capsules, and others, because it exhibits chemical and biological inertness and has no taste, color and odor (Kambli *et al*., 2017; Nwajiobi *et al*., 2019). Most of the time MCC is used as directly compressible excipient as filler. In addition to its use in direct compression, MCC is used as a diluent in tablets prepared by wet granulation, and for the production of spheres (Gohel and Jogani, 2005).

In recent years, there has been a great interest in producing MCC for pharmaceutical use because of its high compactness under minimum compression pressures, high binding capability, and

ability to prepare tablets that are extremely hard, stable, yet disintegrate rapidly. All the above properties make MCC particularly valuable as a filler and binder for tablet formulations prepared by direct compression (Setu *et al*., 2015). MCC can also be considered as dry binders since they improve the compactibility or tabletability (Nwajiobi *et al*., 2019).

1.9.1. Application as compressibility enhancers

More than 80 percent of all dosage forms available in the market or administered to humans are tablets. The main reason of this great popularity is the advantages of tablets over other dosage forms of pharmaceuticals. Some benefits of tablet dosage forms are ease of manufacturing, convenience dosing and greater stability than liquid or semisolid dosage forms (shokri and Adibkia, 2013). The simplest and fastest kind of tablet compression is called direct compression method in which the drug and all of other excipients are mixed and compressed, in one-stage process with proper compression force to form tablet. However, due to its poor physical properties, such as compactibility, flowability and compressibility, only a few excipients can be directly compressed into tablets. In order to determine the suitability of an excipient for direct compression, it is necessary to evaluate its functional properties, such as compactibility, binding properties, compatibility with other excipients or different drugs, distribution of particle size to provide favorable mixing condition, as well as the carrying capacity of the active pharmaceutical ingredient (Alfa *et al*., 2006). Compressibility is the capacity of the powder to deform under pressure, and compactibility is the ability to form mechanically strong compacts with low pressure (Santl *et al*., 2011). The most important functional property is compactibility, which is related to the deformation mechanism that occurs when a pressure is applied to bind particles together to form a compact. Due to its excellent compactability at low pressures, superior disintegration properties and also high dilution capacity, MCC is considered as one of the best and most useful fillers / binder (Kalita *et al*., 2013). MCC exhibits the highest capacity and compressibility of all known direct compression excipients, because of the extremely good bonding properties as a dry binder (Alfa *et al*., 2006). The compressibility and compactibility of processed MCC vary according to the source used in processing (Rojas *et al*., 2013). Avicel PH-101 has high plastic deformation following application of a minimum level of pressure which results in appreciable amount of inter particulate bonding (Alfa *et al*., 2017; Gohel and Jogani,

2005). During compression MCC plastically deforms and therefore maximizes the area of inter particle bonding of hydrogen groups. This proximity of hydrogen groups on adjacent cellulose molecules allows the formation of numerous hydrogen bonds, which account almost exclusively for the strength and cohesiveness of compacts, even under low compression forces. The tabletability of MCC enhanced by mechanical interlocking of irregularly shaped and elongated particles (Thoorens *et al*., 2014).

1.9.2. Application as Directly compressible tablet Diluents/fillers

Diluents are incorporated into tablet or capsule dosage forms to increase dosage form volume or weight, and as such they can also be referred to as fillers. MCC, the frequently used diluent and also considered as dry binders because MCC improve the compactibility or tabletability of the APIs. Good DC binders are functional even at low use levels and provide great tabletability (Thoorens *et al*., 2014).

Dilution potential is defined as the minimum amount of excipient needed in the blend with an active ingredient to form tablets of adequate compactibility and friability (<1%), or it is the amount of an active ingredient that can be satisfactorily compressed in to tablets with the given directly compressible excipient and it is one of the most crucial property in a direct compression excipients (Rojas *et al*., 2013; Gohel and Jogani, 2005).

In order for the final dosage form to have a minimum possible weight directly compressible excipients, should have high dilution potential. The dilution potential is influenced by the compressibility, compactabiliy of the APIs (Gohel and Jogani, 2005). Most of the time, dilution potential is evaluated by comparing the crushing strength versus compaction force (pressure) curves for various binary mixtures of the filler and some poorly compactible APIs, such as metrendazole, ascorbic acid and acetaminophen (Habib *et al*., 1996). MCC exhibits a high dilution potential which makes it suitable for the formulation of low dose and potent drugs (Nwachukwu and Ugoeze, 2018). Owing to its low bulk density, strong crystallinity and high compactability, MCC has a high dilution potential (up to 60%) (Habib *et al*., 1996; Gohel and Jogani, 2005).

2. SIGNIFICANCE OF THE STUDY

Commercially available cellulose and its derivatives are mainly derived from wood pulp and also purified cotton linters (Kambli *et al*., 2017). However there is a decrease in wood availability with the increasing demand for market pulp in some rapidly developing countries in Asia, Africa, and Latin America (Costa *et al*., 2015). Currently our world faces shortage of natural resources and energy, as well as worsening environmental pollution and global warming. These problems are leading to a serious crisis (Xu *et al*., 2018). This fact makes the raw materials expensive to obtain and increase the cost of cellulose and its derivatives as well (Cao *et al*., 2007).

On the other hand the accumulation of agricultural residues can leads to environmental pollution. Some farmers burning agricultural residues to alleviate this problem. However burning agricultural residues also causes environmental problems such as air pollution, soil erosion, and a decrease in soil biological activity (Kambli *et al*., 2017; Cao et al., 2007).

Cellulose and its derivatives are widely used in textile industries, papermaking and packaging industries, food industries and pharmaceutical industries. Because of these, Ethiopia import cellulose and its derivatives from foreign countries which requires large amount of foreign currency.

Finding the alternative sources of cellulose is necessary to fulfill the current demand of cellulose and its derivatives in different industrial sectors. Therefore production of cellulose from alternative sources especially from non-expensive, readily available and renewable lingo cellulosic by products is highly valuable. Thus the present study will try to investigate corn husk, corn cob and lupine husk as potential sources of cellulose and by modifying this cellulose for various pharmaceutical applications.

Therefore this research tries to answer to the following questions.

1. What is the yield of cellulose and MCC extracted from corn husk, corn cob, or lupine husk?
2. What are the physico-chemical characteristics of CH, CC, and LH cellulose and MCC?
3. What is potential application of CH-MCC, CC-MCC, or LH-MCC as a directly compressible excipient?

3. OBJECTIVES

3.1. General Objective

- To extract and characterize native and microcrystalline corn husk, corn cob, lupine husk, cellulose and evaluate MCC as directly compressible excipient.

3.2. Specific objectives

- To extract cellulose from, corn husk, corn cob, and lupine husk.
- To characterize cellulose from corn husk, corn cob, and lupine husk.
- To prepare and characterize MCC from native cellulose.
- To evaluate MCC extracted from corn husk, corn cob, and lupine husk as directly compressible excipient.

4. MATERIALS AND METHODS

4.1. Plant Materials

Three different agricultural wastes i.e corn husk, corn cob, and lupine husk was collected from Injibara, Awi Zone, Amara Region, Ethiopia.

4.2. Materials

Acetic acid (99.5%), Sodium lauryl sulphate (Sigma-Aldrich, Germany), Formic Acid (85%), Potassium Iodide, Zinc Chloride (97%), Xylene (98%, extra pure), Copper sulphate (Pentahydrate, 98.5%) (Loba Chemie Pvt. Ltd, India), Sodium hydroxide, Sulphuric acid, Nitric acid, Hydrogen peroxide, Magnesium stearate (Bulvinos Chemicals Ltd, England), Sodium chloride (99.8), Ethanol (96%) (UNI-CHEM, India), Toluene (99.5%) (Fisher Chemicals, UK) Ammonium hydroxide (28%) (Farmatalia Carlo erba reagents S.P.A/Carlo erba reagents S.A.S, France), Hydrochloric acid (37%) (BDH Chemicals Ltd, England), MCC (Avicel PH101), were used as received. Distilled water was used in the extraction and modification of cellulose. Mebendazole powder was kindly donated by Cadila Pharmaceutical Company.

4.3. Methods

4.3.1. Extraction of Cellulose from CH, CC, and LH

Cellulose was extracted following the method described by Ranganagowda *et al*., (2019) with slight modification (treat the fibers with different concentration of $H_2O_{2)}$. The raw fibers were dewaxed with toluene and ethanol (2:1) for 6 h in a soxhlet apparatus. Each fiber was taken in Erlenmeyer flask and suspended in 10% NaOH, followed by 10% H_2O_2 at a fiber to liquor ratio of 1: 20. The flask was covered by aluminum foil and maintained at 121^0c and 1.5 bars in an autoclave for 1h. Then the fiber was filtered through nylon cloth and washed thoroughly with distilled water. The delignification of autoclaved fibers was carried out by soaking them in a 1:1 (v:v) mixture of 20% formic acid and 10% H_2O_2. The mixture was maintained at a temperature of 85^oc for 2h on water bath. The fiber was filtered through nylon cloth and initially washed with

10% formic acid and repeatedly washed with distill water. The cellulose fiber extracted was light yellow in color. Bleaching of cellulose was carried out with 4%, 6%, 8% and 10% H_2O_2 and 8% NaOH for 90 min at 60°c. The white suspension obtained was filtered and washed several times with distilled water until it becomes neutral and oven dried at 50°c (KOTTERMANN 2711, Germany) until constant weight attained.

4.3.2. Preparation of MCC

MCC was prepared according to the method developed by Battista (Battista, 1950). A 2.5_N HCl was prepared and poured into volumetric flask then boiled on a hot plate. Cellulose was added to the boiling acid (1:20 fiber-to-liquor ratio) and allowed to boil for 30 min at 105°C with constant agitation (125 rpm) using magnetic rod. After completion of the reaction time, the mixture was filtered and washed with distilled water followed by 5% ammonium hydroxide solution. The filtrate was then washed repeatedly with distilled water till it became neutral. The resulting MCC was dried in air circulating oven (Kottermann® 2711, Germany) at 100 °C until constant weight was achieved. Finally, it was ground with pestle in a glass mortar and sieved through 224_µm mesh size sieve.

4.3.2.1. Determination of percent yield

The Percentage yield of Cellulose was calculated by the following formula.

$$\text{Cellulose (\%)} = \frac{\text{Weight of dry cellulose residue}}{\text{Weight of original fiber sample}} \times 100 \ \ldots\ldots\ldots\ldots\ldots\ldots\ldots\ldots\ldots\ldots\ldots.. \ (1)$$

The percentage yield of MCC was determined by the following formula.

$$\text{MCC yield (\%)} = \frac{\text{Weight of prepared MCC (g)}}{\text{Weight of prepared cellulose (g)}} \times 100 \ldots\ldots\ldots\ldots\ldots\ldots\ldots\ldots\ldots\ldots\ldots \ (2)$$

4.3.3. Hemicellulose and Lignin determination

The amount of hemicellulose and lignin in CH, CC, and LH was determined through the method proposed by Mansor *et al*., 2019. For the experimental process, 3 types of chemicals were used; Acetone, Sodium hydroxide (NaOH-0.5 mol/L), and Sulphuric acid (98 %).

4.3.3.1. Determination of the amount of extractives in biomasses

To 1 g of each fiber (corn husk, corn cob, and lupine husk) (A), 60 mL of acetone was added. The sample was boiled at 90 °C on hot plate for 2 h. The sample was then dried in an oven at 110 °C until constant weight was obtained (B). The amount of extractives was calculated with Eq. 3.

Amount of Extractives (g) = (A) - (B)……. (3)

4.3.3.2. Determination of the amount of hemicellulose in biomasses

One hundred fifty mL of Sodium Hydroxide solution (0.5mol/L) was added to 1 g of each fiber with extractives free (B). The samples were boiled at 80 °C on a hot plate for 3.5 h. After that, the sample was washed with distilled water until it is free from Na^+. The Na^+ was detected by using pH paper and the reading should be close to 7. The sample was dried in an oven at 110°C until constant weight was obtained (C). The amount of hemicellulose was calculated with Eq. 4.

Amount of Hemicellulose (g) = (B) – (C)……. (4)

4.3.3.3. Determination of the amount of lignin in biomasses

Thirty mL of 98 % Sulphuric acid was added to 1 g each fiber free from extractives (B). The sample left at ambient temperature for 24 h before boiled at temperature 100 °C controlled on a hot plate for 1 h. The mixture was filtered and the solid residue was washed by using distilled water until sulfate ion was undetectable. The sample was dried in an oven at 110 °C until constant weight was obtained (D). The final weight of residue was recorded as lignin content.

Amount of Lignin (g) = D……. (5)

4.3.4. Characterization of cellulose and MCC

4.3.4.1. Organoleptic characteristics

The color, odor, taste and physical appearance of cellulose and MCC samples from corn husk, corn cob, and lupine husk were observed.

4.3.4.2. Chemical identification test

Chemical identification test of CH-MCC, CC-MCC, and LH-MCC was performed with iodinated zinc chloride solution. Iodinated zinc chloride solution was prepared by dissolving 20 g of zinc chloride and 6.5 g of potassium iodide in 10.5 ml of distilled water. 0.5 g of iodine was then added and shaken for 15 min at room temperature. The prepared MCC powder (10 mg) was placed on a petri dish and dispersed in 2 ml of iodinated zinc chloride solution. The resulting color of MCC was observed (USP 30/NF25, 2007).

4.3.4.3. Moisture content determination

The moisture content of cellulose and MCC samples was determined as follow. In a tired weighing bottle, 2 g of sample (A) was taken. The weighing bottles carrying the sample was kept in oven at 105° ± 1 °C (4 h) for drying. After drying, it was cooled in desiccator and weighed accurately until a constant weight (B) was obtained. The moisture content was calculated by using the following formula (Kambli *et al*., 2017).

$$\text{Moisture content (\%)} = \frac{A - B}{A} \times 100 \quad \text{..... (6)}$$

4.3.4.4. Degree of polymerization

The DP is defined as the number of monomeric units in a macromolecule or polymer. DP of cellulose and MCC samples were determined following the method described elsewhere using cuprammonium hydroxide [Cu $(NH_3)_4$ $(H_2O)_2$]$(OH)_2$) solution as solvent. Cuprammonium hydroxide was prepared from freshly precipitated copper hydroxide and ammonium hydroxide solution. Initially, 28 g of $CuSO_4 \cdot 5H_2O$ was dissolved in 600 mL distilled water to which 14 mL of NH_4OH (25%) was added and the precipitate, $Cu(OH)_2$, was filtered and repeatedly washed with distilled water to make it sulfate free. The precipitate was then dissolved to 500 mL with NH_4OH (25%) to form cuprammonium hydroxide solution. Finally, certain amount of cellulose or MCC was dissolved in the freshly prepared cuprammonium hydroxide solution at 25 ^{O}C for about 5 min (Kambli *et al*., 2017; Karande *et al.*, 2011).

An appropriate volume of the solution was then transferred to Ostwald viscometer. The flow times (in seconds) of blank cuprammonium hydroxide solution (t_0) and cellulose or MCC solution (t) between the 2 marks on the viscometer were recorded and specific viscosity was determined from Eq (7).

Where, η spec = specific viscosity, $(\eta / \eta_0 - 1)$ …… (7)

(η / η_0) = relative viscosity and (η and η0 are the time (seconds) required for the sample and blank solutions, respectively, to travel from upper to lower mark. The DP value was then calculated from the specific viscosity according to Eq 7.

$$DP = \frac{2000 \times \eta spec}{c \times (1 + 0.29 \times \eta spec} \quad \text{…..……. (8)}$$

Where 'c' is concentration (in g/L) of cellulose or MCC, and 0.29 is viscometer constant. Average viscosity molecular weights of cellulose and MCC samples were determined as product of their respective DP value and the molecular weight of monomer units (162g/mole).

4.3.4.5. Density and related property of MCC

I. Bulk and tapped density

To determine the bulk density of the MCC, 30g of MCC powder was accurately weighed and poured into 250 ml of clean, dry graduated measuring cylinder. The cylinder was stopped and the bulk density D bulk was recorded without tapping it. Then the D bulk was calculated by dividing weight by volume of the powder CH-MCC, CC-MCC, and LH-MCC samples.

$$D\ bulk = \frac{W}{V_0} \quad \text{……... (9)}$$

To determine tapped density (D tap) of MCC, The bulk in the cylinder was tapped 500 times using tapping densitometer (ERWEKA, Germany) to a constant volume (i.e., until no more settling of powders occurred) and the final or constant volume was recorded as tapped volume. Tapped density was then calculated based on the ratio of weight to tapped volume.

$$D\ tap = \frac{W}{V_1} \quad \text{……. (10)}$$

II. True density

True density of the CH-MCC, CC-MCC, and LH-MCC powder was determined by specific gravity bottled method using xylene was displacement liquid according to the method described by Nwadiogb et al., (2015) and Kambli et al., (2017). A cleaned glass bottle was filled with xylene followed by wiping off all spilled over xylene with a tissue paper and then its weight was noted (a). The same bottle was emptied and cleaned thoroughly, and then 2 g of MCC powder was added into it. The weight of the MCC powder was noted as (w). The bottle was then half filled with xylene, stirred with glass rod to release air bubbles and was allowed to stands for 10 min. Finally the bottle was completely filled with xylene and the weight of bottle was noted as (b). True density of MCC was calculated using the following equation,

$$Dt = \frac{W}{[(a+w)-b]\times S} \qquad (11)$$

Where, Dt is the true density of MCC and the specific gravity of xylene, S = 0.86.

III. Carr's Index and Hausner's Ratio

Carr's index is the percentage compressibility index was determined as the difference between tapped and bulk density to the tapped density times 100.

$$\text{Carr's Index} = \frac{\text{Tap density} - \text{bulk density}}{\text{Tap density}} \times 100 \qquad (12)$$

Hausner's ratio is the ratio of tapped density to bulk density. It was calculated using the equation given below.

$$\text{Hausner's Ratio} = \frac{\text{Tap density}}{\text{Bulk density}} \qquad (13)$$

IV. Porosity

The porosity of MCC Powders (E) was calculated from the values of the bulk and tapped density, by using the formula stated by Kambli *et al.*, 2017.

$$E = 1 - \frac{Db}{Dtrue} \qquad (14)$$

Where, Db is bulk density, Dtrue is true density of MCC.

4.3.4.6. pH determination

One g of the powder sample was shaken with 50 ml of distilled water for 5 min and the pH of the supernatant liquid was determined using a pH meter (Kambli *et al*., 2017).

4.3.4.7. Water soluble substances

Two g of the sample in 32 ml of water was shaken for 10 min and filtered using filter paper. The filtrate in a tarred beaker was evaporated to dryness, dried at 100–105°C for 1 h and weighed. The amount of water soluble substance was the difference between the weight of beaker along with residue and the weight of empty beaker. The experiment was performed in triplicates and the average of three determinations taken (Kambli *et al*., 2017).

4.3.4.8. Ash value determination

With American Society for Testing and Materials (ASTM (E 1755-01)) test method, the ash content in the sample was determined. The sample was placed in a crucible and accurately weighed. The sample was carbonized by igniting over the Bunsen flame. After carbonization, the crucible was transferred to a muffle furnace along with the sample. Ashing was done at 575 ± 25 °C, till it attained a constant weight (Kambli *et al*., 2017).

4.3.4.9. Particle Size Analysis

The particle size and particle size distribution of MCC from corn husk, corn cob, and lupine husk were determined with laser diffraction particle-size analyzer (Mastersizer 2000, Malvern Instruments Ltd, and Worcestershire, WR14 1XZ, UK). The analysis was done under the following conditions: Range (0.05–900 µm, 300RF); active beam length (2.4 mm); sample unit (MS1: Small Volume Sample Dispersion Unit); Polydisperse; standard-wet, Presentation (3OHD). Small amount of MCC powder was dispersed in the dispersion media i.e. distilled water till obscurity becomes 0.20. The result was compared to Avicel PH 101. The test was repeated using Avicel PH 101 as a reference (Suryadi *et al*., 2018).

4.3.4.10. Moisture sorption capacity

One g of CH-MCC, CC-MCC, LH-MCC and Avicel PH-101 powders were weighed accurately and distributed evenly over the petri dish. A large desiccator containing distilled water in its reservoir (RH = 100%), saturated solution of NaCl (RH=75.6 and RH= 80), and NaOH (RH= 20 and RH=40) was used to place the samples in the desiccator at room temperature. The weight gained was recorded at 4 weeks equilibrated. Water sorption capacities of the MCC samples were expressed as percent moisture uptake. Results were expressed as a mean of three parallel determinations. The weight difference was used to calculate the amount of water absorbed with the following equation,

$$\text{Moisture sorption capacity} = \frac{W2-W1}{W1} \times 100 \quad \ldots\ldots (15)$$

Where W1 is the weight of the sample before exposure and W2 is the weight of the sample after exposure (Greenspan, 1977; Mihranyan *et al*., 2004).

4.3.4.11. Fourier transform infrared spectroscopy (FTIR)

Perkin Elmer Fourier Transform Infrared Spectrophotometer (L1600400 Spectrum TWO DTGS, SN: 108152, LIantrisant, UK) was used to study the functional groups and chemical structure of CH-C, CC-C, LH-C, CH-MCC, CC-MCC, LH-MCC and Avicel PH-101 in the frequency range of 4000 – 400 cm^{-1}.

4.3.4.12. X-ray Diffraction (XRD)

The crystalline structure of cellulose and MCC from CH, CC, and LH were analyzed by XRD-7000 X-ray diffractometer MAXima (SHIMADZU Corporation, Japan) at 40 KV. The crystallinity index was calculated according to equation (16).

$$CI = \frac{Ic(002)-I(am)}{Ic(002)} \times 100 \quad \ldots\ldots (16)$$

Where: Ic is crystallinity index (%); I (002) is maximum diffraction peak intensity which represents the crystalline material; and I (am) is minimum intensity of the diffraction peak that represents the amorphous material.

Crystal size was estimated using the Scherrer equation (17)

$$L = \frac{0.94 \times \lambda}{\beta_{1/2} \times \cos\theta} \quad \ldots\ldots (17)$$

Where, L is the crystal dimension (in nanometers) perpendicular to the diffracting planes with Miller indices of hkl, λ is the wavelength of X-ray radiation (λ = 1.542Å), Scherrer constant (K = 0.94) represents the shape factor (depends on the shape of the crystallites), β1/2 is the full width at half maximum (FWHM) of the diffraction peaks, in radians, at a height half-way between background and the peak maximum, and θ is half of the (002) Bragg diffraction peak position (2θ max position) (Trache *et al*., 2014).

4.3.4.13. Scanning electron microscopy (SEM)

The morphological analysis of the isolated celluloses, MCCs and Avicel PH-101 were analyzed with scanning electron microscope, under vacuum conditions and at a voltage of 20 kV. All images were taken at magnifications of 200, 500 & 1000X.

4.3.4.14. Thermo gravimetric analysis (TGA)

The thermal stability of the CH-MCC, CC-MCC, LH-MCC, Avicel PH-101, CH-C, CC-C, and LH-C was determined by TGA measurements performed by DTG (Differential Thermo Gravimetry)-60H (SHIMADZU Corporation, Japan). All measurements were performed under a nitrogen atmosphere with a gas flow of 60 mL/ min by heating the material from room temperature to 700 ◦C at a heating rate of 10 ̊C /min.

4.3.5. Preparation and Evaluation of MCC tablets

Before evaluation of the crushing strength, tensile strengths, friability and disintegration time tablets were allowed for 24 h post compression relaxation time.

4.3.5.1. Preparation of microcrystalline cellulose tablets

To study the compressibility and compactability of CH-MCC, CC-MCC, and LH-MCC plain tablets, CH-MCC, CC-MCC, LH-MCC, and Avicel 101 powders were compressed at different

compression forces. Plain tablets were compressed at crushing strength of 50_N, 75_N, 100_N, 125_N and 150_N with (Eco Press200 India) tablet compression machine. Avicel PH-101 was used to adjust the desired compression force. Because of poor flow properties, 200 mg of the powder was individually weighed and manually filled into the tablet press through the hopper to give the targeted weight.

To study the dilution potential of CH-MCC, CC-MCC, and LH-MCC, binary mixtures of 200mg of mebendazole and excipients were prepared in the ratios 1:1, 1:2, 1:3 and 1:4 as reported by Eraga, *et al*. (2015). These mixtures (CH-MCC, CC-MCC, LH-MCC and Avicel PH101 mixed with mebendazole) were prepared in Turbula® mixer (Willy A. Bachofen AG, Maschinefabrik, Basel, Switzerland) for 10 min. Mebendazole tablets were prepared using tablet compression machine (Eco Press200, India) at a constant compression force (adjusted to achieve between 4-10KN) crushing strength for the standard Avicel PH-101 using flat punches of diameter 8.6 mm.

Lubricant sensitivity of CH-MCC, CC-MCC, LH-MCC, and Avicel PH-101 were evaluated following the method described by Rojas *et al.* (2013). Binary blends of excipient : lubricant (99.5%:0.5%) were prepared in a Turbula® mixer (Willy A. Bachofen AG, Turbula® 2TF, Basel, Switzerland) for 5 min. Lubricated and unlubricated compacts (200 mg) of 8.6 mm in diameter were compressed with a rotary tablet compression machine at constant compression pressure adjusted to give plain Avicel PH-101 tablets with a hardness of 100 N.

4.3.6. Evaluation of tablets

4.3.6.1. Drug-MCC compatibility studies

The compatibility study of mebendazole and CH-MCC, mebendazole and CC-MCC, mebendazole and LH-MCC, and mebendazole and Avicel PH- 101 (at a mixture of 1:1 ratio) was checked in their FTIR spectra taken with PerkinElmer Fourier Transform Infrared Spectrophotometer (L1600400 Spectrum TWO DTGS, SN: 108152, LIantrisant, UK) in the frequency range of 4000 – 400 cm ˉ1.

4.3.6.2. Lubricant sensitivity

The lubricant sensitivity test (LST) was carried out with tablets containing LH-MCC, CH-MCC, CC-MCC, and Avicel PH-101 compressed with and without fixed concentration of magnesium stearate at fixed compression force.

The lubricant sensitivity was expressed as the lubricant sensitivity ratio (LSR)

$$LSR = \frac{So - S_{lub}}{So} \quad \ldots\ldots (18)$$

Where, So is compact crushing strength without lubricant, and Slub is compact crushing strength with added lubricant.

4.3.6.3. Weight and thickness

From each batch, randomly selected twenty tablets were weighed individually on the analytical balance and the average weight and standard deviation was calculated. Tablet thickness and diameter (fixed 8.6 mm) were measured a sliding caliper scale (Nippon Sokutei, Japan).

4.3.6.4. Crushing strength test

The crushing strength of the tablets was determined after 24 h of compression (time for stress relaxation of compression) using an electronic hardness tester (Caleva Model THT2, England). Ten tablets from each batch were used for the hardness test. Each of the tablets to be tested was placed between the spindle and the anvil then applied the pressure. Then the value of the individual tablet was recorded and the average and standard deviation of ten tablets was used to determine the crushing strength of the tablets.

4.3.6.5. Tensile Strength

The dimensions of the tablets were measured with a digital vernier caliper. The crushing strength was determined after 24 h of compression (time for stress relaxation), using an electronic hardness tester (Caleva Model THT2, England). From the values of the diameter (D, cm), thickness (L, cm), and crushing strength (F, kg), the tensile strength (T, MPa) of the tablets was calculated the following equation (Chauhan *et al*., 2016).

$$T = \frac{2F}{\pi.D.L} \quad \text{..... (19)}$$

Where F is the maximal force recorded (crushing strength), D the tablet diameter and h its thickness.

4.3.6.6. Friability test

The weight of ten tablets was determined on an electronic balance. The tablets were then placed in the drum of a Friability tester (ERWEKA, TAR 20, Germany), revolving at 25 rpm for 4 min. After 4 min, the tablets were brought out, de-dusted and reweighed. The weight was then recorded and friability calculated as percentage loss in weight (Eraga *et al*., 2015).

4.3.6.7. Dilution potential

The dilution potential of CH-MCC, CC-MCC, and LH-MCC was evaluated using the poorly compressible model drug mebendazole (Chauhan *et al*., 2016).

4.3.6.8. Disintegration test

The disintegration test was performed using (ERWAKA, DT504, Germany) Disintegration tester; six tablets were placed in the tube of USP disintegration test apparatus. The assembly was suspended in the beaker with 900 ml distilled water as medium at 37 ± 2ºC at 50 rpm. The time required to disintegrate for each tablet was measured.

4.3.6.9. Construction of calibration curve of Mebendazole

A stock solution containing 100 µg/ml of mebendazole in 0.1M HCL containing 1% sodium lauryl sulfate was prepared. Different volumes of stock solutions were taken and then diluted to provide nine different concentrations (1, 2, 3, 4, 5, 6, 7, 8 and 9 µg/ml) of Mebendazole in 0.1M HCL containing 1% sodium lauryl sulfate. The UV absorbance readings of these solutions were measured at 260 nm using UV/Visible spectrophotometer (UV/VIS Spectrophotometer, T92+, PG instruments limited). 0.1M HCL containing 1% sodium lauryl sulfate was used as a blank solution.

4.3.6.10. In vitro drug release studies

The dissolution profiles of the Mebendazole tablets were determined using the BP paddle method for the various batches of the tablets (Caleva ST7, G.B. Caleva Ltd., Dorset, UK). A dissolution medium of 900 mL of 0.1_M HCl containing 1% sodium lauryl sulphate solution maintained at (37 ± 0.5) °C with a paddle revolution of 50 rpm was used. A 5 mL volume of dissolution fluid was withdrawn at 5, 10, 15, 20, 30, 45, 60, 120 min time intervals and replaced with an equivalent volume maintaining the sink condition at the same temperature (37 ± 0.5) °C of the dissolution medium. The samples were filtered and diluted with an equal volume of 0.1 M HCl containing 1% sodium lauryl sulphate. This was continued for 120 min. The absorbance of the resulting solutions was measured spectrophotometrically at λmax of 260 nm (UV/VIS Spectrophotometer, T92+, PG instruments limited, Germany). The percentage drug released at each time interval was determined the equation from the standard calibration plot obtained for the pure drug. A minimum of triplicate determinations were carried out for all experiments and the results were reported as mean ± SD.

4.3.7. Statistical Analysis

The statistical analysis was carried out using Analysis of Variance (ANOVA) with statistical software Origin 2019 (OriginLab™ Corporation, USA). Tukey multiple comparison test was used to compare the individual difference in the physicochemical and tablet properties of the MCC. At 95% confidence level, p values less than or equal to 0.05 were considered statistically significant.

5. RESULTS AND DISCUSSION

5.1. Extraction conditions of cellulose, and MCC

During the preliminary study, six different pretreatment methods i.e., (NaOH pretreatment method, H_2SO_4 pretreatment method, Acetic acid- nitric acid mixture pretreatment method, steam explosion pretreatment method, NaOH with glacial acetic acid pretreatment method and steam with NaOH and H_2O_2 pretreatment method) were used for cellulose isolation from corn husk, corn cob and lupine husk. Among those steam with NaOH and H_2O_2 pretreatment method was the most effective one according to the yield and organoleptic property (Ranganagowda *et al*., 2019). Organoleptically, the corn husk, corn cob, and lupine husk cellulose extracted using steam with NaOH and H_2O_2 pretreatment were white and fibrous materials (Figure 4 a, b, and c).

Fig.4. Cellulose extracted from corn husk(a), corn cob(b),lupine husk(c),and MCC from corn husk(d),corn cob(e),and lupine husk(f)

Steam pretreatment removes the major part of the hemicellulose from the lignocellulosic biomass and makes the cellulose more susceptible (Ibrahim *et al*., 2011). According to Ranganagowda et al., (2019) the high energy steam produced in an autoclave during the pretreatment process support the diffusion of sodium hydroxide and hydrogen peroxide for partial oxidation and dislocated the hemicellulose and lignin fibers arrangement.

Hydrolysis of the different kinds of pulps for the preparation of MCC was carried with either sulfuric or hydrochloric acids. The hydrolysis of cellulose by strong acid leads to the degradation of the glycosidic bonds of cellulose chains and produced the more crystalline form of cellulose. The preparation of CH-MCC, CC-MCC, and LH-MCC was derived from 0.1M of HCL acid hydrolysis of the α-cellulose prepared from CH, CC, and LH through pulping and bleaching process. The obtained CH-MCC, CC-MCC, and LH-MCC were white, tasteless, and odorless, which was similar to commercial-MCC (Avicel PH 101) (Figure 4 d, e, f).

5.1.1. Yield of Cellulose and MCC

The yield of cellulose and MCC extracted from corn husk, corn cob and lupine husk were 42%, 33%, and 36% respectively and the yield of CH-MCC (80%), CC-MCC (76%), and LH-MCC (78%). The yields of CH-C and CC-C were comparable to the values reported by Kampeerapappun, (2015) 40%, and 38%, respectively.

Compared to the other biomasses, such as MCC prepared from Luffa cylindrica fiber (60.69 %) and jute (48 %), the yields of CH-MCC, CC-MCC, and LH-MCC were greater (Jahan *et al.*, 2010). In spite of that, the yields of CH-MCC, CC-MCC, and LH-MCC were lower than MCC from Sorghum caudatum (83%), MCC from Sacred Bali bamboo (83.4%), MCC from cotton (85%), MCC from cotton linter (99.8%), MCC from Flax fibres (97.9%) (Khali *et al*., 2018; Leppanen *et al*., 2009; Ohwoavworhua and Adelakun, 2010; Haque *et al*., 2015). Different researchers believed that the differences in MCC yields were most probably influenced by the sources of raw materials and their processing methods (Khali *et al*., 2018; Leppanen *et al*., 2009; Trache *et al*., 2014). The results indicate that corn husk, corn cob, and lupine husk fiber is promising potential source of cellulose and MCC.

5.2. Composition of the untreated plant materials and physical properties of cellulose and MCC

5.2.1. Hemicellulose and lignin determination

The amount of extractives, hemicellulose and lignin in corn husk, corn cob, and lupine husk are shown in Table 1.

Table 1. The amount of extractives, hemicellulose and lignin from corn husk, corn cob and lupine husk.

	Corn husk	Corn cob	Lupine husk
Amount of extractives (%)	15	20	19
Amount of hemicellulose (%)	23	28	18
Amount of lignin (%)	20	19	27

As can be seen in table 1, lupine husk contains higher amount of lignin and lower amount of hemicellulose compared to corn husk, and corn cob. Corn cob exhibits high amount of hemicellulose and low amount of lignin.

5.2.2. Organoleptic characteristics

The organoleptic properties of the prepared CH-C, CC-C, LH-C and CH-MCC, CC-MCC and LH-MCC samples fulfilled USP/NF specification (USP 30/NF 25, 2007). All the prepared cellulose and microcrystalline cellulose were white, odorless and tasteless, and the physical appearances of cellulose are fibrous and MCC are fine powders.

5.2.3. Identification test results

The result of the identification test of CH-C, CC-C, LH-C, CH-MCC, CC-MCC, and LH-MCC was in agreement with (USP 30/NF 25, 2007) specifications. In the iodinated zinc chloride solution, the color of both cellulose and MCC changed to violet-blue. According to USP 30/NF 25 (2007), the color of cellulose and MCC must be violet-blue in iodinated zinc chloride solution.

5.2.4. Degree of polymerization (DP)

The DP of cellulose depends on the method of isolation. The DP of cellulose samples is usually determined from intrinsic viscosities of solutions of cellulose in cupper-ammonium hydroxide solution (Setu *et al*., 2014). It is used as an identity test for cellulose and MCC, as pharmacopoeial MCC is defined by a DP below 350 glucose units, compared to DPs in the order of 10,000 units for the native cellulose (Kambli *et al*., 2017).

The DP and molecular weight of CH-C, CC-C, LH-C and CH-MCC, CC-MCC, LH-MCC and Avicel PH-101 are presented in Table 2. The DP values of cellulose and MCCs are in the range of the values that are mentioned in different literatures. According to various publications in the literature the DP of cellulose ranges from 500-2249 and the molecular weight is also ranges from 81,000-364,340 g/mol (Liu *et al*., 2006; Mishra *et al*., 2018; Lida *et al*., 1997).

The DP of cellulose decreased with temperature while crystallinity increased, indicate hydrolysis occurred in amorphous regions of cellulose and also any kind of pretreatment method decreases the DP of cellulose (Lida *et al*., 1997; Mishra *et al*., 2018).

The DP of corn husk cellulose and MCC were found to be 735.73 and 303.3 respectively. This result was in accordance with the pharmacopeial specification of MCC (< 350) and it was slightly higher than that reported by Kambli *et al*., (2017) the DP of MCC prepared from corn husk fiber was 282. However, the DP of CH-MCC, CC-MCC, and LH-MCC was lower than the result reported by Pachuau *et al*. (2019), the DP of MCC from Ensete glaucum was reported to be as 323.

Table 2. DP and molecular weight of CH-C, CC-C, LH-C, CH-MCC, CC-MCC, LH-MCC and Avicel PH-101.

Samples		DP	Molecular weight (g/mol)
Cellulose	CH-C	735.73	119,188.26
	CC-C	667.29	108,100.98
	LH-C	576.75	93,433.5
MCC	CH-MCC	303.3	49,110.3
	CC-MCC	315.15	51,078.6
	LH-MCC	272.65	44,169.3
	Avicel PH-101	247.86	40,153.32

5.3. Densities and related properties of MCC

5.3.1. Bulk density and tapped density

A powder 's capacity to flow from its hopper into the die cavity of a rotary compression tablet machine is estimated by bulk density, while tap density is determines how well it can be packed into a confined space on repeated packing. Powder that has high bulk and tap density indicates good flow property (Kambli *et al*., 2017; Nwajiobi *et al*., 2019). Hence, as MCC prepared has low packing density, it can be considered non-free-flowing powders (Doelker *et al*., 1987).

All MCC samples exhibited low value of bulk and tapped densities. The bulk density of CH-MCC, CC-MCC, LH-MCC, and Avicel PH-101 are 0.19, 0.27, 0.3, and 0.33 g/cm^3 respectively. This shows that the bulk density of LH-MCC is comparable to that of Avicel PH-101 which might be attributed to small particle size and low moisture content (Nwajiobi *et al*., 2019). The bulk density of LH-MCC is comparable to the bulk density reported for African breadfruit seed hull MCC (0.33 g/ml) (Nwajiobi *et al*., 2019), and higher than *Sorghum caudatum* (0.27 g/ml) (Ohwoavworhua and Adelakun, 2010). On the other hand, corn husk has the lowest bulk density than corn cob, lupine husk and Avicel PH101. This may be due to the sources of the plant origin. Zuliahani et al., (2016), reported that MCC of cotton stalks had significantly higher tapping and bulk densities than rice straw and sugarcane bagasse. This may be due to the presence of the large amounts of pith (non-fibrous materials). MCC with low bulk density have a higher dilution potential and may improve the poor tableting properties of active pharmaceutical ingredients (Thoorens *et al*., 2014; Nwajiobi *et al*., 2019). Crystallinity, moisture content and particle size may influence the bulk and tap density of MCC. However, bulk and tapped densities are not significantly affected by acid concentration and acid type during hydrolysis (El-Sakhawy and Hassan, 2007; Zuliahani *et al*., 2016). According to Zuliahani et al., (2016), report the bulk densities of rice husk treated with 1M HCl, 2M HCl, 1M HNO_3 and 2M HNO_3 were 0.34, 0.36, 0.29 and 0.32 g/cm^3 respectively and the tapped densities of rice husk treated with 1M HCl, 2M HCl, 1M HNO_3 and 2M HNO_3 were 0.56 g/cm^3, 0.53 g/cm^3 0.48g/cm^3 and 0.48 g/cm^3 respectively.

5.3.2. True density

The true density indicates the crystallinity state of the material when determined in a non-polar liquid. High true density indicates high crystallinity of the powder material (Nwajiobi *et al* 2019), as the degree of crystallinity of MCC increases the true density of MCC also increases. The true density of 100% crystalline natural cellulose is between 1.582 and 1.599 g/cm^3. However, the crystallinity of MCC is substantially less than 100%; the true density of MCC is expected to be lower than 1.582 g/cm^3 (Sun, 2005). The true density value of CC-MCC (1.336g/ml) < CH-MCC (1.368g/ml) < LH-MCC (1.41g/ml) < Avicel PH 101 (1.46g/ml). This indicates the crystallinity index of the MCC is directly related to the true density value. The crystallinity index of Avicel PH-101 is greater than LH-MCC greater than CH-MCC greater than CC-MCC.

According to Sun's, (2008) report, the true density of MCC is affected by the moisture content. The true density of MCC increases initially with increasing moisture content up to 3.3%. This may be due to anti-plasticization effects of water on amorphous polymers. This effect of water resulted in reduced free volume of MCC with increasing water content, corresponding to the increasing true density. Between 3.3% and 5.1% moisture content, true density of MCC remains constant. However, at higher moisture contents (5.1–9.0%), true density decreases because the moisture is more than 5% the weight gain of MCC decreased, which also reduces volume (Sun, 2005).

5.3.3. Carr's index and Hauser's ratio

Carr's index and Hausner's ratio are indirect measures of powder compressibility and flowability respectively. The Hausner's ratio indicates inter particle friction and measures cohesion between particles and Carr's index measures the compressibility of the powder (Kambli *et al*., 2017; Haque *et al*., 2015).

The Carr's index values stated in different pharmacopeias indicates that the material's flow properties range from 5 to 15 (excellent), 12 to 16 (good), 18 to 21 (fair), 23 to 25 (poor) and 33 to 38 (very poor) (Nwajiobi *et al*., 2019). HR values 1.00-1.11, 1.12-1.18, 1.19-1.25, 1.26-1.34, 1.35-1.45, 1.46-1.59, and > 1.6 represent excellent, good, fair, passable, poor, very poor and very, very poor flow properties, respectively (USP <1174>, 2016).

The Carr's index of CH-MCC, CC-MCC, LH-MCC and Avicel PH-101 was 29.63, 28.95, 26.86, and 23.26 respectively, and the Hauser's ratio of CH-MCC (1.42%), CC-MCC (1.4%), and LH MCC (1.36). This indicates that the flow property of each of CH-MCC, CC-MCC, and LH-MCC is poor. However, the HR of Avicel PH101 (1.3%) indicates that Avicel PH-101 has passable flow property. The high values of Carr's index and Hausner's ratio indicate that increased inter particulate friction between the particles (Umeh *et al*., 2014). Hydrolysis cannot influence the value of CI and HR value. On the other hand, CI and HR values are strongly influenced by the morphology of the sample. According to Krivokapic et al., (2020) wheat straw hydrolyzed with 64% H_2SO_4 for 1 h and wheat straw hydrolyzed by 64% H2SO4 for 2 h have higher Carr's index value. It can be assumed that both samples are highly compressible powders. This is because of the rod-like particle morphology of MCC samples which causes dense packing of particles during tapping.

5.3.4. Porosity

Porosity is inter- and intra- void spaces of particles. The space between particles is referred to as void and the volume occupied by this void is called void volume (Nwajiobi *et al*., 2019). Porosity may be influenced by bulk, tapped and true densities of powder. The porosity of CH-MCC, CC-MCC, LH-MCC and Avicel PH-101 is 86, 81, 79, and 77%; attributed to the bulk and tap densities of Avicel PH-101 which are greater than LH-MCC greater than CC-MCC greater than CH-MCC. As the powder bulk and tap densities increased, the porosity of the powder decreased (Rojas *et al*., 2013).

Table 3. Densities and related properties of CH-MCC, CC-MCC, LH-MCC, and Avicel PH-101

Parameters	CH-MCC	CC-MCC	LH-MCC	Avicel PH 101
Bulk density (g/ml)	0.19	0.27	0.3	0.33
Tap density (g/ml)	0.27	0.38	0.41	0.43
True density (g/ml)	1.336	1.368	1.41	1.46
Carr's index	29.63	28.95	26.86	23.26
Husner's ratio (%)	1.42	1.4	1.36	1.3
Porosity (%)	86.0	81.0	79.0	77.0

5.4. Moisture sorption capacity

The moisture sorption capacity is a measure of the moisture sensitivity of the powder material. Moisture sorption can occur either on the surfaces or in the bulk of a material. In the case of cellulosic materials moisture sorption is predominantly occurring in the bulk of disordered regions (Mihranyan *et al*., 2004). Ohwoavworhua, and Adelakun (2010) reported that the crystalline portion of cellulose does not adsorb water and that the extent of water adsorption by cellulose should thus be proportional to the amount of the amorphous cellulose present.

The study of moisture sorption capacity of MCC is important because it reflects the relative physical stability of tablets during storage under humid condition (Khalil *et al*., 2018). Figure 5 shows the moisture absorption capacities of CH-MCC, CC-MCC, LH-MCC and Avicel PH-101 at different relative humidity (RH) (20, 40, 75.5, 80, and 100 %) for one month.

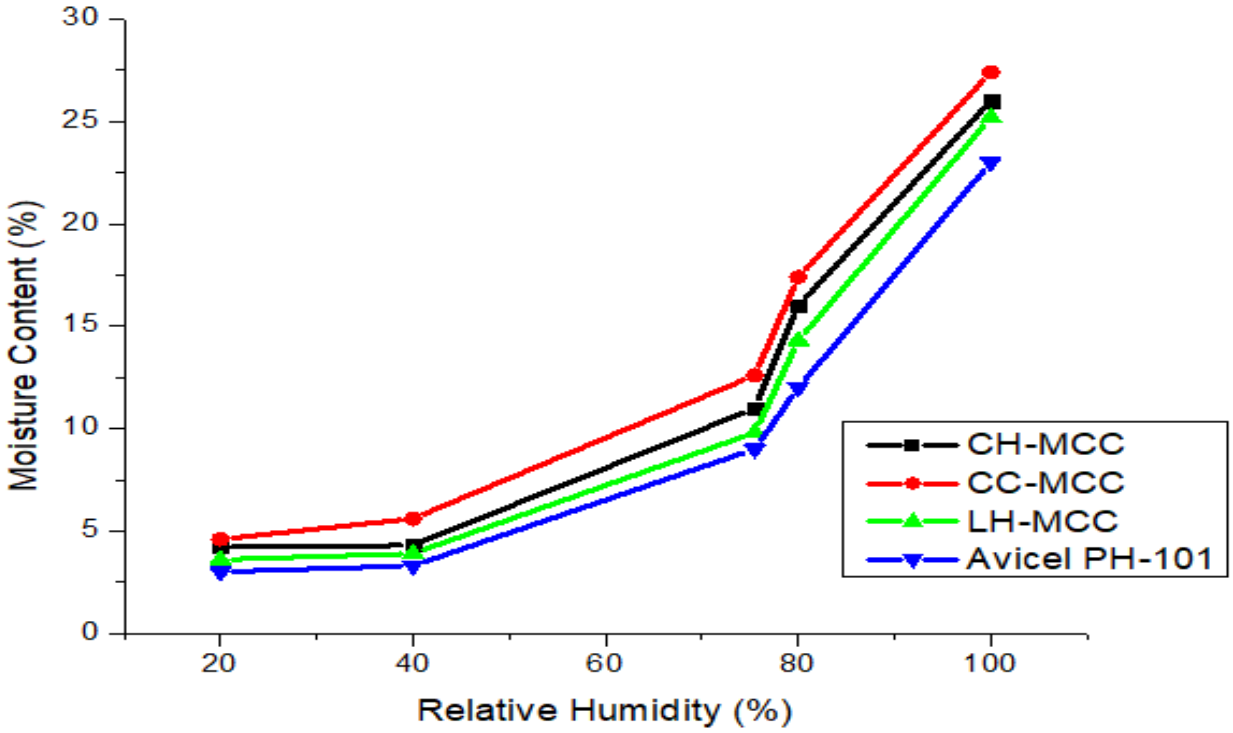

Fig. 5. Moisture sorption pattern of CH-MCC, CC-MCC, LH-MCC, and Avicel PH-101 at room temperature

As shown in Fig.5, moisture uptake of all MCC powders slightly increases with increase in RH. The moisture sorption capacity of Avicel PH-101 and LH-MCC are lower than those of CH-

MCC and CC-MCC. This is due to high crystallinity index of Avicel PH-101 and LH-MCC (Greenspan 1977; Mihranyan *et al*., 2004). Higher moisture sorption of the CC-MCC and CH-MCC indicates a possible higher susceptibility to moisture during storage and this induces change in quality. Therefore, MCC prepared from corn cob, or corn husk requires good control of moisture as compared to Avicel PH-101 and LH-MCC.

5.5. Ash value, pH, moisture content and water soluble substances of MCC

The total Ash content, of MCC is important to assess the purity, and it indicative of that the inorganic compounds that are available in the sample (Ohwoavworhua and Adelakun, 2010). The ash value of MCC from corn husk was found to be 0.04%, which is in agreement with the value reported by Kambli et al., (2017) the ash content of MCC from corn husk fiber was 0.05%. According to USP/NF specification the ash content of MCC should not be more than 0.1% (USP 30/NF 25, 2007). The total ash content obtained from CH-MCC, CC-MCC, and LH-MCC were very low. This indicates that all samples of MCC are nearly free of inorganic compounds.
The PH and water soluble substances that are present in all samples of MCC were within the acceptable range stated in USP/NF, PH 5-7 and water soluble substances not more than 0.2% (USP 30/NF 25, 2007).

The moisture content is the most important parameter that affects the mechanical and flow properties of MCC during manufacturing. Compaction properties, tensile strength, and viscoelastic properties are the mechanical properties of MCC that are influenced by moisture content. Water molecules within the pores of MCC may act as an internal lubricant, reduce frictional forces between the particles, reduces the adhesion between the tablet and the die wall, and facilitate slippage and plastic flow within the individual microcrystals (Thoorens *et al*., 2014: Abu-Thabit *et al*., 2020).The moisture content of CH-MCC, CC-MCC, LH-MCC and Avicel PH-101 was determined by drying MCC at 105 ^{o}C for 3 hours and expressed as percent loss of drying. The percent loss of drying of CH-MCC, CC-MCC, LH-MCC, and Avicel PH-101 is 5.5, 5.2, 5 and 4 %, respectively. The moisture content of all MCC powders are within the range of USP specification should not exceed 7 %. The loss of drying obtained in this study was found almost similar compared with loss of drying value obtained for Sacred Bali Bamboo 4.5% (Khalil *et al*., 2018; Thoorens *et al*., 2014). MCC used in pharmaceutical industry should have

low moisture content because the presence of high molecules of water could act as plasticizers by altering the mechanical properties of the MCC, resulting in lower tablets hardness (Khalil, *et al*., 2018).

Water soluble substances of CH-MCC, CC-MCC, and LH-MCC were within the range of British Pharmacopeia specification < 0.25% (BP, 2009). This may be due to the absence of traces sugar components of hemicellulose (Nwajiobi *et al*., 2019).

Table 4. Ash value, pH, moisture content and water soluble substance of CH-MCC, CC-MCC, LH-MCC and Avicel PH-101

Test	CH-MCC	CC-MCC	LH-MCC	Avicel PH 101	Standard as per USP/NF
PH	5.5±0.2	5.67±0.21	6.3±0.28	6.2±0.3	5-7
Ash (%)	0.04	0.02	0.028	0.06	Not more than 0.1
Moisture content (%)	5.5	5.2	5	4	Not more than 7
Water soluble substances (%)	0.08±0.2	0.05±0.19	0.04±0.12	0.09±0.2	Not more than 0.25

5.6. Particle size analysis

The particle size distributions (normal particle size distribution curve and cumulative percent particle size) of the various MCCs are depicted in Figures 6-9. The particle size and size distribution of Avicel PH-101 are higher than corn husk, and lupine husk. However, the particle size of corn cob is greater than the others. Particle size of MCC depends upon the extent of degradation of cellulose molecule. It has very little effect on the tabletability of pure MCC, i.e., not lubricated nor blended with other excipients or active pharmaceutical ingredients (APIs) (Thoorens *et al*., 2014). However, the effect of particle size is significant when MCC blended with other excipients and APIs. Finer particle size of MCC promotes tablet (compact) strength (kambli *et al*., 2017). However reducing the particle size of MCC can certainly affect its flowability, as a result of its increased cohesiveness. The particle size may impact not only the flowability of the powder but also tablet hardness, friability and disintegration (Thoorens *et al*., 2014). Laser diffraction particle size analysis is a preferred method for determination of particle size and particle size distribution of a wider range of particles (20 nm–2000 μm) (Keck, and

Muller, 2008). In addition, SEM, TEM and sieving methods are also used to analyze the particle size of MCC (Kian *et al*., 2017; Adel *et al*., 2011).

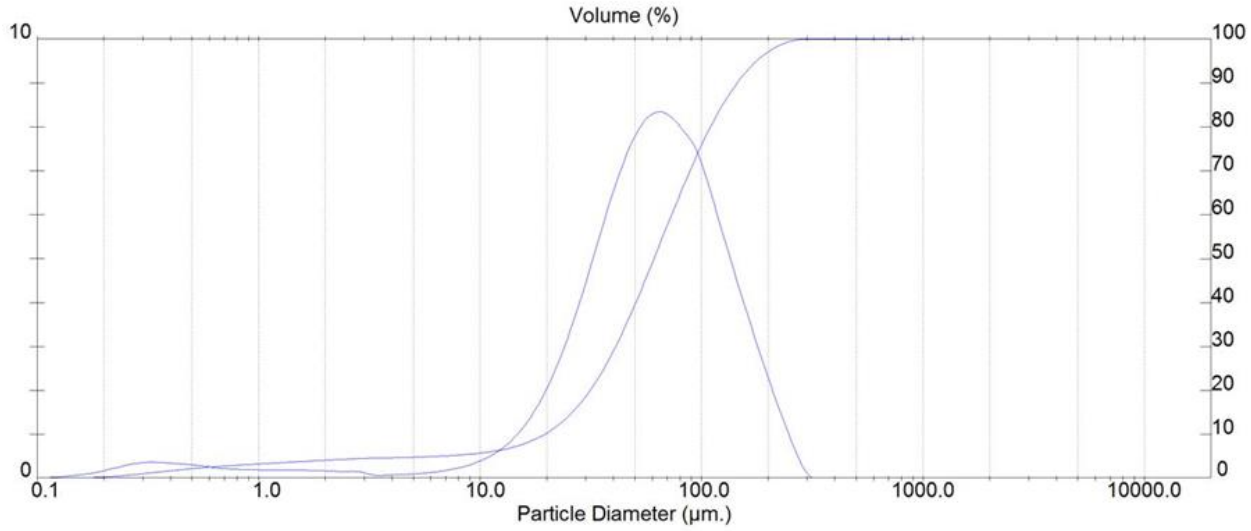

Fig.6.Volumeteric Particle size distribution of corn cob MCC

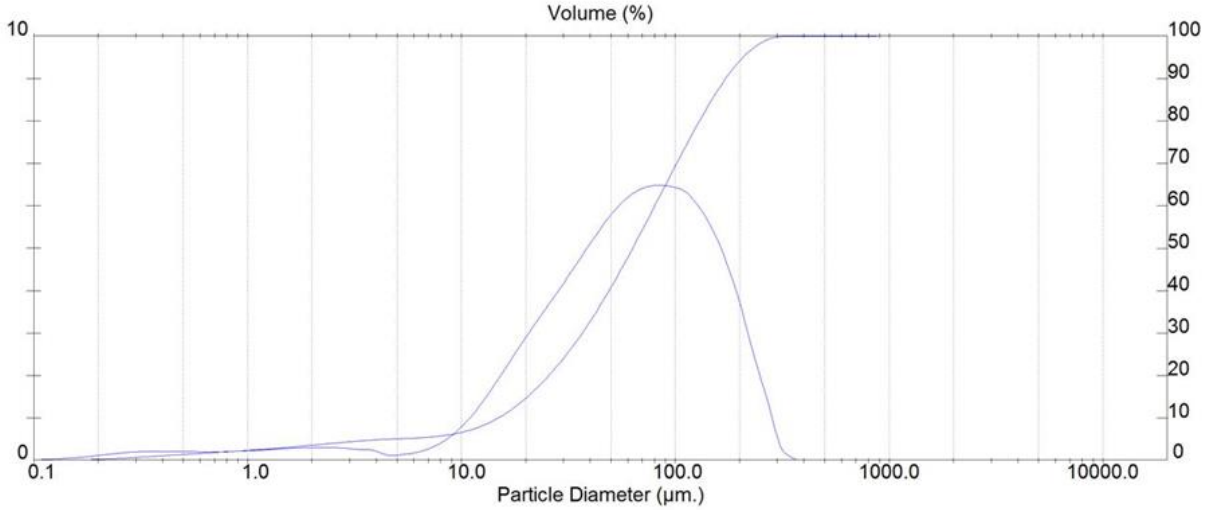

Fig. 7. Volumetric Particle size distribution of Lupine husk MCC

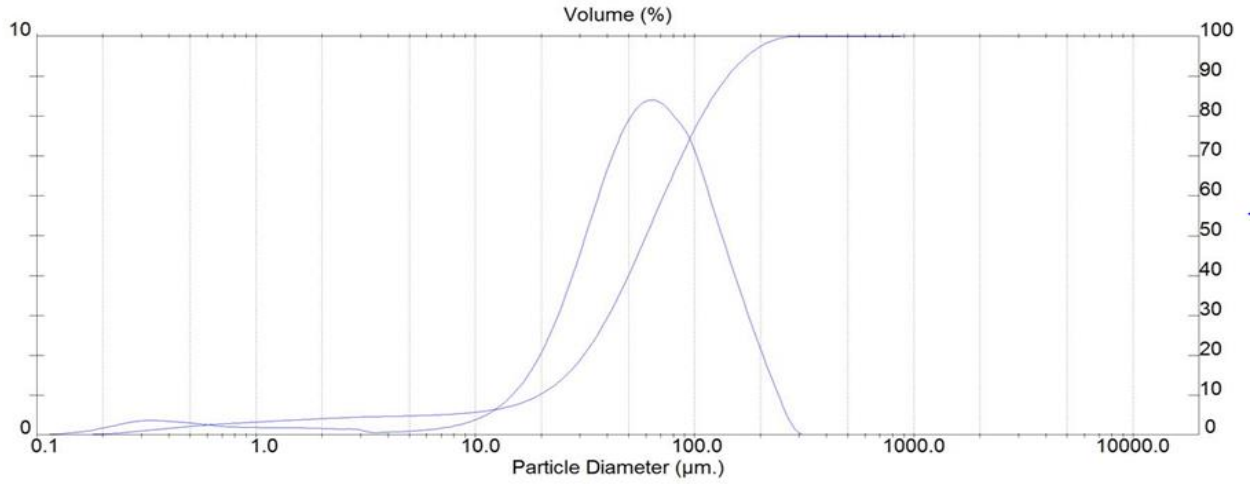

Fig. 8. Volumetric Particle size distribution of Avicel PH 101

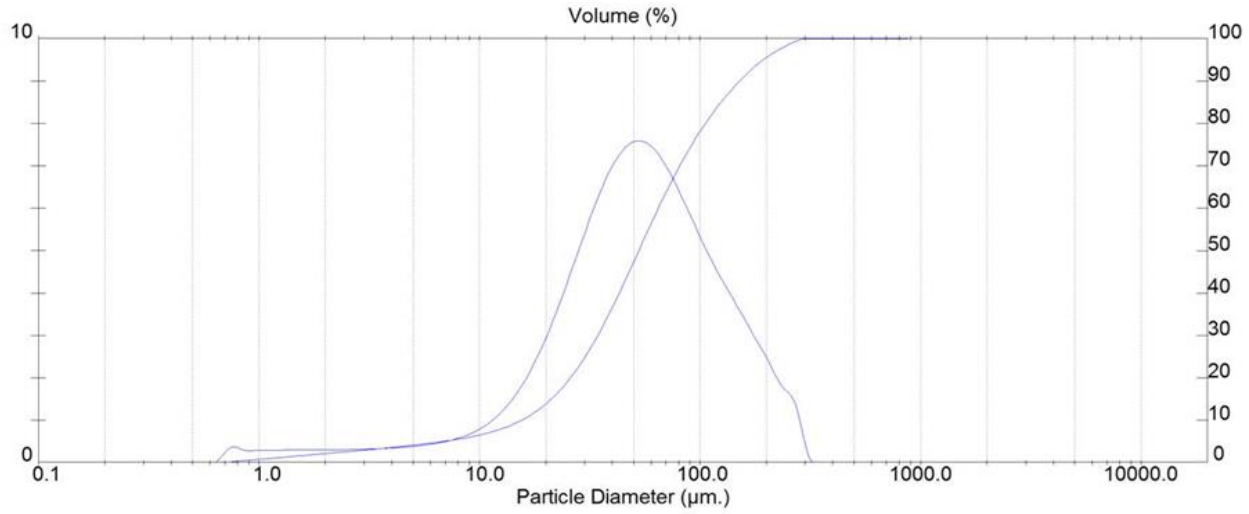

Fig. 9. Volumeteric Particle size distributions of corn husk MCC

Table 5. Particle size and size distribution of CH-MCC, CC-MCC, LH-MCC, and Avicel PH-101

Parameters	CH-MCC	CC-MCC	LH-MCC	Avicel PH-101
Mean particle size (µm)	69.99±0.745	90.22±1.373	69.26±1.719	72.11±0.71
Dv10 (µm)	15.61±0.212	21.81±2.523	14.49±0.552	19.47±0.0755
Dv50 (µm)	52.89±0.413	72.07±1.496	65.64±2.15	60.35±0.527
Dv90 (µm)	152.31±2.12	155.52±1.48	153.75±2.045	143±1.635
SSA (m2/g)	0.238±0.0021	0.124±0.011	0.46±0.0128	0.542±0.0022
Span	2.604E+00	2.258E±00	2.788E+00	2.056E+00

D10: 10% of particles below, D50: 50% of the particles below, D90: 90% of particles below, SSA: Specific surface area, Span= (D90 - D10)/D50

According to FMC, (2003) Specification the Dv10, Dv50, and Dv90 of Avicel PH 101 are in the range of 14-30, 40-75, and 77-156 respectively. The CH-MCC, CC-MCC, LH-MCC and Avicel PH-101 of Dv10, Dv50, and Dv90 values are within the range stated in FMC specification. The mean particle size of Avicel PH-101 must be in the range of 35-50μm (FMC, 2003). In this study the mean particle size of CH-MCC, CC-MCC, and LH-MCC were higher than the FMC specification. This may be due to processing conditions. The physicochemical, thermal and mechanical properties of MCC may be affected by processing conditions. Avicel PH-101 were also shows higher particle size than FMC specification. This may be due to moisture absorption during the storage. The temperature and the duration of hydrolysis, nature and concentration of acid as well as the fiber to acid ratio play the important roles in the particle size, morphology, crystallinity, thermal stability and mechanical properties of MCC (Trache *et al*., 2016). El-Sakhawy and M.L. Hassan, (2007) reported that the nature of acid used during hydrolysis can affect the particle size of MCC based on the plant sources. In the case of MCC prepared from sugarcane bagasse the kind of acid used did not affect the particle size, however in the case of MCC prepared from cotton stalks and rice straw with H_2SO_4 in the hydrolysis process, shows larger particle size.

The specific surface area of MCC has positive impact on its tabletability, potentially because of the numerous hydrogen bonds between the large bonding surface areas of adjacent particles and to the mechanical interlocking of irregular particles. However large specific surface area may affect the flowability of direct compression binders by increasing the cohesiveness of powders (Thoorens *et al*., 2014). The specific surface area of CH-MCC, CC-MCC, LH-MCC, and even Avicel PH-101 is less than the value described by Pesonen et al., (1989), the specific surfaces area of Avicel PH-101 was 1.26m^2/g.

5.7. FTIR study

There are two main absorbance regions of FTIR spectra. The first one is found at high wavenumbers (2800–3500 cm^{-1}) and the second one is found at low wavenumbers (500–1700 cm^{-1}) (Haafiz *et al*., 2013). The FTIR spectra of corn husk, corn cob, lupine husk cellulose,

MCC, and Avicel PH101 are illustrated in Figure 10, and 11, respectively. All spectra of cellulose and MCC were comparable this is an indication that all samples have identical chemical compositions. The broad absorption band around 3320cm^{-1}, 3329cm^{-1}and 3332cm^{-1}of all samples of cellulose spectrum observed due to O-H groups stretching vibration. The other peak at 2889cm^{-1}, 2891cm^{-1} and 2894 cm^{-1} indicates C-H stretching vibrations. In all cellulose spectra, the peaks at 1634 cm$^{-1,}$ 1648cm^{-1}, and 1652cm^{-1} and at 1630 cm^{-1}, 1632 cm^{-1}, 1634 cm^{-1}, and 1635 cm^{-1} of MCC corresponds to the absorption of water molecule, due to the strong interactions between cellulose and water molecules and difficulty to remove the adsorbed water, even after appropriate drying process. Both sets of peaks are ascribed to the stretching of hydrogen bonds and bending of hydroxyl (OH) groups bound to the cellulose structure (Abu-Thabit *et al*., 2020).

The disappearance of the absorption peak around 1740 cm $^{-1}$and 1533 cm $^{-1}$in the spectrum indicates the absence of lignin and hemicellulose in all celluloses and microcrystalline celluloses. This absorption peak 1740cm^{-1} and 1533cm^{-1} indicates that C-O stretching of the acetyl and uronic ester groups of hemicellulose or the ester linkage of carboxylic groups of ferulic and p-coumaric acids of lignin, respectively (Sheltami *et al*., 2012; Rasheed *et al*., 2020; Haafiz *et al*., 2013; costa, *et al*., 2015). The peak at 1595 cm $^{-1}$ is associated with an aromatic ring stretch that is strongly associated with the aromatic C–O stretching band (Setu, *et al*., 2014: Adel, *et al*., 2011). The bands at 1316cm^{-1}, 1320cm^{-1}, and 1325 cm^{-1}are related to –CH or –CH2 vibrations associated with intermolecular hydrogen bonds at the C group and the OH in plane bending vibration, respectively (Haque *et al*., 2015; Adel *et al*., 2011). The other significant peak at 1026cm, 1027cm, and 1028cm indicating that the stretching of C-O-C pyranose ring skeletal vibration (Adel *et al*., 2011; Kian, *et al*., 2017). While, the peak located at 890 cm^{-1} - 895 cm^{-1} is related to the β (1-4) glycosidic linkage vibration of cellulose and MCC (Kian *et al*., 2017).

No significant differences were observed between the spectra corresponding to cellulose and microcrystalline cellulose. The results indicate that the cellulose molecular structure remains unchanged following acid hydrolysis. However, in the case of MCC the stretching absorbance increased because acid hydrolysis removes the amorphous part of cellulose on the surfaces. Therefore, C-OH, C-O-C, and C-C bonds were more exposed (Haque *et al*., 2015). In addition to this there was an increase in intensity at absorbance peak of 1454 cm-1 and 893 cm-1 in the

MCC spectrum, this indicates that the increase of crystallinity and complete removal of hemicellulose during acid hydrolysis process (Zhang *et al*., 2019).

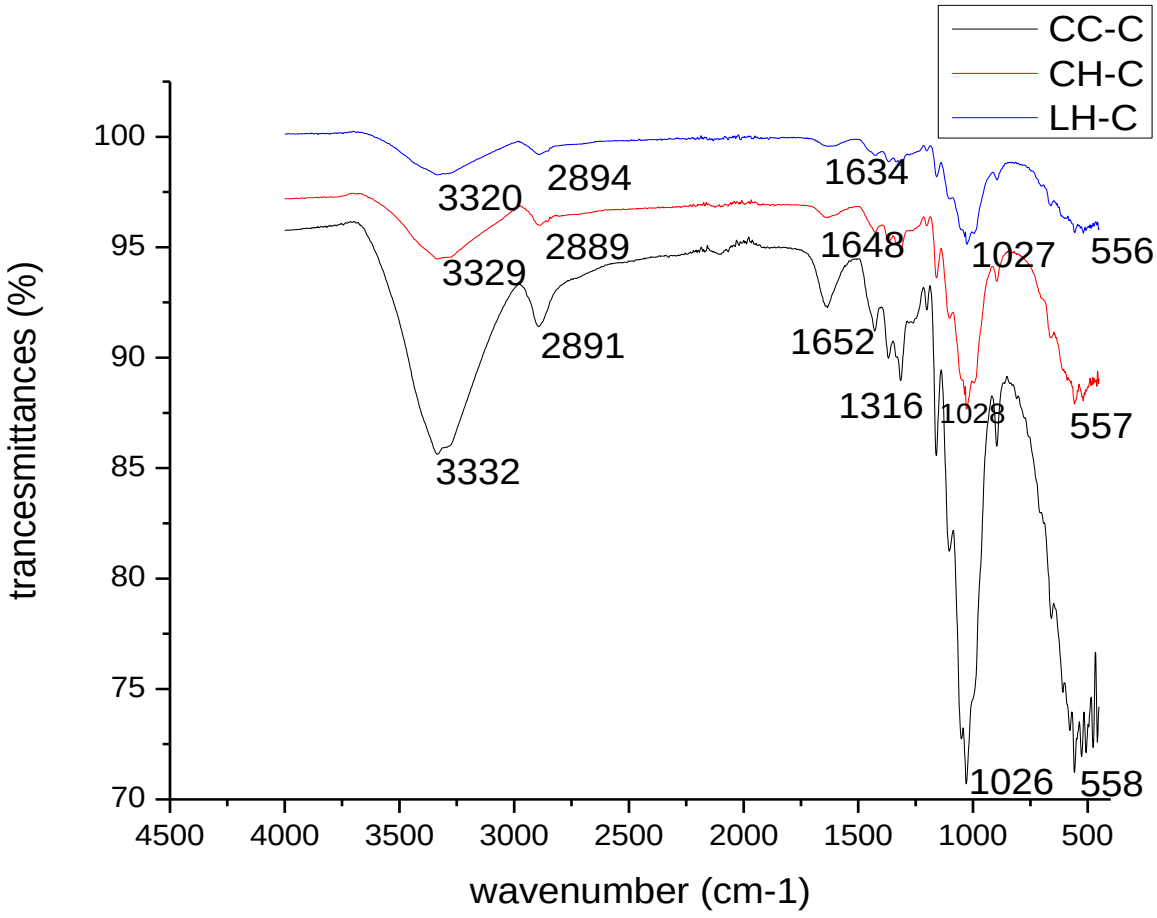

Fig. 10. FTIR spectra of cellulose from corn cob (CC-C), corn husk (CH-C) and lupine husk (LH-C).

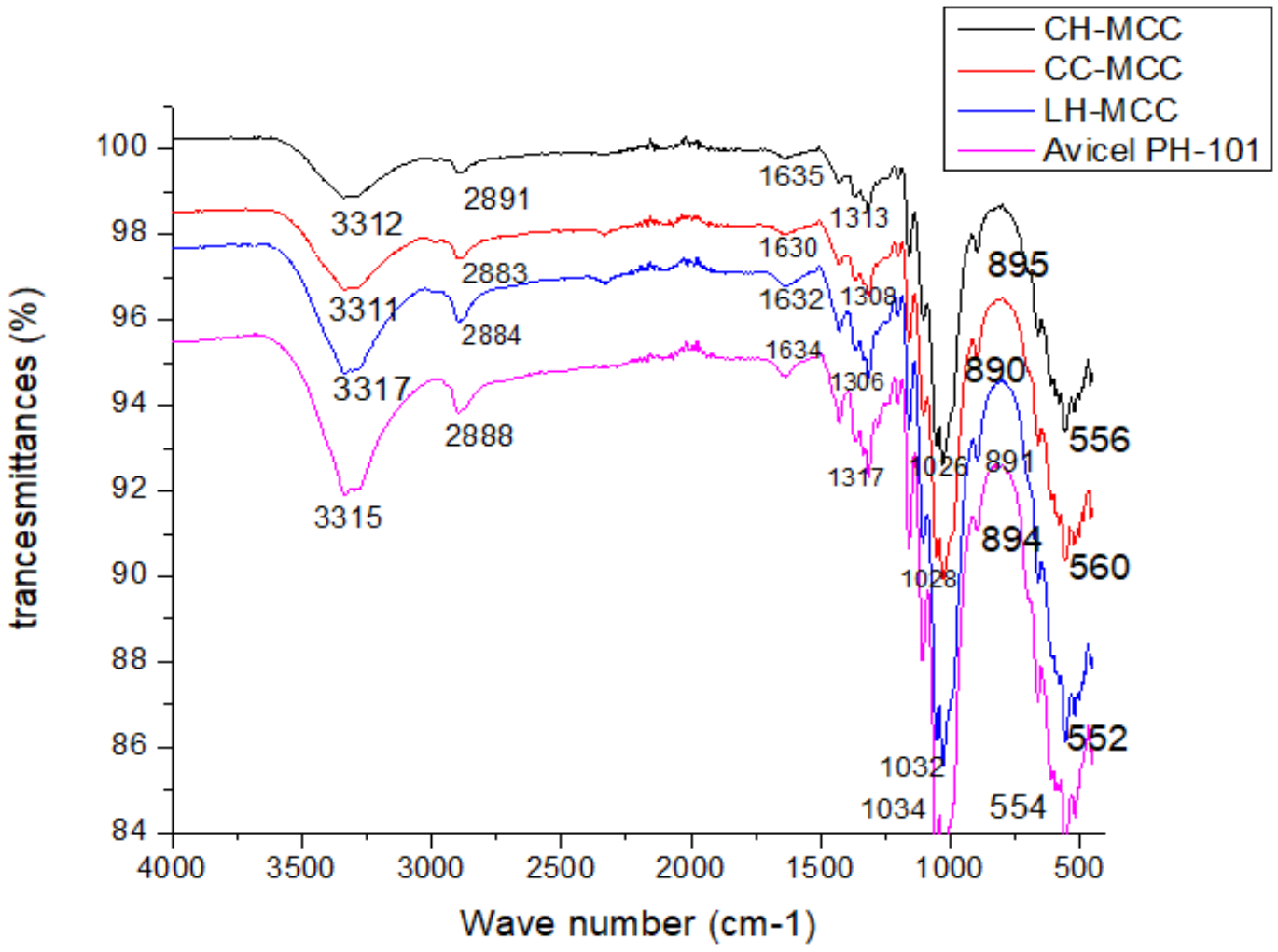

Fig.11. FTIR spectra of MCC from corn husk, corn cob, lupine husk, and Avicel PH-101

5.8. Crystallinity

X-ray diffraction (XRD) gives information directly related to the crystal and amorphous portions of cellulose. Crystalline cellulose gives strong signals with sharp peaks, whereas amorphous (non-crystalline) portion is represented by weak and broader signals in the diffraction pattern (Karimi and Taherzadeh, 2016). Crystallinity appears to be more dependent on the plant source rather than on processing conditions. The XRD pattern of CH-C, CC-C, LH-C, CH-MCC, CC-MCC, LH-MCC, and Avicel PH-101 are illustrated in (Figure 12 and 13).

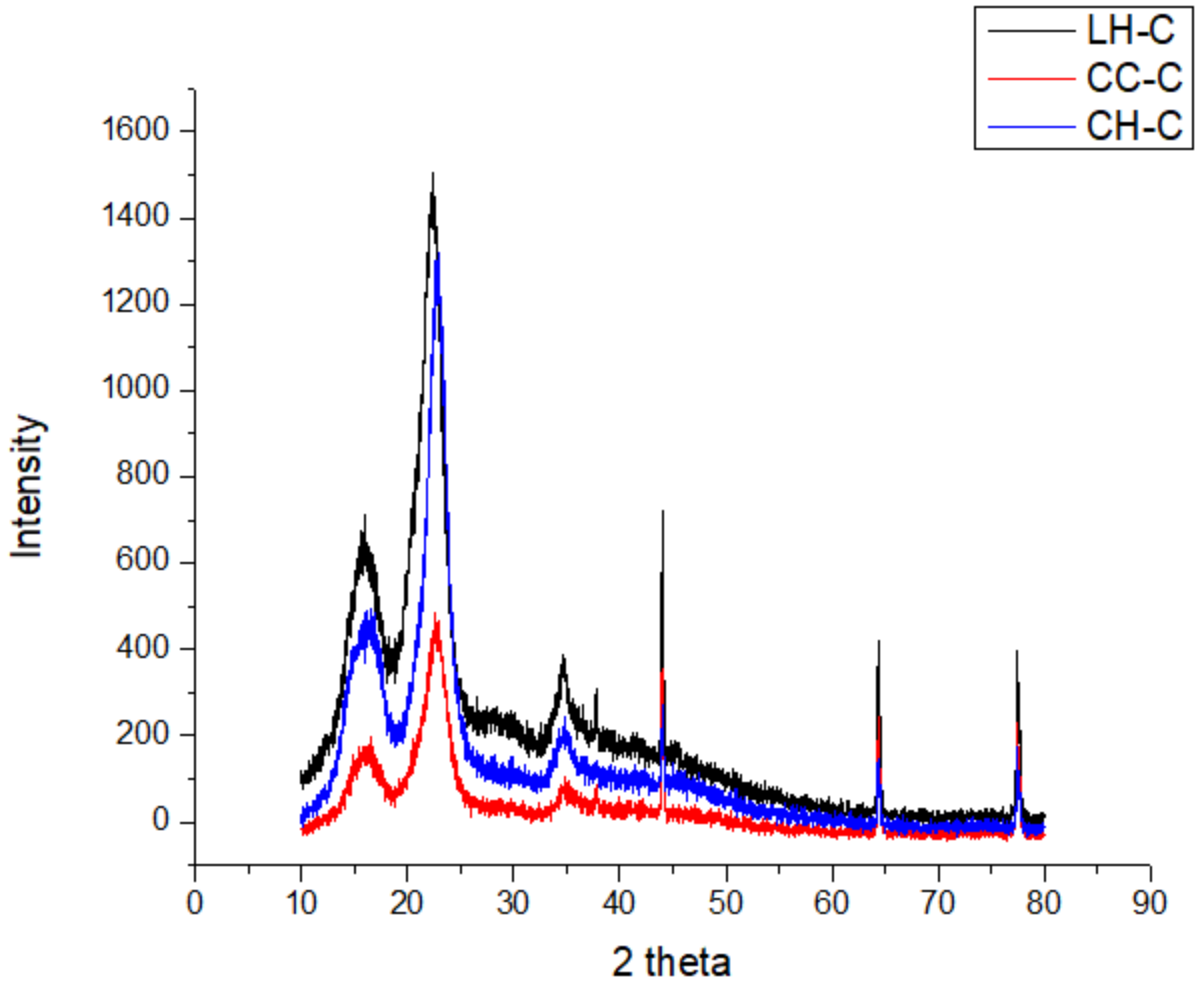

Fig. 12. X-ray diffraction pattern of CH-C, CC-C and LH-C.

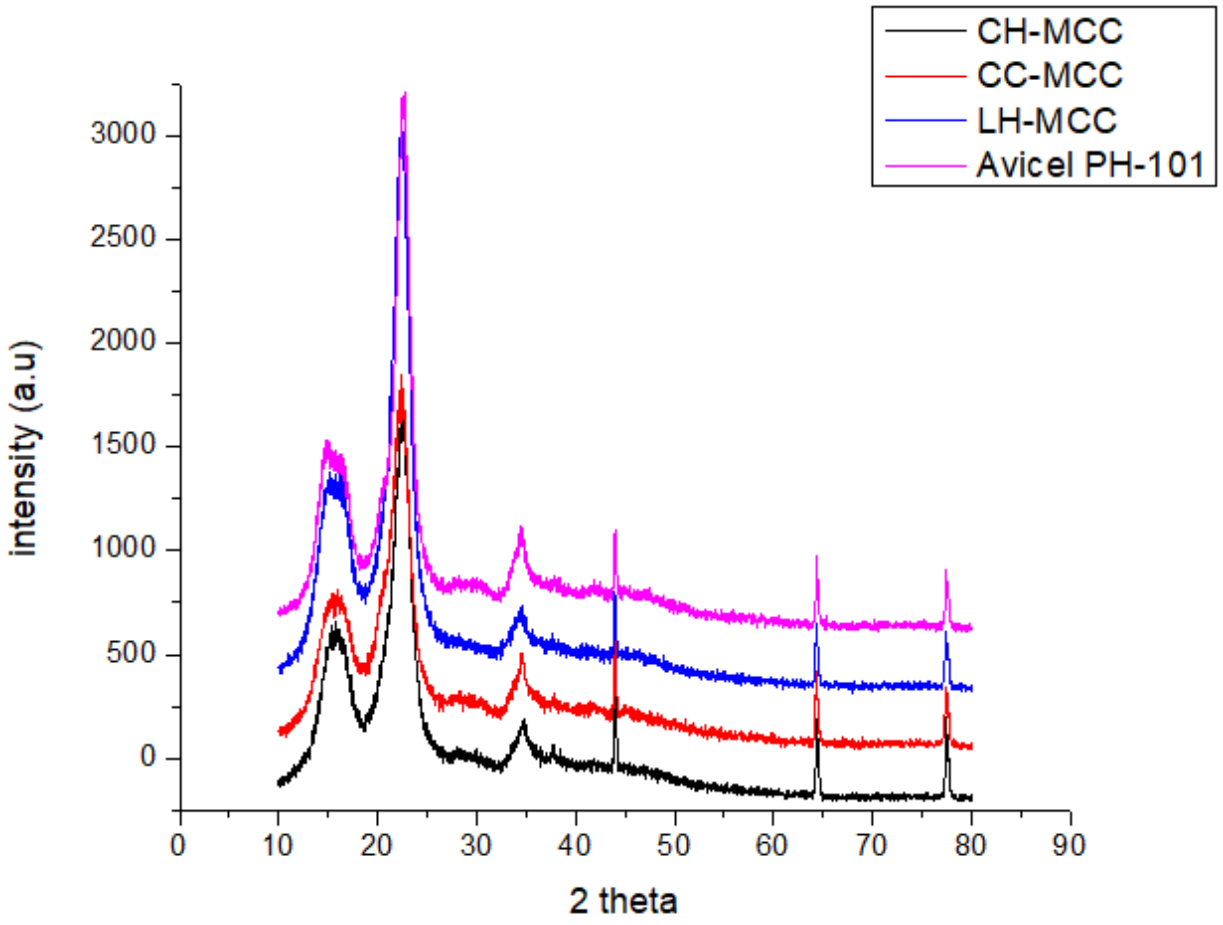

Fig. 13. X-ray diffraction pattern of CH-MCC, CC-MCC, LH-MCC, and Avicel PH-101

As seen on the difractogram of all samples of cellulose, there is no doublet peak at the 002 plane which indicates that all the samples are comprised of cellulose-I polymorph without cellulose-II (Haafiz *et al*., 2013; Deraman *et al*., 2001). Different literatures reported that the typical peaks of cellulose-I are usually found at 2θ values of around 15^{o} and 22.6^{o} (Chio *et al*., 2018; Rasheed *et al*., 2020). There was no typical peaks at 2θ = 20.4°, 25°, and 33° of all cellulose and MCC samples extracted from corn husk, corn cob, and lupine husk and also Avicel PH-101. This indicates that the complete removal of hemicellulose from the sample (Abu-Thabit *et al*., 2020). As seen in the difractogram, there is a similar pattern of XRD of cellulose and MCC. This indicates that cellulose structure did not change during the acid hydrolysis (Zhang *et al*., 2019). However, the peak around 2θ＝22.6^{o} of CH-MCC, CC-MCC, LH-MCC, and Avicel PH 101 was sharper than that of the CH-C, CC-C, and LH-C. This is due to the higher degree of crystallinity

of MCC than cellulose (Choi *et al*., 2018). The subsequent increase of the CI value upon acid hydrolysis of purified cellulose CH, CC, and LH were indicative of the dissolution of amorphous cellulosic domains. During the strong acid hydrolysis process, hydronium ions can penetrate the more accessible amorphous regions of cellulose and allow the hydrolytic cleavage of glycosidic bonds, which eventually releases individual crystallites (Johar *et al.*, 2012).

The crystallinity index CI (%) of all samples was displayed in Table 6. A number of studies suggested that the CI (%) of MCC is in the range between 60 and 80% (Haafiz *et al*., 2013; Sun, 2008). In this study, the CI (%) of CH-MCC, CC-MCC, and LH-MCC was 78.1, 77.01, and 81.41% respectively; these results were observed higher compared with Muli bamboo-MCC (68 %) and Rawnal bamboo (72.5 %) rice husk (63.9%) (Ahmad *et al*., 2016; costa *et al*., 2015). The CI of lupine husk MCC is higher than Bamboo MCC however; the CI of corn husk MCC is similar to Bamboo MCC (78%) (Khali *et al*., 2018; Haafiz *et al*., 2013). This result was due to different processing variables involved in the preparation of MCC, such as reaction temperature, duration, drying conditions, acid concentration and plant origin (Khalil *et al*., 2018).

In this study, the crystallinity of cellulose increases from CC-C (72.86%) to CC-MCC (77.01%), CH-C (74.54%) to CH-MCC (78.1%) and LH-C (75.39%) to LH-MCC (81.41%). This phenomenon indicated that partial removal of amorphous during acid hydrolysis process (Khali *et al*., 2018).

The apparent crystallite size (L) of cellulose and MCC from CH, CC, and LH were calculated following the Scherrer equation. As can see in table 6 the crystal size (L) of cellulose and MCC from lupine husk was higher than that of cellulose and MCC from corn husk and corn cob. This may be due to the sources of the plant and the corresponding crystallinity index. Crystallite size of Avicel PH-101 is higher than the others.

Table 6. The CrI of CH-C, CC-C, LH-C, CH-MCC, CC-MCC, LH-MCC and Avicel PH-101

	Corn husk	Corn cob	Lupine husk	Avicel PH 101
CrI of cellulose (%)	74.54	72.86	75.39	
CrI of MCC (%)	78.1	77.01	81.41	85.48
L(nm) cellulose	2.76	2.64	2.81	
L(nm)MCC	3.21	3.02	3.35	4.5

5.9. Morphology of cellulose and MCC

The particle morphology and surface characteristics of cellulose from corn husk, corn cob, and lupine husk and MCC from these sources was investigated using SEM and compared to commercial MCC (Avicel PH-101). The studies of SEM micrographs for corn husk, corn cob, lupine husk cellulose and MCC, as well as Avicel PH-101 are presented in figure 14 and 15, respectively. The microgram of CH-C, CC-C, and LH-C shows individualized, curled, soft-flat shape and also has rough pits on the surfaces, which is due to the removal of hemicellulose and lignin (Collazo-Bigliardi *et al*., 2018; Kale *et al*., 2017). These features of cellulose increase its specific surfaces area and favor chemical reactions like acid hydrolysis (Kale *et al*., 2017).

It can be observed from the SEM micrographs that CH- MCC, CC-MCC, and LH-MCC have short fiber strands which appeared to rod- like shape; irregular fiber fragments and also showed a network-structure. This result is consistent with the findings of various researchers (kambli *et al*, 2017; Adel *et al*., 2011; El-Sakhawy and Hassan, 2007). Compared to round-shaped particles, rod shaped (fibrous) particles resulted in higher tablet tensile strengths (Thoorens *et al.*, 2014). Avicel PH- 101 shows a similar morphological topography as compared to CH-MCC, CC-MCC and LH-MCC.

a. 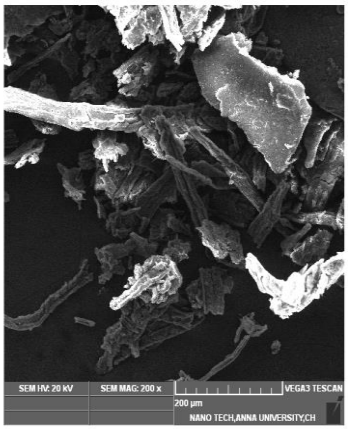

b. 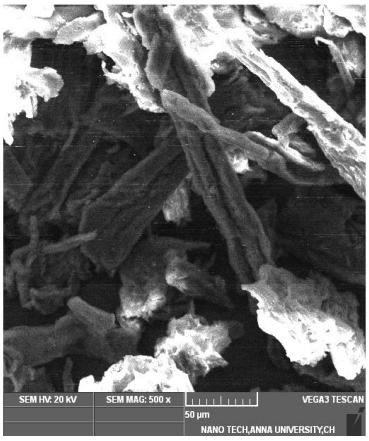

c. 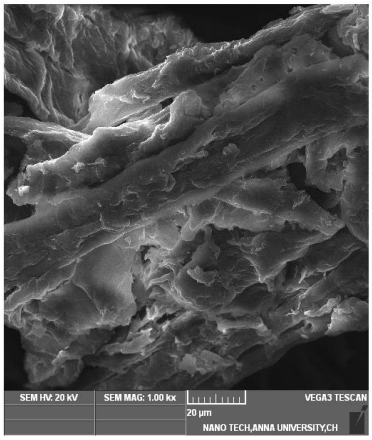

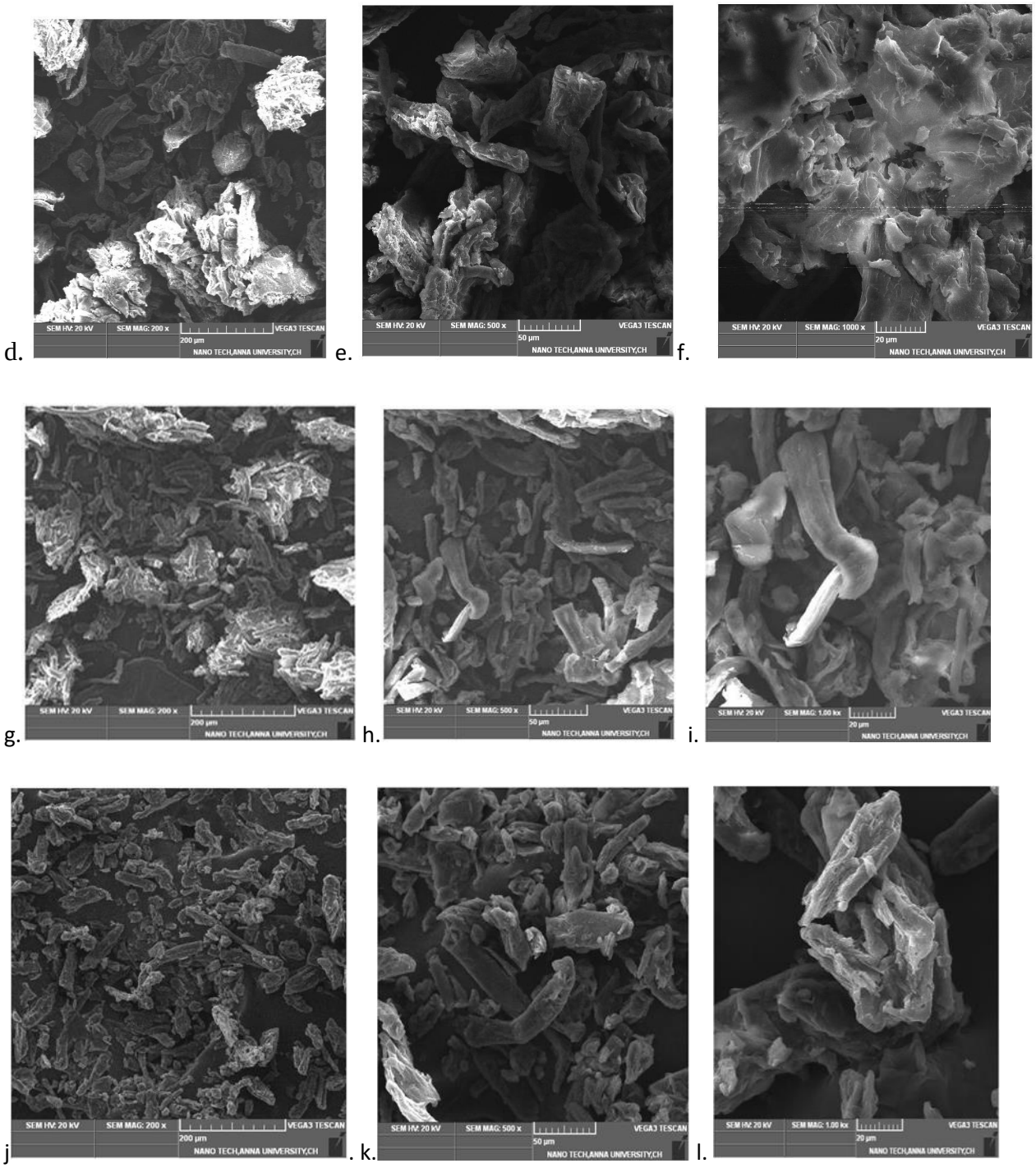

Fig. 14. SEM image of MCC from corn husk(a,b,c), corn cob(d,e,f),lupine husk(g,h,i),and Avicel PH 101 (j,k,l) at 200,500, and 100 magnification.

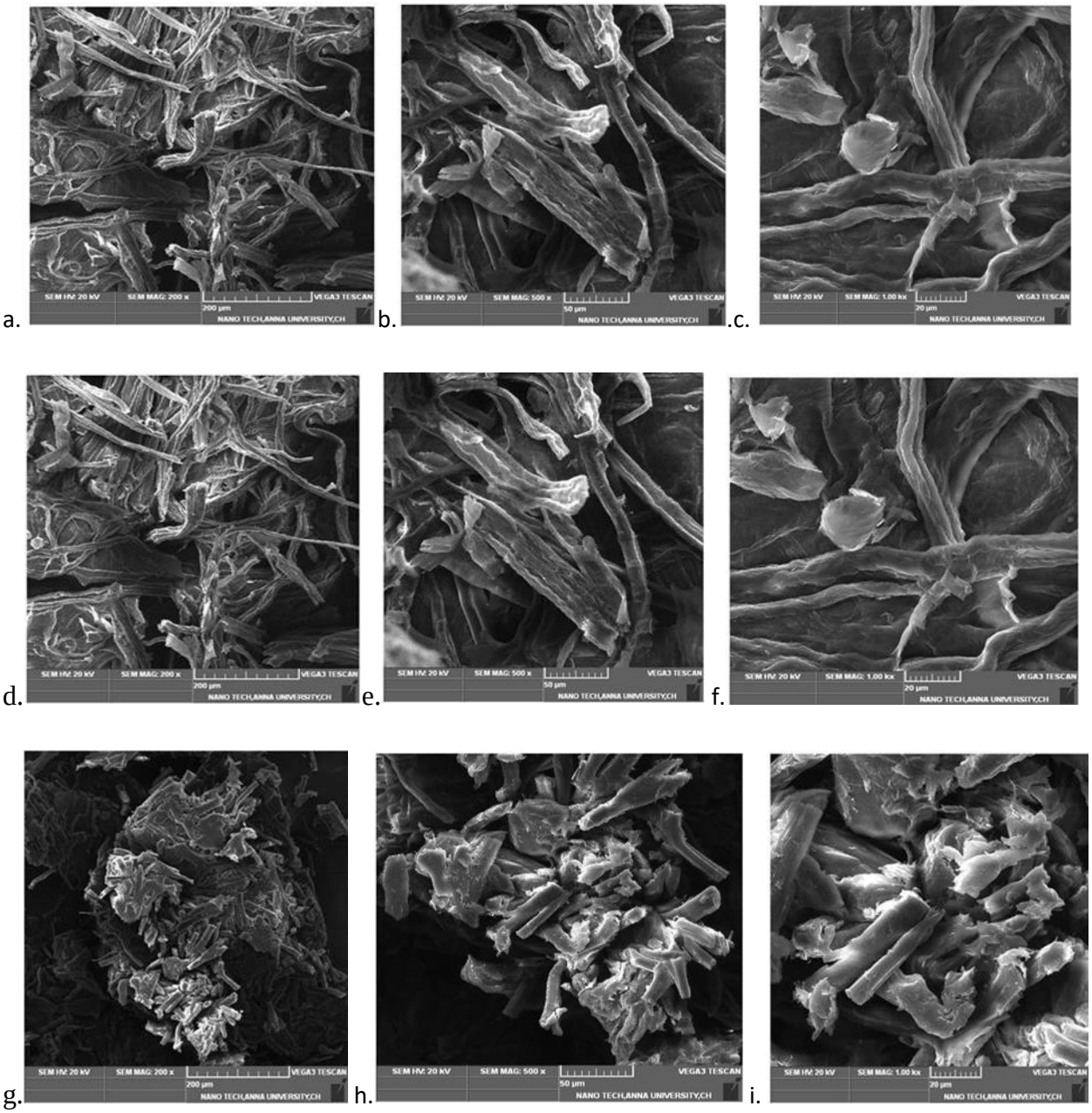

Fig. 15. SEM image of cellulose from corn husk (a,b,c,), corn cob (d,e,f), and lupine (g,h,i) at 200,500,and 1000 magnification.

5.10. Thermo gravimetric analysis

Thermo-gravimetric analysis provides a method for the determination of mass change in the polymer as a function of time and temperature. These techniques reflect reactions which appear at the molecular level of the materials (Princi *et al.*, 2005). The thermal analysis of cellulose and

MCC is necessary in order to determine the future application. Both TGA and DTG commonly used methods to investigate the thermal and degradation properties of cellulose and MCC sample (Trache *et al*., 2016). The thermal studies of Cellulose, MCC prepared and commercial MCC (Avicel PH-101) by thermogravimetric analysis (TGA) and derivative thermogram (DTG) are presented in figure 16 (A) and (B).

The TGA curves of MCC show two degradation curves, which indicate the weight loss of the sample. The first curve indicates the evaporation of water within the cellulose at the region between 60 and 150 ◦C. The second curve indicates the dehydration, decarboxylation, depolymerization and decomposition of glycosyl units in cellulose in the range of 250–450 ^{o}C, followed by the char residue formation in the range of 450 -700 ^{o}C (Trache *et al*., 2016).

In the TGA curve the first stage weight loss was observed in the temperature range of 57-100 ^{o}C, 63-101^{o}C and 63-108 ^{o}C, 66-112 ^{o}C, 65-107 ^{o}C, 64-114 ^{o}C, and 64- 110 ^{o}C for CH-C, CC-C, LH-C, CH-MCC, CC-MCC, LH-MCC and Avicel PH101, respectively, with corresponding weight loss of 9.6%, 12.48%, 10.3%, 5.67%, 4.03%, 6.37% and 5.81%. The presence of this endothermic peak on thermograms of cellulosic materials is as a result of the evaporation of loosely bound water on the surface of the samples (Nwajiobi *et al*., 2019; Haafiz, *et al*., 2013). The second decomposition peak of CH-C, CC-C, LH-C, CH-MCC, CC-MCC, LH-MCC and Avicel PH-101 appeared at 213 - 371 ^{o}C, 219-371 ^{o}C, 218-367 ^{o}C, 279-374 ^{o}C, 280-373^{o}C, 274-377^{o}C, and 285-378 ^{o}C, respectively. These temperature ranges revealed that decarboxylation, depolymerization and decomposition of cellulose (Kian, *et al*, 2017). Cellulosic materials degrade at low to moderate temperatures. Early decomposition of hemicelluloses begins below 400 ◦C followed by pyrolysis of lignin (Haafiz *et al*., 2013). In the second degradation peak CH-MCC,CC-MCC,LH-MCC, and Avicel PH-101 started to decompose at 279 °C, 280°C, 282°C, and 285 °C, respectively, which were higher temperatures compared to the thermal degradation temperature of CH-C (213 °C), CC-C (219°C), and LH-C (220°C). This result would suggest that cellulose with higher crystallinity exhibited higher thermal stability. This may be due to absence of hemi-cellulose and lignin, as well as the removal of the amorphous part presents in the cellulose during acid hydrolysis process (Liu *et al*., 2018).

50% weight loss decomposition temperature of cellulose and MCC occurred at CH-C (325.22 ^{o}C), CC-C (326.85 ^{o}C), LH-C (335.17 ^{o}C), CH-MCC (333.32 ^{o}C), CC-MCC (333.79 ^{o}C), LH-MCC (335.14 ^{o}C) and Avicel PH-101 (336.46 ^{o}C). This result is because of the thermal stability

of the cellulose and MCC increased with its purity. The reason for this relatively higher thermal stability of the pure cellulose and MCC is probably due to the substantial removal of less stable hemi-cellulose and lignin (Sun *et al*., 2004; Liu *et al*., 2018).

Avicel PH-101 shows the highest onset temperature (354.8 °C) followed by LH-MCC (351.1°C), CH-MCC (349.81°C) and CC-MCC (347.36°C). This is due to the high crystallinity percentage of cellulose found in Avicel PH-101 and LH-MCC than CH-MCC and CC-MCC. According to Kuthi et al., (2016) report; the reorientation of the crystals in cellulose facilitates to arise in onset temperature of degradation. The onset temperature of cellulosic materials also influenced by surface morphology. Aggregated crystals in the surface morphology show high degradation temperature (Nwajiobi *et al.*, 2019).

$T_{10\%}$ decomposition of cellulose and MCC appeared at temperature of 239.23 ^{o}C CH-C), 233.41 ^{o}C (CC-C), 241.74^{o}C (LH-C), 300.17 ^{o}C (CH-MCC), 297.32 ^{o}C (CC-MCC), 304.03^{o}C (LH-MCC), and 308.82 ^{o}C (Avicel PH-101). This is attributed to the high degree of crystallinity of MCC, which requires high heat energy for thermal degradation than cellulose samples (Kian *et al*, 2017).

A.

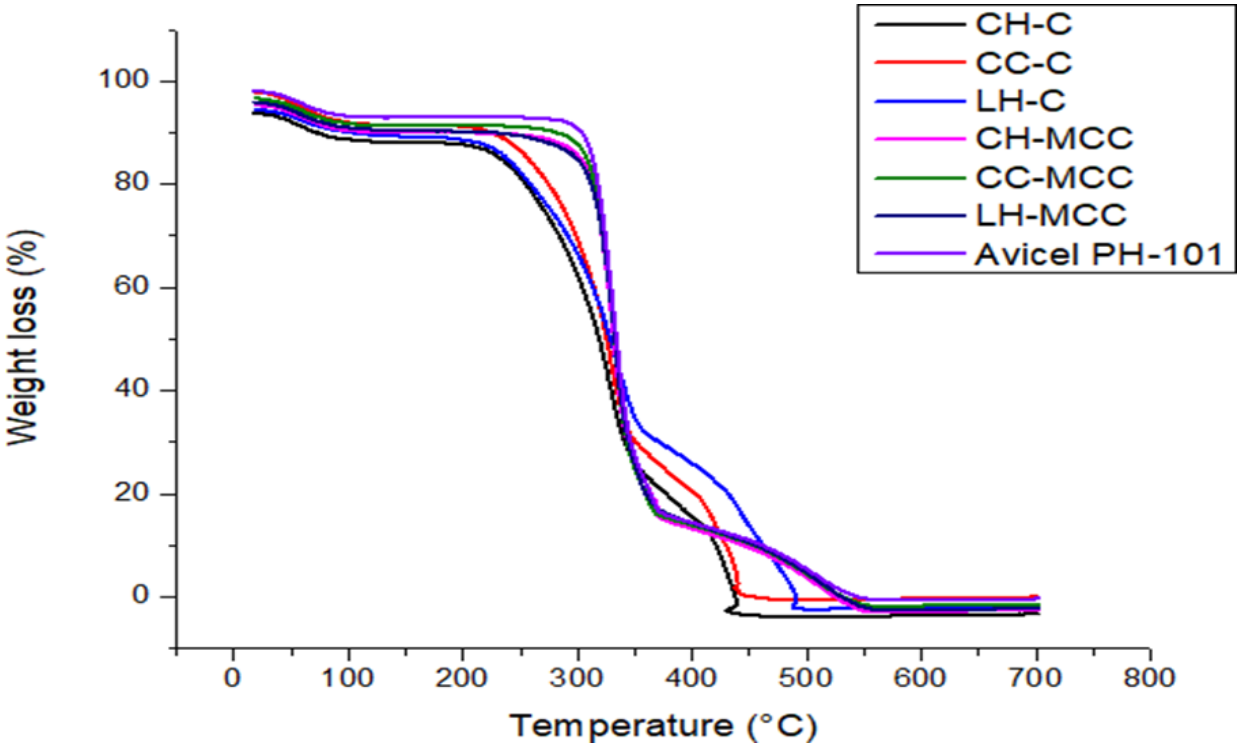

B.

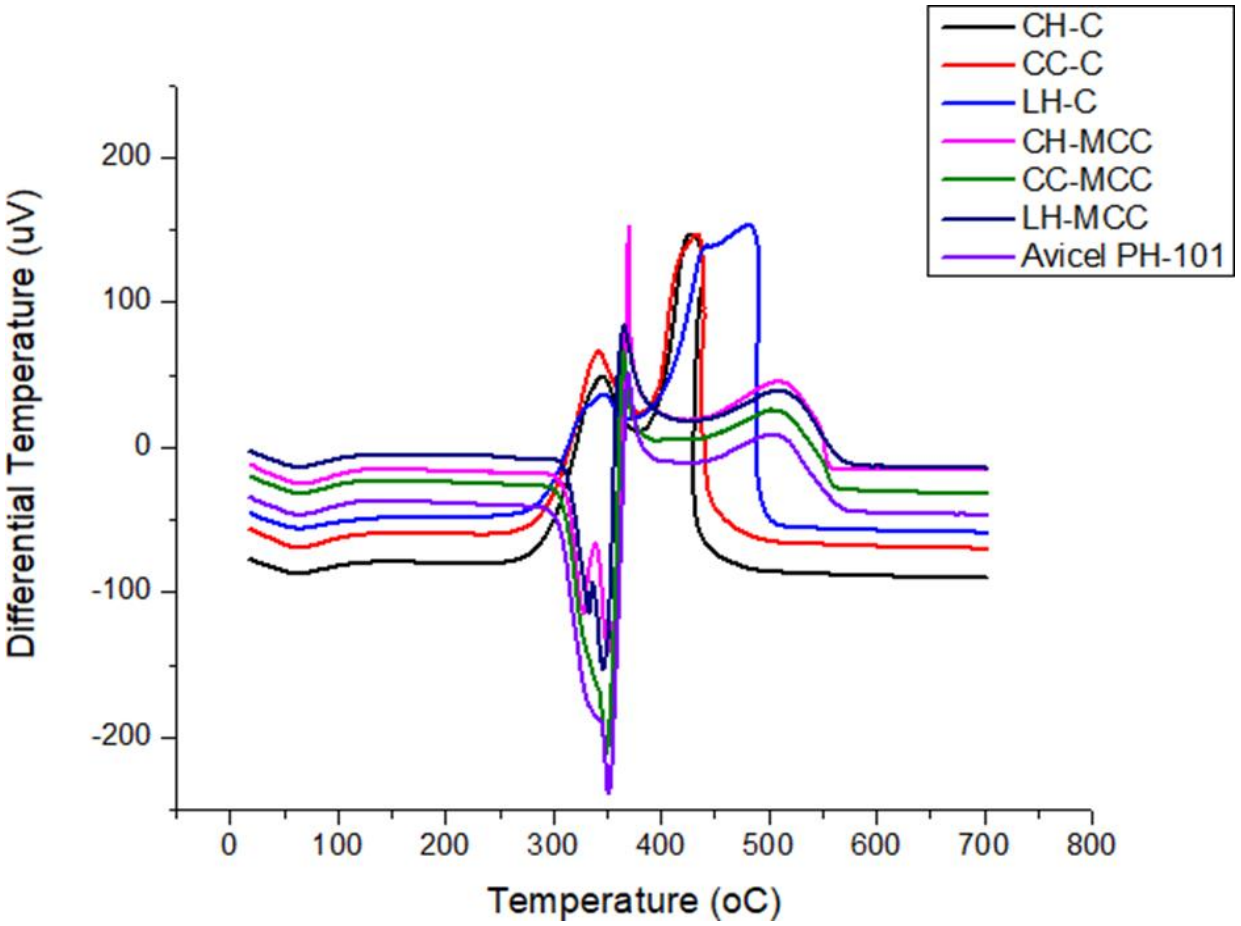

Fig. 16. TGA (A) and DTG (B) curve of CH-C, CC-C, LH-C, CH-MCC, CC-MCC, LH-MCC and Avicel PH-101

The DTG thermogram of all cellulose and MCC preparations contained both endothermic and exothermic peaks. A very small endothermic peak observed in the DTA of CH-C, CC-C, LH-C, CH-MCC, CC-MCC, LH-MCC and Avicel PH-101 at a temperature range of 63-120 ^{o}C due to water evaporation on the surface of the particles was also observed in the TGA study. The area of second endothermic (major) peak related with the proportion of crystallinity of the sample, higher area implying higher crystallinity (Kalita *et al*., 2013). As seen in figure 16 (B), in the second endothermic peak, the area of Avciel PH-101> LH-MCC> CH-MCC> CC-MCC. This shows that the crystallinity index of Avciel PH-101 and LH-MCC higher than CH-MCC> CC-MCC. The char residue at 700 ^{o}C was 2.64% (CH-C), 1.94% (CC-C), 3.24% (LH-C), 1.76% (CH-MCC), 1.49% (CC-MCC), 1.67% (LH-MCC), and 1.32% (Avicel PH-101. The high residual weight of all cellulose samples than MCC was likely due to the char formation from

flame retardant compounds (Kian *et al*., 2017; Adel *et al*., 2011). However, the impurities present in all cellulose samples is low compared to other studies such as; roselle fibers cellulose 12.57%, jute fiber 12-14%, and rice husk 30% (Kian *et al*., 2017; Johar *et al*., 2012; Jahan *et al*., 2010).

5.11. Evaluation of tablet properties

5.11.1. Drug-excipient compatibility study

Drug-Excipient compatibility studies were conducted to evaluate interaction between mebendazole and CH-MCC, CC-MCC, LH-MCC and Avicel PH-101. The FTIR spectra of mebendazole, physical mixture (1:1) of mebendazole and CH-MCC, mebendazole and CC-MCC, mebendazole and LH-MCC, mebendazole and Avicel PH-101 are displayed in Figure 17 and 18, respectively. Mebendazole contains different functional groups including –NH, C=O, CH_3-O, Aromatic ring, and Amide (Honorato *et al*., 2012).

The absorption peaks of mebendazole at 3369- 3415 cm^{-1}, 3000 cm^{-1}, 1730 cm^{-1} and 1647cm^{-1} shown that the presence of N-H stretching, aromatic C-H, CO-NH amide stretching and C=O stretching, respectively. The presence of an absorption band around 1516 cm−1 confirmed the C-N stretching of the primary or secondary amines (Roque-Flores *et al*., 2020; Agatonovic-Kustrin *et al*., 2008). All characteristic peaks of mebendazole were observed in the FTIR spectra of the 1:1 physical mixture of mebendazole and CH-MCC, mebendazole and CC-MCC, mebendazole and LH-MCC, and mebendazole and Avicel PH-101.

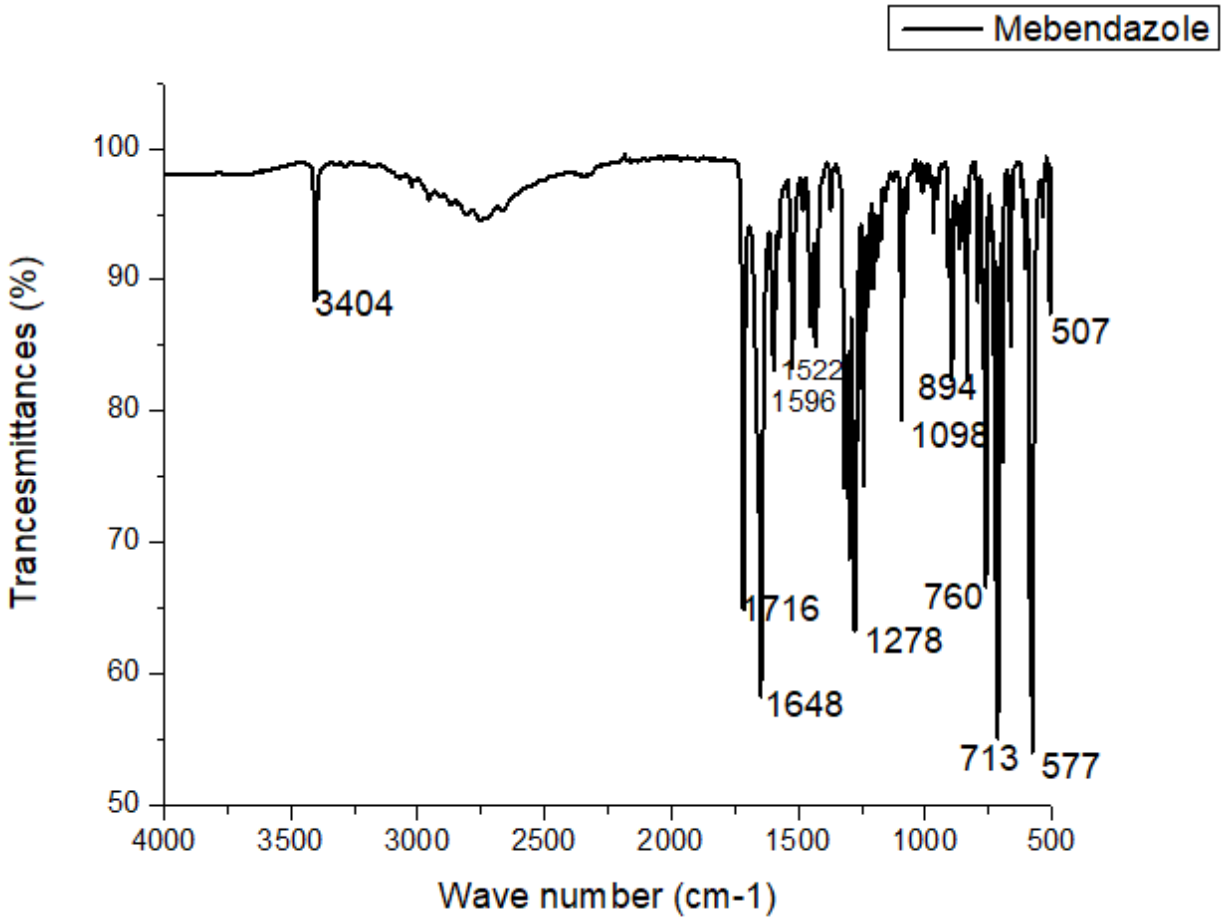

Fig. 17. FTIR spectra of Mebendazole

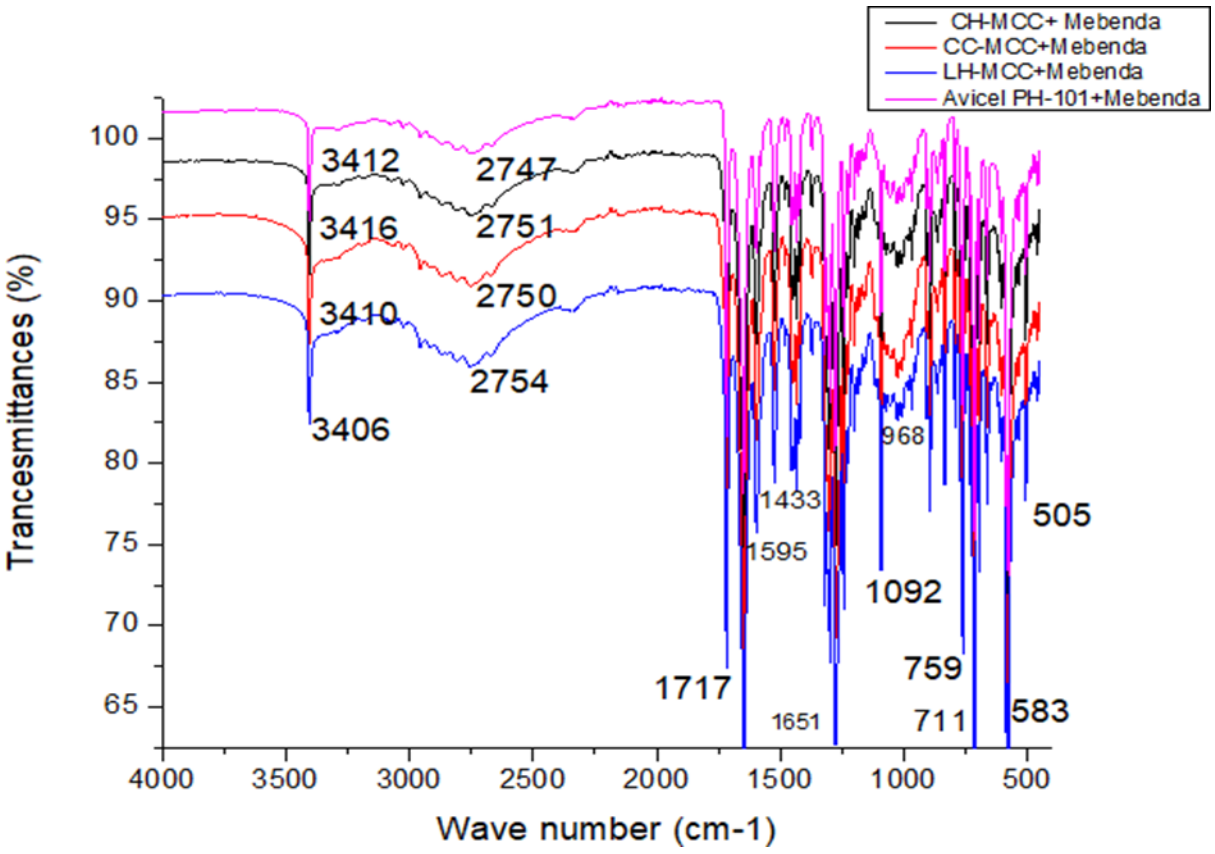

Fig. 18. FTIR spectra of CH-MCC+Mebendazole, CC-MCC+Mebendazole, LH-MCC +Mebendzole, and Avicel PH101+Mebendazole

The sharp peak at 3406 cm-1, 3420 cm^{-1}, 3412 cm^{-1}, and 4416 cm^{-1} seen in the physical mixture of mebendazole and CH-MCC, CC-MCC, LH-MCC, and Avicel PH-101 is attributed to the N-C stretching. The broad band at 2747 cm-1, 2750 cm-1, 2751 cm-1, and 2754 cm-1 is indicated to the aromatic C-H group. The peak around 1717 cm-1, 1651 cm-1, and 1595 cm-1 are associated with CO-NH amide starching, C=O stretching, and C-N stretching of the primary or secondary amines, respectively. The peaks at 1410 cm^{-1}- 1460 cm^{-1} show that CH_3-O stretching. The FTIR spectra of the mixture of mebendazole and all MCC suggested that there were no interactions between mebendazole and MCC samples, which indicate the compatibility between the samples.

5.11.2. Lubricant sensitivity ratio

In solid dosage form formulations, lubricants are essential additives to reduce die wall friction during tablet compression and ejection. Magnesium stearate is the most widely used lubricant

among the different lubricants that are utilized in the pharmaceutical industry because of its low friction coefficient and high covering potential. It facilitates the compaction process by reducing wall friction during tablet compression and ejection and decrease in solid–solid contact (Almaya and Aburub, 2008; Rojas *et al*., 2013). However, it has adverse effects on the compactibility and compressibility of tablet excipients and on the mechanical properties (tensile strength and hardness), disintegration and dissolution behaviors and the stability of the tablets, especially with excessive amounts of lubricant and/or prolonged mixing times. The effect of lubricant on compact strength depends on a number of factors, such as its nature, concentration, mixing time, particle size, and specific surface area (Aly 2012; Rojas *et al*., 2013; Almaya and Aburub, 2008). There are other properties of the excipients themselves that influence their sensitivity to lubricant. The sensitivity of MCC to magnesium stearate depends on the particle size. The effect of mixing time on tablet crushing strength decreased as the particle size of MCC increased. This may be due to the larger shear forces generated by the larger particles in a mixer (Almaya and Aburub, 2008).

In this study the crushing / tensile strength of all MCC powders that has 0.5% magnesium stearate were reduced. According to Aly, (2012) investigation the crushing / tensile strength of the tablets compressed from a lubricated formulation decreased because of isolation effect of magnesium stearate layer film, and also the friability of the tested tablets increased and their disintegration rates decreased. Therefore, the sensitivity to lubricant (magnesium stearate) has been used to characterize the general properties of excipients (Rojas, *et al*., 2013).

Table 7. Tensile strength and LSRs of the lubricated and un- lubricated MCC tablets

Samples	**Tensile strength in Kg/cm^2**		**LSR**
	Un-Lubricated (without 0.5% magnesium stearate)	Lubricated (with 0.5% magnesium stearate)	
CH-MCC	6.2	4.226	0.318
CC-MCC	5.08	3.26	0.358
LH-MCC	2.84	1.8	0.366
Avicel PH 101	15	9.34	0.377

Lubricated (MCC with 0.5% magnesium stearate) tablets are softer compacts than un-lubricated MCC tablets. These results are in accordance with the result reported by Doelker, et al., (1987) when MCC samples were mixed with 0.5% magnesium stearate, all samples give softer compacts than those of MCC without 0.5% magnesium stearate. This is because of the particles of magnesium stearate can interfere with the interactive bonding forces between the particles of MCC, thus reducing the eventual strength of the tablets (Cabiscol, *et al*., 2018). According to Haruna, et al., (2020) study MCC has 79% sensitive to magnesium stearate. Avicel PH-101 exhibits highest lubricant sensitivity this is because of its least porous structure, highest bulk density and good flow property, which facilitates the formation of a continuous lubricant film (Rojas, *et al*., 2013; Doelker, *et al*., 1987; Cabiscol, *et al*., 2018).

Sensitivity to magnesium stearate was ranked (most to least sensitive) as follows: Avicel PH-101 > LH-MCC > CC-MCC > CH-MCC. This is due to the high bulk density and low porosity of Avicel PH-101 and LH-MCC relative to CC-MCC and CH-MCC. High bulk density and low porosity provides less void space to accommodate lubricants, resulting in a high LSR (Rojas, *et al*., 2013).

5.11.3. Mechanical properties of CH, CC, and LH-MCC tablets

MCC is the best excipient for direct compression tableting (Doelker, *et al*., 1987). Its popularity in direct compression is due to the excellent bonding properties as a dry binder. MCC exhibits the highest compactability and compressibility of all known direct compression excipient (Alfa, *et al*., 2006). The physico-chemical properties of MCC vary according to the source of the plant used. It was reported that MCCs extracted from bagasse and corn cobs showed better physico-chemical property than celluloses extracted from rice husks and cotton linters, respectively (Aly, 2012). Table 8 showed that the tensile strength, crushing strength, friability, and disintegration time of CH-MCC, CC-MCC, LH-MCC and Avicel PH-101 compressed tablets at different compression forces (CF1-CF5).

Tensile strength indicates the bonding strength and provides information about tablet capping and lamination (Krivokapic, *et al*., 2020). The compactability of the powder can be influenced by particle size, DP, and morphology (particle shape) of MCC obtained from different sources. The tablets formed from CH-MCC, CC-MCC, and LH-MCC was good and acceptable as none had

surface defects. The tensile strength of Avicel PH-101 and LH-MCC was comparable. This may be due to high crystalinity and smaller particle size. The compactibility of pure materials (both crushing and tensile strengths), the strongest compacts were obtained with the finest powder (Doelker, *et al*., 1995). Adel et al., (2011) reported that tablets made from rice husk MCC had higher tensile strength than that made from bean hull MCC. The difference in compressibility of rice and bean hull MCC powder is probably due to the difference in their DP and/or particle morphology. SEM image of rice husk MCC showed that irregular shapes. This irregular shape of rice husk MCC provides mechanical interlocking to strengthen MCC compacts. The DP of MCC was higher the tensile strength of the MCC tablet was lower. The DP of bean hull MCC was higher than that of rice husk MCC. Other study also shows that tablets made from rice straw MCC had higher tensile strength than that made from bagasse MCC (El-Sakhawy, and Hassan, 2007). The tensile strength of MCC powder is higher for the finest particle size. Most of the time, a decrease in particle size results in an increase in surface area available for bonding which eventually leads to increased tensile strength (Alfa, *et al*., 2017). The tensile strength of tablets depends on the area of intimate contact between particles and the attractive forces over the entire contacting area (Cabiscol, *et al*., 2018; El-Sakhawy, and Hassan, 2007). Alfa, et al., (2017), reported that in MCC from Andropogon Stalks , about 75% of the particles size fraction is found to be within 0 to 91.25 µm range whereas that of MCC from Sorghum is within 0 to 140 µm. The median particle diameters were 52.50 µm and 80.0 µm for Andropogon Stalks MCC and Sorghum MCC, respectively. Andropogon Stalks shows that high tensile strength than Sorghum MCC based tablets because of finest particles.

Tablet crushing strength gives an indication of the ability of tablets to withstand pressure. Measurements of crushing strength can also be important tool for the selection of potential direct compression excipient (Ohwoavworhua and Adelakun, 2010). The crushing strength of tablets prepared from CH-MCC, CC-MCC, LH-MCC and Avicel PH-101 were in the order of Avicel PH-101 tablets >LH-MCC > CH-MCC>CC-MCC at different compression forces. This result may be due to high bulk density of Avicel PH-101 than MCC from LH, CH, and CC. Crushing strength of MCC is not only affected by bulk density and crystallinity index but also DP. The DP of MCC was higher the crushing strength of the MCC tablet was lower (Doelker *et al*., 1987; El-Sakhawy and Hassan, 2007).

Friability is related to the strength of the tablets and its ability to withstand abuse during normal handling, packaging and transportation. Such abuses can lead to capping, chipping, abrasion or even breakage of the tablets. The friability test values of MCC tablets must be less than 1 % (Ohwoavworhua and Adelakun, 2010; Doelker *et al*., 1987). Except CF1, the friability of all formulation of CH-MCC, CC-MCC, LH-MCC, and Avicel PH-101 were less than 1%. The relatively low weight loss of all compacts of MCC could be due to the strength of all compacts. All compacts (except CF1) of Avicel PH-101 tablets had a relatively low value of friability. This was due to their high tensile and crushing strength. In general, at comparable crushing strength, all MCC tablets had comparable percentage friability.

According to British Pharmacopeia the disintegration limit of conventional drugs are 15 min (BP, 2009). Tablets containing MCC disintegrate rapidly in water because of the swelling capacity of the MCC particles and destruction of the bonding forces holding them together (Ejikeme, 2008). All formulation of CH-MCC, and CC-MCC, shows low disintegration time than LH-MCC, and Avicel PH-101. This was due to low crystalinity and high porosity of the compacts. The disintegration time of MCC tablets can be affected by not only porosity but also compaction forces. Yassin et al., (2015) reported that MCC tablets that have 40% porosity break apart after approximately 15s. However, MCC tablets that have 10% porosity retain their shape throughout the experiment and do not break within 3.5min. This result due to the difference of the magnitude of compaction forces that act on the MCC powder during the tableting process. To produce MCC tablets that have 10% porosity approximately 7.0 kN of force was applied, in contrast only 0.4 kN forces was applied for 40% porous MCC tablets. The disintegration time of all MCC tablets increased with an increase in compaction force. Doelker, et al., (1987), stated that disintegration time is very rapid up to a certain compaction pressure, beyond which it strongly increases.

Table 8. Crushing strength, tensile strength, friability, and disintegration of plain tablets of CH-MCC,CC-MCC,LH-MCC, and Avicel PH-101

Excipients	Parameters	CF1	CF2	CF3	CF4	CF5
MCC-CH	Crushing strength (N)	20.66±0.88	47.04±5.76	69.776±8.532	101.44±6.07	128.968±9.64
	Tensile strength (Kg/cm2)	2.78 ± 0.49	5.01±0.54	6.94±0.58	8.87±0.62	11.99±0.39
	Friability (%)	1.4	0.8	0.7	0.5	0.3
	Disintegration time (min)	0.3±0.33	0.37±0.068	1.78±0.073	2.56±0.41	4.34±0.195
MCC-CC	Crushing strength (N)	18.37±1.18	38.02±8.49	57.193±6..79	88.664±4.77	102.148±748
	Tensile strength (Kg/cm2)	2.31±0.34	4.97±0.47	6.01±0.39	8.07±0.74	10.87±0.65
	Friability (%)	1.12	0.77	0.64	0.4	0.3
	Disintegration time (min)	0.22±0.023	0.32±0.067	1.67±0.34	2.97±1.08	4.92±1.02
MCC-LH	Crushing strength (N)	22.06±0.79	51.42±7.66	70.69±7.52	97.02±7.22	115.51±6.739
	Tensile strength (Kg/cm2)	3.1± 0.54	6.27±0.49	8. 33 ±0.68	9.94±0.59	13.89±0.81
	Friability (%)	1	0.8	0.6	0.5	0.4
	Disintegration time (min)	0.34±0.015	0.88±0.331	2,25±0.868	4.54±1.06	5.34±1.04
Avicel PH-101	Crushing strength (N)	45.144±4.08	72.072±6.6	101.2±5.33	122.56±4.88	148.047±8.06
	Tensile strength (Kg/cm2)	5.11±0.58	8.44±0.77	11.06±0.87	14.01±0.91	18.7±0.69
	Friability (%)	1.1	0.7	0.6	0.4	0.3
	Disintegration time (min)	0.8±0.17	1.07±0.074	2.16±0.167	4.19±1.04	5.7±1.08

CF = target crushing strength: CF1 (50N), CF2 (75N), CF3 (100N), CF4 (125N) and CF5 (150N).

5.11.4. Weight variation and thickness

The weights of the tablets were within acceptable range of weight variation (± 7.5%) as per the British Pharmacopoeia for tablets weighing more than 80 mg or less than 250 mg (BP, 2009). MCC tablets shows good weight uniformities, and there were no any significant variations ($P > 0.05$) in the mean tablet thickness of all formulations, this is because of MCC powders have high compressibility and compactability (Doelker *et al*., 1987).

Table 9. Mebendazole tablet weight and thickness at different mebedazole and MCC concentration

Parameters	Drug: Excipient conc.	CH-MCC	CC-MCC	LH-MCC	Avicel PH-101
Weight (mg)	1:1	194.32±5.053	192.36±4.73	200±5.33	201.44±6.41
	1:2	194.4±7.82	193.76±8.6	198.76±8.6	199.1±5.01
	1:3	199.52±7.81	194.44±8.08	201.26±5.93	197.74±4.97
	1:4	197.3±3.25	196.7±6.11	197.46±7.63	200.54±3.88
Thickness (mm)	1:1	4.256±0.05	4.3±0.046	4.28±0.033	4.34±0.023
	1:2	4.334±0.053	4.36±0.011	4.29±0.046	4.13±0.43
	1:3	4.343±0.059	4.38±0.053	4.43±0.05	4.44±0.033
	1:4	4.412±0.033	4.38±0.034	4.33±0.053	4.37±0.019

5.11.5. Dilution potential

Dilution Potential is the ability of directly compressible excipients to carry high amounts of active pharmaceutical ingredient and it measure the proportion of poorly compactible drug which can be incorporated into an excipient to produce satisfactory (sufficient mechanical strength) tablets (Rojas *et al*., 2013). Dilution potential depends on the compaction behavior of the excipients and API. MCC exhibits the highest capacity of active pharmaceutical ingredient (Habib *et al*., 1996). This is due to plastic deforming materials tend to have better dilution potential than that of brittle fracture deforming (elastic) materials (Almaya and Aburub, 2008). Dilution potential of CH-MCC, CC-MCC, LH-MCC, and Avicel PH-101 was evaluated using mebendazole as a model drug at a fixed compression force. Mebendazole is BCS class II drug, is a common benzimidazole anthelmintic used in the treatment of ascariasis, uncinariasis, oxyuriasis, trichuriasis and more than one worm infection at a time (Kumar *et al*., 2008). According to Haruna et al., (2020), the dilution potential of MCC is up to 60% of API. It is higher than that of other excipients. According to the tensile strength of tablets in the present study, MCC-LH and Avicel PH-101 shows closely related dilution capacity for the model drug used. Yet CC-MCC has lower dilution potential than Avicel PH-101, LH-MCC, and CH-MCC.

5.11.6. Crushing strength, tensile strength and friability

MCC containing tablet formulations have good hardness/tensile strength and can also disintegrate rapidly in water due to MCC particles have high swelling capacity and the interruption of the hydrogen bonding (Nwachukwu *et al*., 2015; Nwajiobi *et al*., 2019).
The hardness/crushing strength of mebendazole tablets containing CH-MCC, CC-MCC, LH-MCC and Avicel PH-101 increase, as the amount of MCC in the tablet increased. In addition to this the hardness of tablets also increased with increase weight and thickness of the tablet. This is in accordance with Nwachukwu et al., (2015) investigation, the hardness of ciprofloxacin tablet found to increase as the quantity of MCC contained in the tablet increased and the weight and thickness/height of tablets increased.

The mean crushing strength values were between 40.16 and 69.94N for all tablets of all mebendazole concentrations; hardness values greater than or equal to 40N are considered to be the minimum for a satisfactory tablet. In addition to this USP specification describes that, directly compressible tablets should have the hardness of 4 to 10 KN (40-100N) (USP/NF, 2007).

The tensile strength describes the mechanical strength that present in a tablet in relation to the proportionality of its hardness to the surface area and thickness of the tablets (Nwachukwu *et al*., 2015). The tensile strength of mebendazole containing CH-MCC, CC-MCC, LH-MCC, and Avicel PH- 101 tablets are depicted in table 10. CC-MCC exhibits low tensile strength than LH-MCC and CH-MCC at all concentration of mebendazole. Avicel PH-101 gave tablets with high tensile strength than LH-MCC, CH-MCC and CC-MCC at 20, 25, 33 and 50% of mebendazole concentrations. However, there are no significant ($P > 0.05$) differences between the tensile strength of all tablets. The tensile strength of mebendazole tablets formulated with CH-MCC, CC-MCC, LH-MCC, and Avicel PH-101 decreased as the proportion of mebendazole in the formulation increased. This is due to mebendazole decreases the plastic recovery of MCC (Haruna *et al*., 2020).

The friability test is one of the confirmatory tests whether the prepared tablets can withstand the physical force like to capping, chipping, abrasion or even breakage during transportation or not (Setu *et al*., 2014). According to BP the weight loss of conventional tablets should be less than

1.0% of their weight (BP, 2009). As can be seen in the table 10 the friability value of CH-MCC-mebendazole, CC-MCC-mebendazole, LH-MCC-mebendazole, and Avicel PH-101-mebendazole tablets were within the range. The concentration of mebendazole increases the friability of tablets also increase. This may be due to the low hardness value of tablets that has high concentration of mebendazole.

Table 10. Crushing strength, Tensile strength and friability of tablets prepared from different concentration of mebendazole

Samples	Parameters	Mebendazole concentration			
		50%	33%	25%	20%
CH-MCC	CS(N)	41.18±0.74	46.84±0.83	50.71±0.278	60.96±0.249
	TS(Kg/cm^2)	7±0.88	7.9±1.03	8.5±0.98	10±1.36
	Friability (%)	0.72	0.66	0.5	0.34
CC-MCC	CS(N)	40.16±0.456	44.1±0.44	50.18±0.829	58.82±1.276
	TS(Kg/ cm^2)	6.6±0.93	7.4±0.75	8.4±1.22	9.8±0.99
	Friability (%)	0.68	0.5	0.4	0.4
LH-MCC	CS(N)	43.67±1.195	51.27±0.397	59.31±1.093	63.92±0.919
	TS(Kg/ cm^2)	7.2±0.64	8.4±0.58	9.7±0.93	10.7±0.78
	Friability (%)	0.82	0.55	0.35	0.25
Avicel PH-101	CS(N)	46.26±0.68	54.49±1.09	61.74±1.67	69.58±1.22
	TS(Kg/ cm^2)	7.7±.058	9.6±0.86	10.08±1.26	11.6±0.98
	Friability (%)	0.57	0.44	0.4	0.31

Mean ± SD (n = 10), CS: crushing strength, TS: tensile strength.

5.11.7. Disintegration time of directly compressed mebendazole tablets

Evaluation of disintegration time is a key step in formulation development, manufacturing, and clinical practice (Nwachukwu *et al*., 2015). Disintegration of tablets occurs when water molecules penetrate in to the interparticular capillary pores of MCC (Lowenthal, 1972; Nwachukwu *et al*., 2015). Therefore, the disintegration time of tablets depends on hardness and porosity. In this study, the disintegration times of mebendazole loaded CH-MCC, CC-MCC, LH-MCC, and Avicel PH-101 tablets were less than 15 min, which is recommended for conventional dosage forms in the USP/NF specification (USP 30/NF 25, 2007).

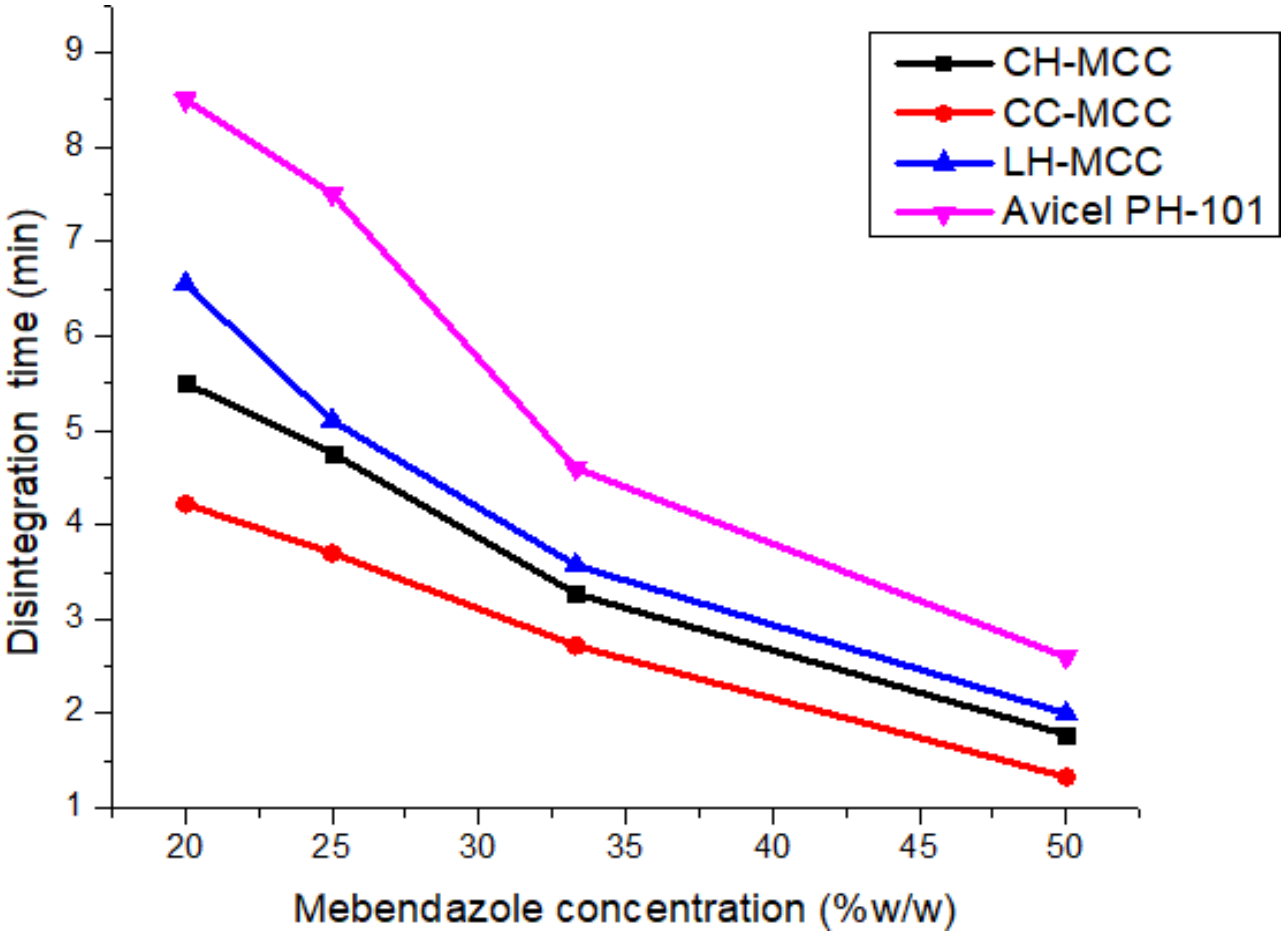

Fig. 19. Effects of mebendazole concentration on the disintegration times of tablets containing, CH-MCC, CC-MCC, LH-MCC and Avicel PH-101.

As can be seen in Figure 19 there is no significant differences between the disintegration time of tablets prepared from CH-MCC, CC-MCC, LH-MCC and Avicel PH-101 at all concentrations of mebendazole. However, Avicel PH-101 and LH-MCC shows the delayed disintegration time than CH-MCC and CC-MCC. This is because of their high crystalinity index and low porosity values. The disintegration time of all tablets prepared from CH-MCC, CC-MCC, LH-MCC, and Avicel PH-101 increased up on increasing of MCC concentration. This may be due to the tablet hardness increases when the concentration of MCC increased (Alfa *et al*., 2006).

5.11.8. UV calibration curve of mebendazole

The absorbance (λ at 260nm) versus concentration of mebendazole in 0.1N HCL containing 1% SLS plot provided a calibration curve with a linear regression equation of Y = 0.069X + 0.078 (Y is the absorbance and X is the concentration in µg/ml). The correlation coefficient (r^2) 0.9998 was obtained as seen in Figure 20.

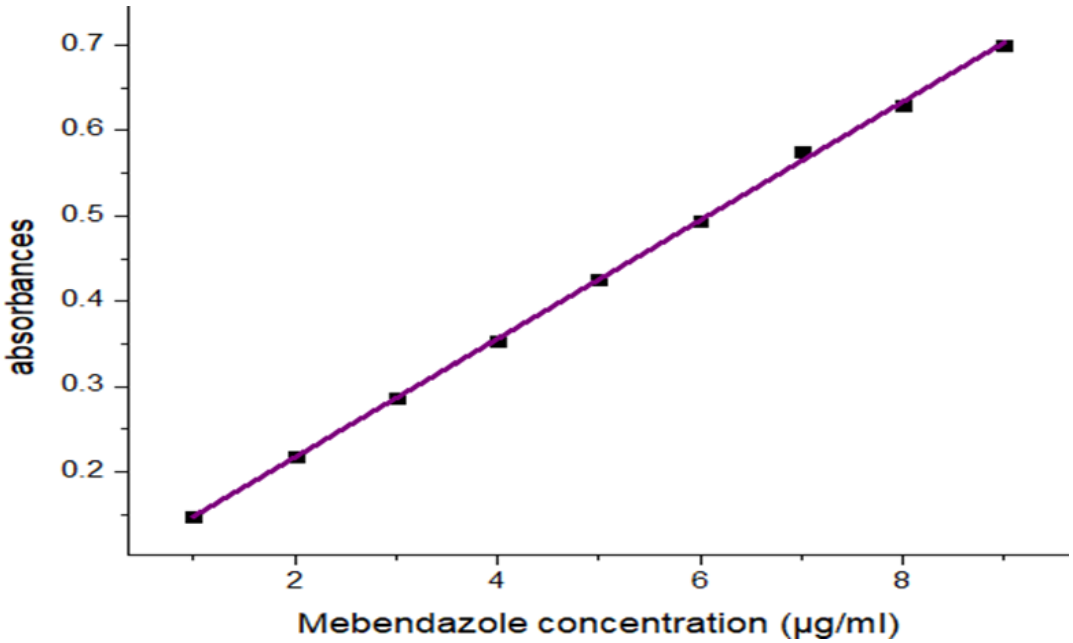

Fig. 20. Absorbance of mebendazole in 0.1_N HCL and 1% SLS at 260nm with 95% confidence level (R^2=0.9998).

5.11.9. Dissolution of directly compressed mebendazole tablets

Dissolution of directly compressible drugs is a necessary criterion for determination of drug bioavailability. It is also used as the single most important control test for assuring batch-to-batch bioequivalence, once the bioavailability of directly compressible tablets determined (Swanepoel *et al*., 2003). The dissolution of the drugs influenced by the physical characteristics of the drug, the wettability of the drug, the penetration ability of the dissolution medium, the disintegration, disaggregation and swelling process of the dosage forms(Alfa *et al*., 2006).

The dissolution profiles of the mebendazole tablets prepared from 1:1, 1:2, 1:3, and 1:4 of mebendazole and CH-MCC, CC-MCC, LH-MCC, and Avicel PH-101 are shown in Figure 21.

All formulations that contain different concentrations of CH-MCC, CC-MCC, LH-MCC, Avicel PH-101, and mebendazole fulfilled USP/NF specification (USP 30/NF 25, 2007). According to the USP specification not less than 75% of the drug must be released from the tablet within 120 min.

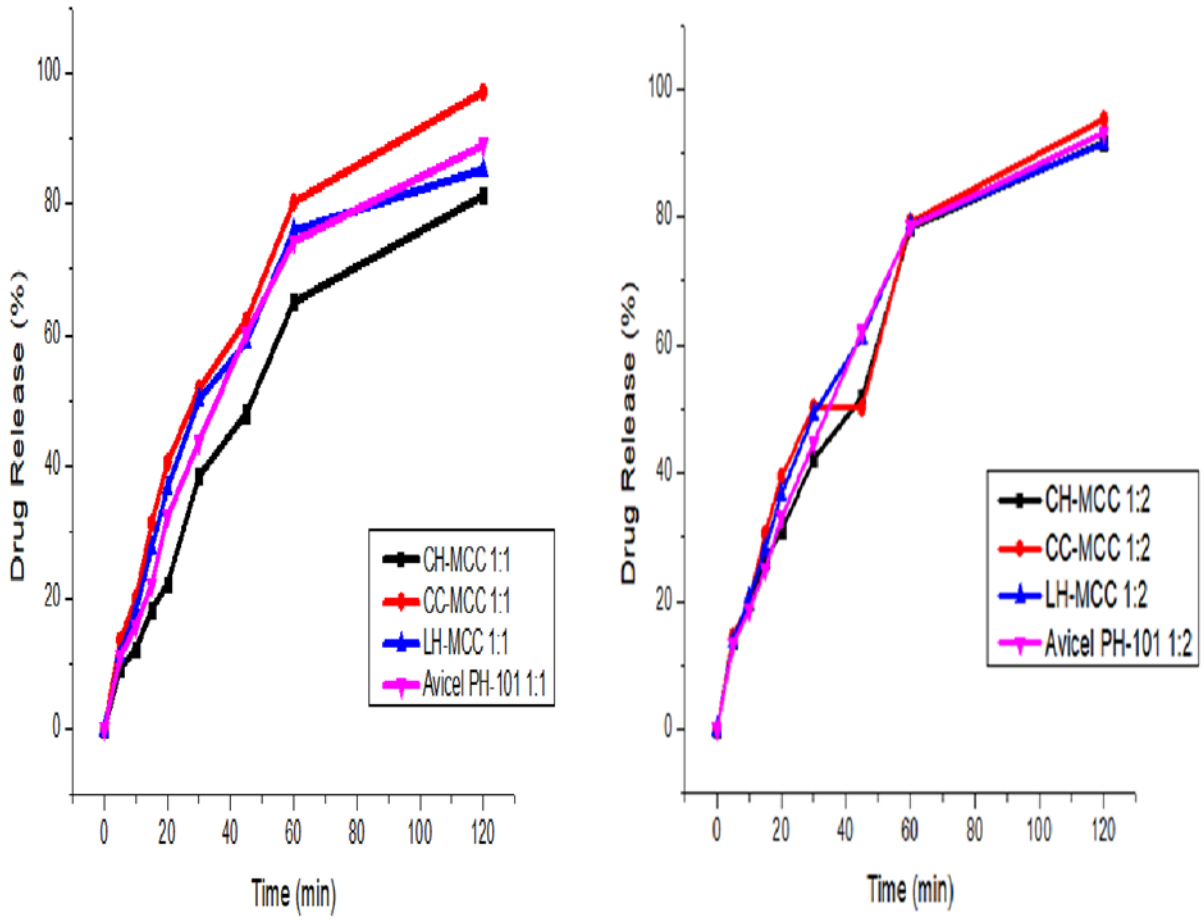

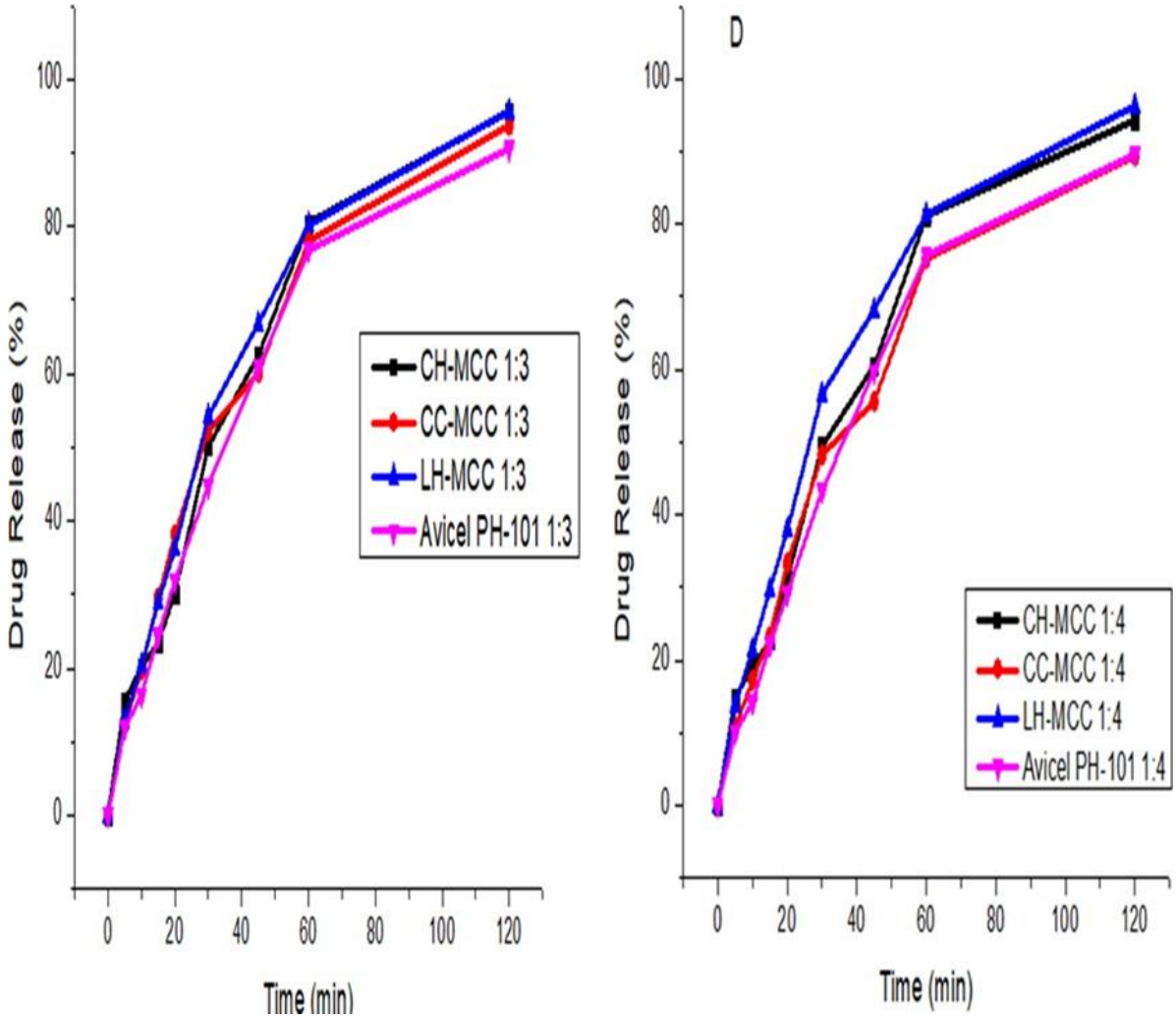

Fig. 21. Dissolution profile of mebendazole loaded CH-MCC, CC-MCC, LH-MCC, and Avicel PH-101 tablets

CONCLUSIONS

Cellulose fibers were isolated from three lignocellulosic plant by-products: corn husk, corn cob and lupine husk through steam exposure and alkaline treatment method. Corn husk yielded the highest cellulose content and corn cob the lowest. The FTIR spectra of both cellulose and MCC from the three sources were comparable. The CI was increased with HCl catalyzed hydrolysis of the isolated cellulose. The SEM images of MCC from the three sources were almost identical to the image of Avicel PH-101. Moisture sorption property, moisture content, ash value, water soluble substances and DP values of MCC from corn husk, corn cob, and lupine husk were within the range set for Avicel PH-101. However, CH-MCC, CC-MCC, and LH-MCC showed slightly lower bulk densities, and tap densities, higher Hausner ratio and Carr's index indicating relatively poor flow in comparison to Avicel PH101. The prepared corn husk, corn cob and lupine husk MCC powders showed better tolerance for lubrication with magnesium stearate than Avicel PH-101. With respect to dilution potential, CH-MCC, CC-MCC, and LH-MCC were able to accommodate 50% of mebendazole with acceptable tablet properties at fixed compression force. Mebendazole loaded MCC tablets exhibited acceptable crushing strength, tensile strength, friability, disintegration, and in-vitro drug release properties. The CH-MCC, CC-MCC, and LH-MCC fulfilled almost all required characteristics of pharmaceutical excipients. Therefore, it is possible to conclude that MCC from CH, CC, and LH can be promising alternative sources of MCC for pharmaceutical applications.

SUGGESTIONS FOR FURTHER WORK

The followings are suggested for further studies:

- Co-processing MCC with other excipients to improve the flow property
- Produces different grades of MCC
- Blending various grades of MCC to design robust formulation.
- Long- and short- term stability studies

REFERENCES

Abu-Thabit, N.Y., Judeh, A.A., Hakeem, A.S., Ul-Hamid, A., Umar, Y. and Ahmad, A., (2020). Isolation and characterization of microcrystalline cellulose from date seeds (Phoenix dactylifera L.). *Int. J. Biol. Macromol.* **155**:730-739.

Adel, A.M., Abd El-Wahab, Z.H., Ibrahim, A.A. and Al-Shemy, M.T., (2011). Characterization of microcrystalline cellulose prepared from lignocellulosic materials. Part II: Physicochemical properties. *Carbohydr. Polym*. **83**:676–687.

Aftab, M.N., Iqbal, I., Riaz, F., Karadag, A. and Tabatabaei, M., (2019). Different Pretreatment Methods of Lignocellulosic Biomass for Use in Biofuel Production. In Biomass for Bioenergy-Recent Trends and Future Challenges. *IntechOpen.*

Agatonovic-Kustrin, S., Glass, B.D., Mangan, M. and Smithson, J., (2008). Analysing the crystal purity of mebendazole raw material and its stability in a suspension formulation. *Int. J. Pharm*. **361**:245-250.

Ahmad, Z., Roziaizan, N.N., Rahman, R., Mohamad, A.F. and Ismail, W.I.N.W., (2016). Isolation and characterization of microcrystalline cellulose (MCC) from rice husk (RH).

Alfa J., Chukwu A. and Udeala O. K. (2017). Compression and Compaction Behaviour of Microcrystalline Cellulose from Sorghum and Andropogon Stalks. *JPRI* .**19**:1-11.

Alfa J., OdeniyI M. A., and Jaiyeob K. T. (2006). Direct Compression Properties of Microcrystalline Cellulose and Its Silicified Product. *East Cent. Afr. J. Pharrn. Sci*. **7**:56-59.

Almaya, A., and Aburub A., (2008). Effect of Particle Size on Compaction of Materials with Different Deformation Mechanisms with and without Lubricants. *AAPS PharmSciTech*. **9**: 414-418.

Aly, S.A.S., (2012). Tabletting Properties and Physical Interaction of Microcrystalline Cellulose with Magnesium Stearate in a Mixture Under Compression/Mikro-kristalin selülozun tabletleme özellikleri ve basim sirasinda karisimin magnezyum stearat ile fiziksel etkilesimi. *FABAD J. Pharm. Pharm. Sci*.**37**: 183.

Amin, F.R., Khalid, H., Zhang, H., u Rahman, S., Zhang, R., Liu, G. and Chen, C., (2017). Pretreatment methods of lignocellulosic biomass for anaerobic digestion. *Amb Express*.7:72.

Aprilia N.A., (2016).Physicochemical characterization of microcrystalline cellulose extracted from Kenaf Bast. *Bio Resources*. **11**:3875-3889.

Azeze, H., Mekbib, F., Dessalegn, Y., Tadele, Z. and Megersa, N., (2016). Challenges on production and utilization of white lupin (Lupinus albus L.) in Ethiopia: A strategic orphan crop. American Journal of Experimental Agriculture. A Strategic Orphan Crop. *AJEA*. **13**: 1-14.

Azubuike, C.P. and Okhamafe, A.O., (2012). Physicochemical, spectroscopic and thermal properties of microcrystalline cellulose derived from corn cobs. *Int. j. recycl. org. waste agric*. **1:**9.

Baruah, J., Nath, B.K., Sharma, R., Kumar, S., Deka, R.C., Baruah, D.C. and Kalita, E., (2018). Recent trends in the pretreatment of lignocellulosic biomass for value-added products. *Front Energy Res.* **6**:141.

Battegazzore, D., Bocchini, S., Alongi, J., Frache, A. and Marino, F., (2014). Cellulose extracted from rice husk as filler for poly (lactic acid): preparation and characterization. *Cellulose*. **21**: 1813-1821.

Behera, S., Arora, R., Nandhagopal, N. and Kumar, S., (2014). Importance of chemical pretreatment for bioconversion of lignocellulosic biomass. *Renew. Sust. Energ. Rev*. **36**: 91–106.

British Pharmacopoeia. (2009). British Pharmacopoeia: The Pharmaceutical Press, HerMajesty‟s Stationery Office, London, vol. I–VI.

Cabiscol, R., Finke, J.H., Zetzener, H. and Kwade, A., (2018). Characterization of mechanical property distributions on tablet surfaces. *Pharmaceutics*.**10**: 184.

Cao, P., Lu, C. and Yu, Z., (2017). Agricultural nitrogen fertilizer uses in the continental US during 1850–2015: a set of gridded time-series data, PANGAEA.

Chauhan, A., Saxena, D.C. and Singh, S., (2016). Physical, textural, and sensory characteristics of wheat and amaranth flour blend cookies. Cogent Food & Agriculture. 2: 1125773.

Ching, Y.C. and Ng, T.S., (2014). Effect of preparation conditions on cellulose from oil palm empty fruit bunch fiber. *BioResources*. ***9*:** 6373-6385.

Choi, M., Kang, Y.R., Lim, I.S. and Chang, Y.H., (2018). Structural characterization of cellulose obtained from extraction wastes of Graviola (Annona muricata) leaf. *Prev Nutr Food Sci*. **23**:166.

Collazo-Bigliardi, S., Ortega-Toro, R. and Boix, A.C., (2018). Isolation and characterization of microcrystalline cellulose and cellulose nanocrystals from coffee husk and comparative study with rice husk. *Carbohydr. Polym.* **191**: 205-215.

Costa L.A, Assis J.D, Gomes V.P.G, de Silva B.A.J, Fonsêcac F.A and Druzian I.J (2015). Extraction and characterization of nanocellulose from corn stover. Materials Today: Proceedings. **2**:287-294.

Deraman, M., Zakaria, S. and Murshidi, J.A., (2001). Estimation of crystallinity and crystallite size of cellulose in benzylated fibres of oil palm empty fruit bunches by X-ray diffraction. Jpn. *J. of Appl. Phys*. **40:**3311.

Doelker E., D. Mordier, H. Iten2 and P. Humbert-Dro (1987). Comparative tableting properties of sixteen microcrystalline celluloses. *Drug Dev Ind Pharm*. **13**:1847-1875.

Doelker. E (1993). Comparative compaction properties of various microcrystalline cellulose types and generic products. *Drug Dev Ind Pharm*.**19**:2399-2471.

Doelkerl E., D. Maswellel, F. Veuillezl and P. Humbert-Droz (1995). Morphological, packing, flow and tableting properties of new avicel types. *Drug Dev Ind Pharm*.**21**: 643-661.

Ejikeme, P.M., (2008). Investigation of the physicochemical properties of microcrystalline cellulose from agricultural wastes I: Orange mesocarp. *Cellulose*. **15**:141-147.

Eraga, S.O., Arhewoh, M.I., Uhumwangho, M.U. and Iwuagwu, M.A., (2015). Characterisation of a novel, multifunctional, co-processed excipient and its effect on release profile of paracetamol from tablets prepared by direct compression. *Asian Pac J Trop Biomed*. **5**: 768–772.

FMC (2003). Avicel® PH-101microcrystalline cellulose NF, Ph. Eur., JP. FMC Corporation, Philadelphia.

Gohel M. C., and Pranav D Jogani (2005). A review of co-processed directly compressible excipients. *J Pharm Pharmaceut Sci.* **8:**76-93**.**

Greenspan, L., (1977). Humidity fixed points of binary saturated aqueous solutions. *J Res Natl Bur Stand*.**81**89-96.

Haafiz, M.M., Eichhorn, S.J., Hassan, A. and Jawaid, M., (2013). Isolation and characterization of microcrystalline cellulose from oil palm biomass residue. *Carbohydr. Polym*. **93**:628–634.

Habib, Y., Augsburger, L., Reier, G., Wheatley, T. and Shangraw, R., (1996). Dilution potential: a new perspective. *Pharm. Dev. Tech.* **1**: 205–212.

Hallac, B.B. and Ragauskas, A.J., (2011). Analyzing cellulose degree of polymerization and its relevancy to cellulosic ethanol. *Biofuel Bioprod Biorefin*. **5**:215-225.

Haque, S.M., Chowdhury, A.A., Rana, A.A., Masum, S.M., Ferdous, T., Rashid, M.A., Sarker, M. and Karim, M.M., (2015). Synthesis of microcrystalline cellulose from pretreated cotton obtained from Bombax ceiba L. and its characterization. *Bangladesh J. Sci. Ind. Res*. **50**:199-204.

Haque, S.M., Chowdhury, A.A., Rana, A.A., Masum, S.M., Ferdous, T., Rashid, M.A., Sarker, M. and Karim, M.M., (2015). Synthesis of microcrystalline cellulose from pretreated cotton obtained from Bombax ceiba L. and its characterization. *Bangladesh J Sci Ind Res*. 50: 199-204.

Haruna, F., Apeji, Y.E., Oparaeche, C., Oyi, A.R. and Gamlen, M., (2020). Compaction and tableting properties of composite particles of microcrystalline cellulose and crospovidone engineered for direct compression. *Future J. Pharm. Sci*. **6**.35.

Honorato, S.B., Farfan, S., Viana, A., Camarão, G.C., Fechine, F.V., Moraes, M.E., Moraes, M.O., Ferro, M., Dabbene, V., Cuffini, S.L. and Ayala, A.P., (2012). Polymorphism evaluation in generic tablets containing mebendazole by dissolution tests. *J Braz Chem Soc*. **23**: 220-227.

Ibrahim M. M., Waleed K. El-Zawawy a, Yasser R. Abdel-Fattah b, Nadia A. Soliman b, Foster A. Agblevor (2011). Comparison of alkaline pulping with steam explosion for glucose production from rice straw. *Carbohydr Polym*. **83**:720–726. *In MATEC Web of Conferences*. **47**: 05013. EDP Sciences.

Jahan M. S., Saeed A., He Z., Ni Y (2011). Jute as raw material for the preparation of microcrystalline cellulose. Cellulose .**18**:451–459.

Jedvert, K. and Heinze, T., (2017). Cellulose modification and shaping–a review. *J Polym Eng*. **37**: 845–860.

Johar N, Ahmad I, Dufresne A (2012). Extraction, preparation and characterization of cellulose fibres and nanocrystals from rice husk. *Industrial Crops and Products.* **37**: 93–99.

Jönsson, L.J. and Martín, C., (2016). Pretreatment of lignocellulose: formation of inhibitory by-products and strategies for minimizing their effects. *Bioresource Technol*. **199**: 103-112.

Kale, R.D., Bansal, P.S. and Gorade, V.G., (2018). Extraction of microcrystalline cellulose from cotton sliver and its comparison with commercial microcrystalline cellulose. *J Polym Environ*. **26**: 355-364.

Kalita D.R, Natha Y, Ochubiojo E.M, Buragohain K.A (2013). Extraction and characterization of microcrystalline cellulose from fodder grass; Setaria glauca (L) P. Beauv, and its potential as a drug delivery vehicle for isoniazid, a first line antituberculosis drug. *Colloids and Surfaces B: Biointerfaces*. **108:** 85– 89.

Kambli, N., Basak, S., Samanta, K.K. and Deshmukh, R.R., (2016). Extraction of natural cellulosic fibers from cornhusk and its physico-chemical properties. *Fibers Polym*. **17**:687-694.

Kambli, N.D., Mageshwaran, V., Patil, P.G., Saxena, S. and Deshmukh, R.R., (2017). Synthesis and characterization of microcrystalline cellulose powder from corn husk fibres using bio-chemical route. *Cellulose*. **24**:5355-5369.

Kambli, N.D., Samanta, K.K., Basak, S., Chattopadhyay, S.K., Patil, P.G. and Deshmukh, R.R., (2018). Characterization of the corn husk fibre and improvement in its thermal stability by banana pseudostem sap. *Cellulose*.**25**:5241-5257.

Kampeerapappun, P., (2015). Extraction and characterization of cellulose nanocrystals produced by acid hydrolysis from corn husk. *J. Met. Mater. Miner*. **25**.

Karande, V.S., Bharimalla, A.K., Hadge, G.B., Mhaske, S.T. and Vigneshwaran, N., (2011). Nano fibrillation of cotton fibers by disc refiner and its characterization. *Fibers Polym*. **12**: 399.

Karimi, K. and Taherzadeh, M.J., (2016). A critical review on analysis in pretreatment of lignocelluloses: Degree of polymerization, adsorption/desorption, and accessibility. *Bioresource Techno*. **203**:348-356.

Keck, C.M. and Müller, R.H., (2008). Size analysis of submicron particles by laser diffractometry- 90% of the published measurements are false. *Int. J. Pharm.* **355**:150-163.

Khalil, H.A., Bhat, A.H., Bakar, A.A., Tahir, P.M., Zaidul, I.S.M. and Jawaid, M., (2016). Cellulosic nanocomposites from natural fibers for medical applications: A review. In Handbook of polymer nanocomposites. Processing, performance and application (pp. 475-511). Springer, Berlin, Heidelberg.

Khalil, H.A., Lai, T.K., Tye, Y.Y., Paridah, M.T., Fazita, M.N., Azniwati, A.A., Dungani, R. and Rizal, S., (2018). Preparation and characterization of microcrystalline cellulose from sacred Bali bamboo as reinforcing filler in seaweed-based composite film. *Fibers Polym*. **19**:423-434.

Kian L.K., Jawaid M., Ariffin H., Alothman O.Y., (2017). Isolation and characterization of microcrystalline cellulose from roselle fibers. *Int. J. Biol. Macromol*. **103**:931–940.

Klemm, D., Heublein, B., Fink, H.P. and Bohn, A., (2005). Cellulose: Fascinating Biopolymer and Sustainable Raw Material Dieter. *Angew. Chem. Int. Ed.* **44**: 3358 -3393.

Kohajdova, Z., KaroVičoVá, J. and Schmidt, Š., (2011). Lupin composition and possible use in bakery-a review. *Czech J Food Sci*.**29**: 203-211.

Krivokapić, J., Ivanović, J., Djuriš, J., Medarević, D., Potpara, Z., Maksimović, Z. and Ibrić, S., (2020). Tableting properties of microcrystalline cellulose obtained from wheat straw measured with a single punch bench top tablet press. *Saudi Pharm J*. **28**: 710-718.

Krstic, M., Maksimovic, Z., Ibric, S., Bakic, T., Prodanovic, J. and Razic, S., (2018). Lignocellulosic biomass as a source of microcrystalline cellulose–chemical and technological characterization and future perspectives. *Cellulose Chem. Technol*. **52**: 577-588.

Kumar, P., Barrett, D.M., Delwiche, M.J. and Stroeve, P., (2009). Methods for pretreatment of lignocellulosic biomass for efficient hydrolysis and biofuel production. *Ind. Eng. Chem. Res*.**48**:3713-3729.

Kumar, S., Chawla, G. and Bansal, A.K., (2008). Spherical crystallization of mebendazole to improve processability. *Pharm Dev Technol*.**13**:559-568.

Kuthi, F.A.A., Norzali, N.R.A.A. and Badri, K.H., (2016). Thermal characteristics of microcrystalline cellulose from oil palm biomass. *MJAS*. **20**:1112-1122.

Leppanen K, Seppo Andersson, Mika Torkkeli, Matti Knaapila, Nina Kotelnikova ,Ritva Serimaa (2009). Structure of cellulose and microcrystalline cellulose from various wood species, cotton and flax studied by X-ray scattering. *Cellulose*.**16**:999–1015.

Lida K., Aoki K., Danjo K., Otsuka A., Chen Y.C., and Horisawa E. (1997). A comparative evaluation of the mechanical property of various cellulose. *Chem. Pharm. Bull*. **45**:217-220.

Liu Y., Ailu Liu a, Salam A. Ibrahim b, Hong Yang a, Wen Huang (2018). Isolation and characterization of microcrystalline cellulose from pomelo peel. *Int. J. Biol. Macromol.* **111**: 717–721.

Liu, C.-F., Ren, J.-L., Xu, F., Liu, J.-J., Sun, J.-X., & Sun, R.-C. (2006). Isolation and Characterization of Cellulose Obtained from Ultrasonic Irradiated Sugarcane Bagasse. J. *Agric. Food Chem*. **54**: 5742–5748.

Lowenthal, W., (1972). Disintegration of tablets. *J P S*. ***61***:1695-1711.

Mansora, A.M., Lima, J.S., Anib, F.N., Hashima, H. and Hoa, W.S., (2019). Characteristics of cellulose, hemicellulose and lignin of MD2 pineapple biomass. *Chem. Eng. Trans*.**72**: 79-84.

Marques-Marinho, F.D. and Vianna-Soares, C.D., (2013). Cellulose and its derivatives use in the pharmaceutical compounding practice. In *Cellulose-Medical, Pharmaceutical and Electronic Applications*. IntechOpen.

Mihranyan, A., Llagostera, A.P., Karmhag, R., Strømme, M. and Ek, R., (2004). Moisture sorption by cellulose powders of varying crystallinity. *Int. J. Pharm*.**269**: 433-442.

Mishra, R.K., Sabu, A. and Tiwari, S.K., (2018). Materials chemistry and the futurist eco-friendly applications of nanocellulose: Status and prospect. *J. Saudi Chem. Soc*. 22: 949-978.

Mishra, R.K., Sabu, A. and Tiwari, S.K., (2018). Materials chemistry and the futurist eco-friendly applications of nanocellulose: Status and prospect. *J. Saudi Chem*.**22**: 949-978.

Mohamed El-Sakhawy, Mohammad L. Hassan (2007). Physical and mechanical properties of microcrystalline cellulose prepared from agricultural residues. *Carbohydr. Polym*. **67**: 1–10.

Morán, J.I., Alvarez, V.A., Cyras, V.P. and Vázquez, A., 2008. Extraction of cellulose and preparation of nanocellulose from sisal fibers. *Cellulose*. 15: 149-159.

Morsyleide, F.R., Medeiros, E.S., Malmonge, J.A., Gregorski, K.S., Wood, D.F., Mattoso, L.H.C., Glenn, G., Orts, W.J. and Imam, S.H., (2010). Cellulose nanowhiskers from coconut husk fibers: Effect of preparation conditions on their thermal and morphological behavior. *Carbohydr. Polym*. **81**:83–92.

Nadal, P., Canela, N., Katakis, I. and O'Sullivan, C.K., (2011). Extraction, isolation, and characterization of globulin proteins from Lupinus albus. *J. Agric. Food Chem*. **59**:2752-2758.

Nigussie, Z., (2012). Contribution of white lupin (Lupinus albus L.) for food security in North-Western Ethiopia: a review. *Asian J Plant Sci*. **11**: 200.

Nuruddin, M., Tcherbi-Narteh, A., Hosur, M., Chowdhury, R.A., Jeelani, S. and Gichuhi, P., (2013). Cellulose microfibrils extracted from wheat straw: a novel approach. Proceedings of the 45th ISTC.

Nwachukwu, N. and Ugoeze, K.C., (2018). Studies on microcrystalline cellulose obtained from saccharum officinarum 2: flow and compaction properties. *J Drug Deliv and Therap*. **8**:54-59.

Nwachukwu, N., Ugoeze, K.C., Okoye, A.C. and Chinaka, C.N., (2018). Application of microcrystalline cellulose from Saccharum officinarum as dry binder in ciprofloxacin tablet formulation. *J.Pharmacy & Bioreso*.**15**:48-55.

Nwadiogb, J.O., Igwe, A.A., Okoye, N.H. and Chime, C.C., (2015). Extraction and characterization of microcrystalline cellulose from mango kernel: A waste management approach. *DerPharmaChemica.***7**:1-7.

Nwajiobi, C.C., Otaigbe, J.O.E. and Oriji, O., (2019). Physicochemical, spectroscopic and tableting properties of microcrystalline cellulose obtained from the African breadfruit seed hulls. *.Afr. J. Biotechnol*. **18**: 371-382.

Ohwoavworhua, F.O. and Adelakun, T.A., (2010). Non-wood Fibre Production of Microcrystalline Cellulose from Sorghum caudatum: Characterisation and Tableting Properties. *Indian J Pharm Sci*. **72**: 295–301.

Pachuau, L., Dutta, R.S., Hauzel, L., Devi, T.B. and Deka, D., (2019). Evaluation of novel microcrystalline cellulose from Ensete glaucum (Roxb.) Cheesman biomass as sustainable drug delivery biomaterial. *Carbohydr. Polym*. **206**:336-343.

Pesonen, T., Paronen, P. and Puurunen, T., 1989. Evaluation of a novel cellulose powder as a filler-binder for direct compression of tablets. *Pharm Weekbl.* **11**: 13-19.

Pointner, M., Kuttner, P., Obrlik, T., Jager, A. and Kahr, H., (2014). Composition of corncobs as a substrate for fermentation of biofuels. *Agron. Res*. **12**: 391-396.

Qian S.Zhang H,Sheng K(2017). Cellulose Nanowhiskers from Moso Bamboo Residues: Extraction and Characterization. *Bio Resources*. **12**:419-433.

Ranganagowda, R.P.G., Kamath, S.S. And Bennehalli, B., (2019). Extraction and Characterization of Cellulose from Natural Areca Fiber. *MSRI*.**16**:86-93.

Rasheed, M., Jawaid, M., Karim, Z. and Abdullah, L.C., (2020). Morphological, Physiochemical and Thermal Properties of Microcrystalline Cellulose (MCC) Extracted from Bamboo Fiber. *Molecules*. **25**: 2824-2838.

Reddy, K.O., Uma Maheswari, C., Muzenda, E., Shukla, M. and Rajulu, A.V., (2016). Extraction and Characterization of Cellulose from Pretreated Ficus (Peepal Tree) Leaf Fibers. *J. Nat. Fibers*.**13**:54–64.

Rojas, J., Lopez, A., Guisao, S. and Ortiz, C., (2011). Evaluation of several microcrystalline celluloses obtained from agricultural by-products. *J. Adv. Pharm. Tech. Res*. **2**: 144-150.

Rojas, O. J., Liu, Y., Stein, H. H., (2013). Phosphorus digestibility and concentration of digestible and metabolizable energy in corn, corn co products, and bakery meal fed to growing pigs. *J. Anim. Sci*. **91**: 5326-5335.

Roque-Flores, R.L., de Oliveira, J.F., de Souza Carvalho, F.M. and do Rosário Matos, J., (2020). Characterization and kinetic studies of the thermal degradation of mebendazole polymorphs a and C. *J Pharm Innov*.**15**:116-124.

Sá R.M., Cleidiene Souza de Mirandaa, Nadia Mamede José (2015). Preparation and Characterization of Nano whiskers Cellulose from Fiber Arrowroot (Maranta arundinacea). *Mater. Res.* **18**: 225-229.

Šantl, M., Ilić, I., Vrečer, F. and Baumgartner, S., (2011). A compressibility and compactibility study of real tableting mixtures: the impact of wet and dry granulation versus a direct tableting mixture. *Int. J. Pharm*.**414**: 131 139.

Setu, M.N.I., Mia, M.Y., Lubna, N.J. and Chowdhury, A.A., (2014). Preparation of microcrystalline cellulose from cotton and its evaluation as direct compressible excipient in the formulation of naproxen tablets. *Dhaka Univ. J. Pharm. Sci***. 13**: 187-192.

Sheltami, R.M., Abdullah, I., Ahmad, I., Dufresne, A. and Kargarzadeh, H., (2012). Extraction of cellulose nanocrystals from mengkuang leaves (Pandanus tectorius). *Carbohydr. Polym*.**88:**772–779.

Shokri, J. and Adibkia, K., (2013). Application of cellulose and cellulose derivatives in pharmaceutical industries. In Cellulose-medical, pharmaceutical and electronic applications. IntechOpen.

Sun J.X., Sun, X.F., Zhao, H., Sun, R.C., (2004). Isolation and characterization of cellulose from sugarcane bagasse. *Polym. Degrad. Stab*. **84**: 331–339.

Sun, C.C., (2005). True density of microcrystalline cellulose. *J Pharm Sci.* **94**: 2132-2134.

Sun, C.C., (2008). Mechanism of moisture induced variations in true density and compaction properties of microcrystalline cellulose. *Int. J. Pharm*. **346**:93-101.

Suryadi, H., Angeline, M. and Murti, M.W., (2018). Characterization of microcrystalline cellulose obtained from enzymatic hydrolysis of alpha-cellulose and its application. *J Young Pharm*, **10**: 87- 92.

Suvachitanont, S. and Ratanapan, P., (2011). Evaluation of microcrystalline cellulose from corn cob for development to the pharmaceutical industry. In *TIChE International Conference, Paper Code: ms012*.

Swanepoel, E., Liebenberg, W., Devarakonda, B. and De Villiers, M.M., (2003). Developing a discriminating dissolution test for three mebendazole polymorphs based on solubility differences. Die Pharmazie-An. *Int. J. Pharm .Sci*. **58**: 117–121.

Szymańska-Chargot, M., Chylińska, M., Gdula, K., Kozioł, A. and Zdunek, A., (2017). Isolation and characterization of cellulose from different fruit and vegetable pomaces. *Polymers*.**9**: 495.

Taherzadeh, M., & Karimi, K. (2008). Pretreatment of Lignocellulosic Wastes to Improve Ethanol and Biogas Production: A Review. *Int. J. Mol. Sci.* **9**:1621–1651.

Thoorens, G., Krier, F., Leclercq, B., Carlin, B. and Evrard, B., (2014). Microcrystalline cellulose, a direct compression binder in a quality by design environment—A review. *Int. J. Pharm*. **473**: 64–72.

Trache, D., Hussin, M.H., Chuin, C.T.H., Sabar, S., Fazita, M.N., Taiwo, O.F., Hassan, T.M. and Haafiz, M.M., (2016). Microcrystalline cellulose: Isolation, characterization and bio-composites application—A review. *Int. J. Biol. Macromol*. **93**:789–804.

Umeh, O.N.C., Nworah, A.C. and Ofoefule, S.I., 2014. Physicochemical properties of microcrystalline cellulose derived from Indian bamboo (Bambusa vulgaris). *Int. J. Pharm. Sci. Rev. Res*. **29**: 5-9.

United States Pharmacopoeia 30th ed. National Formulary 25 ed. (USP 30/NF 25) (2007). The United states Pharmacopeial Convention, Inc., Rockville, Maryland.

United States Pharmacopoeia, Stage 7 Harmonization (USP <717>, 2016). The United States Pharmacopeial Convention.

Uzun, B., Arslan, C., Karhan, M. and Toker, C., (2007). Fat and fatty acids of white lupin (Lupinus albus L.) in comparison to sesame (Sesamum indicum L.). *Food Chemistry*. **102**:45-49.

Vasco-Correa, J., Ge, X., & Li, Y. (2016). Biological Pretreatment of Lignocellulosic Biomass. *Biomass Fractionation Technologies for a Lignocellulosic Feedstock Based Biorefinery. 561–585.*

Xu, L. and Geelen, D., (2018). Developing biostimulants from agro-food and industrial by-products. *Front. Plant Sci*. **9**: 1567.

Yami, M., Meyer, F. and Hassan, R., (2020). The impact of production shocks on maize markets in Ethiopia: implications for regional trade and food security. *Agric. Food Econ.* **8**:1-25.

Yassin, S., Goodwin, D.J., Anderson, A., Sibik, J., Wilson, D.I., Gladden, L.F. and Zeitler, J.A., (2015). The disintegration process in microcrystalline cellulose based tablets, part 1: influence of temperature, porosity and superdisintegrants. *J Pharm Sci*. **104**:3440–3450.

Zhang, Y., Xu, Y., Yue, X., Dai, L. and Ni, Y., (2019). Isolation and characterization of microcrystalline cellulose from bamboo pulp through extremely low acid hydrolysis. *J. Wood Chem. Technol*. **39**: 242-254.

Zheng, Y., Zhao, J., Xu, F., and Li, Y. (2014). Pretreatment of lignocellulosic biomass for enhanced biogas production. *"Prog. Energy Combust. Sci*. **42**: 35–53.

Zuliahani, A., Nurul Nadhirah, R., Rozyanty, A.R., Nawawi, W.I. and Nor Hanani, A.B., (2016). Crystallinity, Tapping and Bulk Density of Microcrystalline Cellulose (MCC) Isolated from Rice Husk (RH). In Applied Mechanics and Materials (Vol. 835, pp. 272-276). Trans Tech Publications Ltd. *Appl. Mech. Mater.* **835**: 272-276.